



HAL
open science

Quadratic Mean Field Games with Negative Coordination

Thibault Bonnemain

► **To cite this version:**

Thibault Bonnemain. Quadratic Mean Field Games with Negative Coordination. Mathematical Physics [math-ph]. Université Cergy Pontoise, 2020. English. NNT: . tel-02524610

HAL Id: tel-02524610

<https://hal.science/tel-02524610v1>

Submitted on 30 Mar 2020

HAL is a multi-disciplinary open access archive for the deposit and dissemination of scientific research documents, whether they are published or not. The documents may come from teaching and research institutions in France or abroad, or from public or private research centers.

L'archive ouverte pluridisciplinaire **HAL**, est destinée au dépôt et à la diffusion de documents scientifiques de niveau recherche, publiés ou non, émanant des établissements d'enseignement et de recherche français ou étrangers, des laboratoires publics ou privés.



CERGY PARIS

UNIVERSITÉ

QUADRATIC MEAN FIELD GAMES
WITH NEGATIVE COORDINATION

THIBAUT BONNEMAIN

Thèse de doctorat pour l'obtention du titre de

DOCTEUR EN PHYSIQUE

délivré par l'Université Cergy-Pontoise

École doctorale n°405 : Économie, Management, Mathématiques, Physique et
Sciences Informatiques (EM2PSI)

Soutenue le 24 Février 2020 devant la Commission d'examen :

M.	Jean-Pierre NADAL	Président
M.	Filippo SANTAMBROGIO	Rapporteur
M.	Max-Olivier HONGLER	Rapporteur
Mme.	Cécile APPERT-ROLLAND	Examinatrice
M.	Olivier GUEANT	Examineur
M.	Thierry GOBRON	Directeur de thèse
M.	Denis ULLMO	Co-directeur de thèse

Travail réalisé conjointement au

LPTMS, CNRS, Université Paris-Saclay, 91405 Orsay, France

et

LPTM, CNRS, Université Cergy-Pontoise, 95302 Cergy-Pontoise, France

entre Février 2017 et Janvier 2020 sous la supervision de

DENIS ULLMO

et

THIERRY GOBRON

*You know I'm born to lose, and gambling's for fools,
But that's the way I like it, I don't wanna live forever*

— Motörhead, Ace of Spades

ABSTRACT / RÉSUMÉ

ENGLISH VERSION

Mean Field Games provide a powerful theoretical framework to deal with stochastic optimization problems involving a large number of coupled subsystems. They can find application in several fields, be it finance, economy, sociology, engineering ... However, this theory is rather recent and still poses many challenges. Its constitutive equations, for example, are difficult to analyse and the set of behaviours they highlight are ill-understood. While the large majority of contributions to this discipline come from mathematicians, economists or engineering scientists, physicist have only marginally been involved in it. In this thesis I try an start bridging the gap between Physics and Mean Field Games though the study of a specific class of models dubbed "quadratic".

The first part constitutes a general introduction to theory of Mean Field Games. The mathematical formalism is introduced heuristically with an emphasis on quadratic Mean Field Games. Some parallels with Physics are drawn, most notably through a mapping onto non-linear Schrödinger equation and its associated hydrodynamic representation. The second part is then divided in three chapters. The first one investigates the integrability of some particular quadratic Mean Field Games models: first in the weak noise limit by way of an analogy with electrostatics, then in the noisy regime by discussing the applicability of Inverse Scattering methods. The second chapter makes use of previous results to study more generic games, toy-models of sort, and construct approximation schemes. The third, and last, chapter examines an alternative approach to deal with the weak noise limit introduced two chapters before by accommodating semi-classical approximation to Mean Field Games.

Keywords: Mean Field Games, optimization, control, stochastic, partial differential equations, non-linear Schrödinger, population dynamics, toy-model.

La théorie des Jeux en Champ Moyen propose un ensemble d'outils puissants lorsqu'il s'agit d'étudier des problèmes d'optimisation stochastique impliquant un grand nombre de sous-systèmes couplés. Cette théorie peut s'appliquer à une grande variété de domaines, de la finance à l'économie, en passant par la sociologie ou l'ingénierie... Cependant, cette dernière étant relativement récente, il reste de nombreux défis à relever. Les équations qui la sous-tendent, par exemple, sont difficiles à analyser, et les comportements ainsi décrits sont mal compris. Alors que la grande majorité des contributions à cette nouvelle discipline provient de mathématiciens, d'économistes ou d'ingénieurs, les physiciens ne s'y sont que peu intéressés. Avec cette thèse, j'essaie de jeter un pont entre Physique et Jeux en Champ Moyen à travers l'étude d'une classe spécifique de modèles qualifiés de "quadratiques".

La première partie est une introduction générale à la théorie des Jeux en Champ Moyen. Le formalisme mathématique y est présenté de manière heuristique à travers le prisme des jeux quadratiques. Des parallèles sont établis avec la Physique, notamment à travers un changement de variable vers l'équation de Schrödinger non-linéaire et la représentation hydrodynamique qui lui est associée. La deuxième partie est ensuite divisée en trois chapitres. Le premier étudie l'intégrabilité de certains modèles particuliers de Jeux en Champ Moyen : d'abord dans la limite de faible bruit à l'aide d'une analogie avec l'électrostatique, ensuite dans le régime bruité pour lequel l'application de méthodes de diffusion inverse est examinée. Le deuxième chapitre utilise les résultats précédemment obtenus pour aborder des problèmes plus généraux, sortes de modèles jouets, et construire des schémas d'approximation. Le troisième et dernier chapitre propose une méthode alternative pour étudier la limite de faible bruit, introduite deux chapitres plus tôt, en adaptant l'approximation semi-classique aux Jeux en Champ Moyen.

Mots-clés : Jeux en Champ Moyen, optimisation, contrôle, stochastique, équations aux dérivées partielles, Schrödinger non-linéaire, dynamique de population, modèle jouet.

PUBLICATIONS

Some ideas and figures have appeared previously in the following publications:

- Thibault Bonnemain and Denis Ullmo. “Mean field games in the weak noise limit: A WKB approach to the Fokker–Planck equation.” In: *Physica A: Statistical Mechanics and its Applications* 523 (2019), pp. 310–325.
- Thibault Bonnemain, Thierry Gobron, and Denis Ullmo. “Universal behavior in non stationary Mean Field Games.” In: *arXiv e-prints*, arXiv:1907.05374 (2019), arXiv:1907.05374. arXiv: 1907.05374 [physics.soc-ph].
- Thibault Bonnemain, Denis Ullmo, and Thierry Gobron. “Schrödinger approach to Mean Field Games with negative coordination.” In: *HAL archives-ouvertes* (2019).

ACKNOWLEDGEMENTS

I know some people really look forward to writing their acknowledgements, but I did not. In fact, this part is the last thing I wrote and I kept postponing it over, and over, and over... It is not that I think everything in this (or any) thesis should be made austere, in the name of science, far from it. It is not that I do not believe in the merits of this tradition either. It is simply that I would like to think that people I am grateful for already know that I am, through other means than such a formal body of text. The exercise ultimately feels artificial to me and I cannot help but end up fairly dissatisfied with the result. I have the utmost respect and admiration for people that manage to turn something so mundane as acknowledgements into three parts epics, sometimes almost ten pages long and written in several languages. Mine, as you may have guessed already, will stay on the more concise and down to earth side of things. I will also keep the name-dropping to a minimum as there are a lot of people that deserve to be mentioned here and I am terrified to forget any.

First I would like to thank my family, my parents, of course, but also my three brothers, six uncles and my aunt, as well as their partners and children. They represent the foundation of my education and are in large part responsible for this thesis.

I would like to thank the *Digging Team*, my oldest group of friends, that still answer the call after all these years. For various reasons it has become increasingly difficult to see each other, but when we do it is like no time has passed. For this you all deserve a kiss on the nose.

I want to express my gratitude to *Les Grelins* (in their more recent, extended version), not only for the great time I had with them over the years but also for the positive influence this group had on me. In particular the older members, Paul-Yves, Pierre and Robin, took the role of mentor figures for the young teenager that I was at the time.

I want to thank the people from *Lycées des Graves*, that I still hang out with to this day. If middle-school was pretty lame, high-school was instead really fun, and it is all thanks to you.

Then comes the *Bordeaux 1* crew (once again in its extended version), full of awesome (and surprisingly diverse) people that reinforced my belief that I made the right call when choosing to go to the university instead of classe prépa. In particular I want to extend my thanks to Lucie who was the first person to proof-read this manuscript.

I thank people from *ENS* that (for the most part) were exceptionally welcoming, even though I joined during the second year, even though

I arrived systematically late in class and even despite my *look de clodo*. Guys you're great.

I also want to give a shout out to *The Magicians* that allowed me to continue nerding at a competitive level when coming to Paris and to meet new people that were in no way related to physics ... be they retired snipers or lyrical singers.

I want to thank my supervisors Denis and Thierry that followed and put up with me these last three years. I also thank the staff from both *LPTM* and *LTPMS*, in particular Jean, Flora and Sylvie on the one side, and Christophe, Claudine, Emmanuel, Karolina, Olivier and Nicolas on the other, for their help and good vibes.

I know I have not been around much in the last few months but I am also grateful for my lab mates, for the ones that left before me as well as for the ones that are still at it, you all made these three years all the more fun.

Finally, I want to thank the members of my jury for taking the time to read my work. Especially, I extend my thanks to Max-Olivier and Filippo who both handled the role of *rapporteur* and provided me with insightful comments.

CONTENTS

I	PROLEGOMENON	1
1	INTRODUCTION	3
2	ELEMENTS OF MEAN FIELD GAMES THEORY	7
2.1	Optimal Control	8
2.1.1	Optimal Control in Physics : principle of least action	8
2.1.2	Dynamic programming and Hamilton-Jacobi-Bellman equation	10
2.2	Game Theory	11
2.2.1	A canonical example	11
2.2.2	Zoology	12
2.2.3	Nash Equilibrium	13
2.2.4	Differential games	14
2.3	Mean Field Approach	15
2.3.1	Mean Field Games equations	15
2.3.2	Long optimization time and ergodic state	17
2.4	Changes of variables	18
2.4.1	Non-linear Schrödinger formalism	19
2.4.2	Hydrodynamic representation	20
2.4.3	Action, and conserved quantities	20
II	KEY FINDINGS	23
3	INTEGRABILITY OF QUADRATIC MEAN FIELD GAMES	25
3.1	Integrable Mean Field Games in the weak noise limit	26
3.1.1	Definition and relevance of the weak noise limit	27
3.1.2	Preliminary simulations	28
3.1.3	Hodograph transform	29
3.1.4	Potential representation	32
3.1.5	Universal scaling solution in the infinite optimization time limit	34
3.1.6	Finite optimization time: impact of higher order multipole moments on the hydrodynamic coordinates	36
3.1.7	Physical meaning of the multipole moments	38
3.1.8	Multipole expansion and the boundary conditions: constructing a numerical ansatz	42
3.2	Complete integrability of Mean Field Games equations	44
3.2.1	Nondimensionalization	46
3.2.2	Zero curvature representation	47
3.2.3	Monodromy matrix	49
3.2.4	Computing conserved quantities	50

3.2.5	Inverse scattering transform and its application to Mean Field Games	53
4	HEURISTIC APPROACH TO 1D QUADRATIC MEAN FIELD GAMES	59
4.1	Static mean field game : the ergodic state	60
4.1.1	Alternative representations in the ergodic state	61
4.1.2	Bulk of the distribution: Thomas-Fermi approximation	62
4.1.3	Tails of the distribution: semi-classical approximation	63
4.1.4	Some properties of the ergodic state	66
4.2	Time dependent problem: the beginning of the game .	68
4.2.1	Large ν regime : Gaussian ansatz	69
4.2.2	Small ν regime : Parabolic ansatz	72
4.3	The entire game	78
4.3.1	Matching small and large ν regimes	78
4.3.2	Matching transient and ergodic states	80
5	SEMI-CLASSICAL ANALYSIS OF FOKKER-PLANCK EQUATION	85
5.1	WKB approximation of a 1d Fokker-Planck equation .	88
5.1.1	Symplectic manifold and classical action	88
5.1.2	Semi-classical approximation for $m(t, x)$	91
5.1.3	Absorbing boundary conditions	92
5.2	Derivation and generalization	93
5.2.1	$R_0 = 0$, Hamilton-Jacobi equation	94
5.2.2	$R_1 = 0$, transport equation	95
5.3	Application to the seminar problem	96
5.3.1	Constant drift	97
5.3.2	Linear drift	99
5.3.3	Coupling the two solutions	101
6	CONCLUSION	107
	III APPENDIX	111
A	NUMERICAL SCHEME	113
A.1	Basic structure	113
A.2	Crank-Nicolson method	114
A.2.1	Discretization scheme	114
A.2.2	Neumann boundaries	115
A.2.3	Von Neumann stability analysis	116
B	METHOD OF CHARACTERISTICS	117
C	RIEMANN INVARIANTS	119
D	GREEN'S THEOREM AND THE LAPLACE EQUATION	121
D.1	Green function of Laplace equation in cylindric coordinates	121
D.2	Solving the boundary value problem	122
E	NON-ABELIAN STOKES THEOREM	125

E.1	Stokes theorem	125
E.2	Generalization to non Abelian forms	125
F	POISSON COMMUTATIVITY OF THE FIRST INTEGRALS OF MOTION	127
F.1	Generalisation of Poisson brackets to infinite dimensional systems	127
F.2	Classical r-matrix	128
F.3	Sklyanin fundamental relation	129
F.4	Involution of the first integrals of motion	130
G	SEMI-CLASSICAL APPROXIMATION FOR QUADRATIC POTENTIAL	131
H	PROOF THAT THE OPERATOR HAS ONLY REAL NON-NEGATIVE EIGENVALUES	133
I	DECREASING SOLUTIONS OF THE EFFECTIVE GAME	135
J	NON-HERMITIAN CORRECTION TO THE SEMI-CLASSICAL TREATMENT OF FOKKER-PLANCK EQUATION	137
K	LIOUVILLE'S FORMULA	139
L	COUPLING TWO SEMI-CLASSICAL SOLUTIONS OF FOKKER-PLANCK EQUATION	141
	List of Figures	145
	BIBLIOGRAPHY	151

ACRONYMS

FP Fokker-Planck

HJB Hamilton-Jacobi-Bellman

IST Inverse Scattering Transform

LPTM Laboratoire de Physique Théorique et Modélisation

LPTMS Laboratoire de Physique Théorique et Modèles Statistiques

MFG Mean Field Game

NLS Non-linear Schrödinger

ODE Ordinary Differential Equation

PDE Partial Differential Equation

WKB Wentzel-Kramers-Brillouin

Part I

PROLEGOMENON

This first part aims to instruct the reader on the basics of Mean Field Games theory in a comprehensive, heuristic fashion. It will provide a short contextualisation of my work as a PhD student, and then introduce elements of both control theory and game theory while trying to relate those to similar notions in physics.

INTRODUCTION

This thesis aggregates the results of my work under the supervision of Thierry Gobron and Denis Ullmo, respectively at the Laboratoire de Physique Théorique et Modélisation (LPTM) and Laboratoire de Physique Théorique et Modèles Statistiques (LPTMS), on models of Mean Field Game theory.

Mean Field Games are a powerful framework introduced a little more than ten years ago in the independent work of J.-M. Lasry and P.-L. Lions [77–79] and of M. Huang, R. P. Malhamé and P. E. Caines [59] to deal with problems of optimization involving an increasingly large number of coupled subsystems. Such optimization problems are traditionally called *games* by the mathematical community and may quickly become technically intricate [67]. Inspired by the notion of *mean field* developed by physicists [112], Mean Field Game paradigms rely heavily on the assumption that the very complexity brought by a large number of subsystems (traditionally called *players* or *agents*) allows for a drastic simplification. In this highly complex configuration, interactions between agents may average out and one may consider that a given player is not really sensitive to the individual choices of their competitors, but only to an averaged quantity representing the decisions made by all the other participants to the game.

Applications of Mean Field Games are numerous, ranging from finance [27, 33, 72] to economy [2, 3, 55], sociology [4, 71, 73] or even engineering [69, 70, 84]. The last few years have seen this new field evolve rapidly, and particularly in two major directions corresponding to two different (if not opposite) philosophies. On the more formal side, many mathematicians have shown great interest for a rigorous description of Mean Field Games, allowing for important results on the existence and uniqueness of a solution to these problems [26, 50, 54], or on the differences and convergence of a many player game to its mean field counterpart [15, 29, 30]. At the same time, significant progress has been made towards developing effective numerical schemes [1, 5, 52] granting the opportunity for more application oriented studies. As such, important contributions largely come from Mathematics, Engineering Sciences or, more recently, Economics.

Then, one may ask, why should a thesis about Mean Field Games be considered theoretical Physics rather than, for example, Mathematics or Economics ? The answer lies in the way the problem is approached. While the mean field assumption provides a substantial simplification of more traditional games, the constitutive equations of Mean Field Game models remain difficult to analyse, even in spite of

This mean field approach was similarly introduced at the end of the 19th century to describe systems of many interacting components, for which an exact treatment is usually unmanageable.

the recent developments. Few exact solutions exist, mainly in simplified settings [13, 34, 51, 60], and the numerical schemes, while quantitatively accurate, do not necessarily yield a complete comprehension of the underlying mechanisms at work. The lack of effective approximation schemes arguably hinders the diffusion of these tools to a significantly larger audience as well. Consequently, there is a need for the discussion of toy-models, simple enough to be understood thoroughly but representative of what Mean Field Games can be, in order to develop a more qualitative understanding of the problem. A physicist's approach, through the evaluation of characteristic scales and the analysis of various limiting regimes, would provide just that: a good intuition of the qualitative behaviours coupled to robust and accurate approximations.

On a larger scale, this work is symptomatic of a recent tendency for physicists to branch out and study subjects that would not strictly be considered Physics by the general public, subjects such as Biology [87, 110], Ecology [12, 17] or Social Sciences [22, 36, 49, 88]. Physics has more or less always influenced (and been influenced) by other fields of research, in particular Economics as highlighted by P. Mirowski [86]. Neoclassical economist I. Fisher wrote his doctoral thesis under the supervision of the physicist J. W. Gibbs [47], R. J. Aumann owes to fluid mechanics for his idea of *continuum of traders* [8], while T. C. Schelling's approach to segregation from individual incentives is reminiscent of statistical mechanics [97]. And if examples of this interplay between Physics and others sciences were indeed numerous already during the 20th century, this phenomenon has exploded since the mid-90s. This stems from the will to apply proven methods of statistical mechanics to domains that are not traditionally looked at as Physics but fall under the definition of *complex systems*. These methods aim for the extraction of macroscopic properties (system wide quantities, correlations, fluctuations, response to perturbations ...) from microscopic characteristics (local interactions, individual wants or needs ...) in systems that, as T. C. Schelling would say, "lead to aggregate results that the individual neither intends nor needs to be aware of, results that sometimes have no recognizable counterpart at the level of the individual". Still, many challenges remain and one has to be wary when looking at transposing techniques that were developed in a specific context to another: it should come as part of a continuing process along with the existing literature... And Mean Field Game theory seems to provide an appropriate framework for physicists to discuss optimization problems in a general and rigorous way.

P. Mirowski [86] notably criticized the use of methods originating from Hamiltonian mechanics in economic problems where the required assumptions for those methods to work, such as conservation of the utility function, were not met.

This manuscript is divided in three parts. The first one, simply titled "Prolegomenon", presents the reader with the fundamentals of Mean Field Game theory. It introduces notions of *Optimal Control* and traditional *Game Theory*, as well as its mean field counterpart,

in an heuristic fashion while drawing parallels with similar concepts in Physics. This part should not be considered as a comprehensive, highly rigorous discussion but rather as an overview of this growing field that is Mean Field Game theory, containing all the basic elements needed to approach the following parts. The second part, "Key Findings", showcases the main results of my work on a specific type of games dubbed *quadratic*. The first chapter of this part, chapter 3, focuses on a particular type of quadratic Mean Field Game models, the constitutive equations of which are characterized as *integrable* and can be solved analytically. These integrable models are interesting in and of themselves as the analytical nature of their solutions can bring a better understanding of what constitutes a Mean Field Game, but those can also be interpreted as limiting regimes of more complex games. Such (more) sophisticated games are then examined in chapter 4, where I use the expertise and intuition developed in chapter 3 to build up various approximation schemes. These approximation regimes are then coupled together to reconstruct the complete solution. Chapter 5, while still dealing with quadratic Mean Field Games, focuses more closely on one of their constitutive equations, namely Fokker-Planck equation, and investigates the applicability of a Wentzel-Kramers-Brillouin approximation to such problems. Finally, chapter 6 contains a summary of the most important results along with some concluding remarks. The third and last part, "Appendix", addresses a few technical aspects (such as details concerning numerical schemes, computations or known mathematical methods) for the sake of self-containedness.

As part of a broader Game Theory, Mean Field Games (MFG) deal with problems of strategic optimization but focus on the limit where the number of agents, or players, becomes large. Players optimize strategically in the sense that the outcome of their optimization depends, inter alia, on the choices (or strategies) adopted by other players.

Such problems of strategic optimization with a large number of players appear naturally when addressing any type of socio-economic conundrum [82]. For example, the notion of *utility*, as coined by utilitarian philosophers J. S. Mill and J. Bentham during the 19th century [85], was introduced in Ethics as a way for a moral agent to decide between two actions: one should make the decision that maximizes the total happiness of the world. A more recent acceptance of utility can be found in microeconomics, where the now quantified *utility function* is frequently adopted to quantitatively represent consumers' preferences, who, in turn, try to maximize their utility (be it happiness, comfort, etc.) by choosing how to spend money within a given budget. In the same way, one can consider industries aim to maximize their profits by adjusting factors of production. Presented strictly in this way the previous examples do not allow for strategic thinking per se, these are plain optimization problems based on some environmental constraints such as prices, wages or production costs ... These problems however become games when one factors in the potential interactions between multiple players and how it can impact their decision making, as highlighted for example through the well-known *Cournot duopoly*.

Naturally these kinds of model become increasingly more complex as the number of players grows. Not only does one need to solve a greater number of individual optimization problems but keeping track of all the interactions between each and every player quickly becomes unmanageable. The idea behind MFG theory is that, in the limit where the number of players goes to infinity, one can assume the interactions average out and each individual only reacts to the overall density of players. Because of this simplifying hypothesis, one may forego the idea of monitoring the behaviour of each player individually in favour of looking at the evolution of their continuous, deterministic distribution.

This chapter aims to provide a general introduction to MFG theory from the basic notions that underlie its formalism to the derivation of its constitutive equations. Important mathematical results integral

An economic model in which two companies compete for profit, knowing that the end prices depend on the overall production [82].

to further discussions will then be addressed before discussing some alternative formulations of the MFG problem.

2.1 OPTIMAL CONTROL

Optimal Control is largely due to the work of L. Pontryagin and R. Bellman in the 50s [25].

Optimal Control is the branch of applied mathematics which deals with dynamical systems that can be controlled in order to optimize an objective function. In many ways, it can be seen as a rather recent extension of the *Calculus of Variations* well-known to physicists. Because of the strong link between optimization and Game Theory it is only natural that Optimal Control serves as the foundations of MFG theory.

2.1.1 Optimal Control in Physics : principle of least action

To bridge the gap between Physics and Optimal Control I will recast a typical model of Physics in the language of optimization.

I shall consider a classical point particle of mass m , and generalised coordinate $\vec{q}(t)$, that goes from \vec{q}_1 to \vec{q}_2 between time t_1 and t_2 , in a potential $V(\vec{q}, t)$. Examples of the possible trajectories of this particle are illustrated Figure (1). Naturally, as any physicist may know, one can deduce the particle's dynamics using Newton's second law

$$\ddot{\vec{q}} = -\vec{\nabla}V . \quad (2.1)$$

However this equation can also be seen as deriving from the more general *principle of least action* which reads [90]:

"The path taken by the system between times t_1 and t_2 and configurations \vec{q}_1 and \vec{q}_2 is the one for which the action is stationary (no change) to first order."

The *action* \mathcal{S} is, then, an abstract physical quantity that needs to be extremized in order to obtain the dynamics of the considered system (here a point particle). It is usually defined as the integral over time of another quantity called *Lagrangian* and denoted L

$$\mathcal{S}[\vec{q}, t_1, t_2] = \int_{t_1}^{t_2} L(\vec{q}, \dot{\vec{q}}, t) dt . \quad (2.2)$$

The Lagrangian is constructed so that the dynamics follows a set of rules or physical principles. For example, in the case of a classical particle in a potential:

- The motion of the particle should be fully defined once \vec{q} and $\dot{\vec{q}}$ are known.
- The dynamics should respect Galileo's principle.

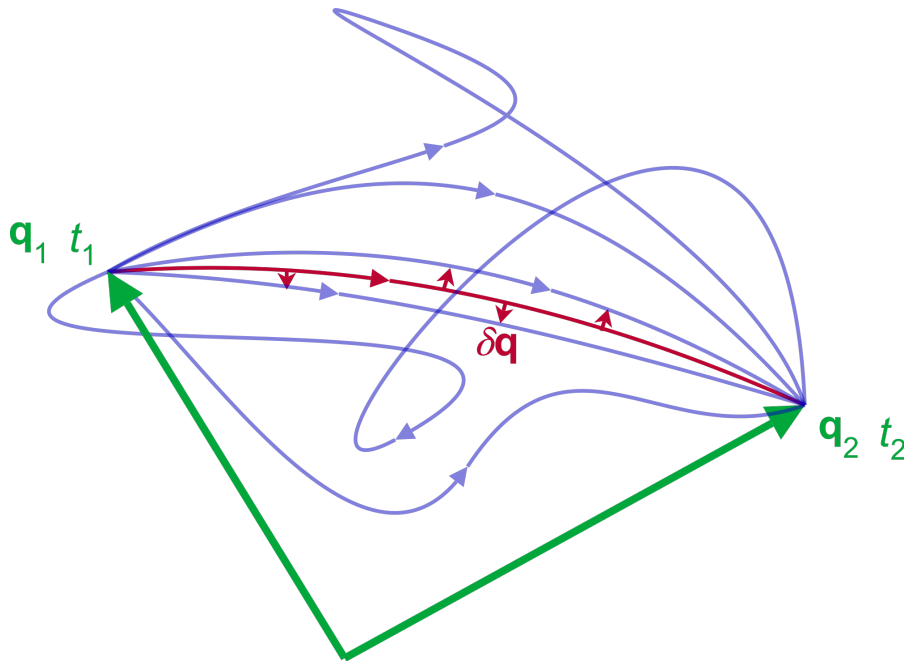


Figure 1: There are infinite possibilities for the system to reach state \vec{q}_2 starting from \vec{q}_1 , however the chosen path (red) is the one that minimizes the action.

- Going through a region where the potential is greater should be penalized.

As discussed by L. D. Landau and E. M. Lifshitz [75], those constraints impose the Lagrangian of classical mechanics to read

$$L = \frac{1}{2}m|\dot{\vec{q}}|^2 - V, \quad (2.3)$$

and the mathematical expression of the principle of least action

$$\frac{\delta \mathcal{S}}{\delta \vec{q}} = \frac{d}{dt} \vec{\nabla}_{\dot{\vec{q}}} L - \vec{\nabla}_{\vec{q}} L = 0, \quad (2.4)$$

also known as Euler-Lagrange equation, is perfectly equivalent to equation (2.1).

In this way, through the principle of least action, it is possible to reformulate a problem of classical mechanics as a problem of optimization. In Physics the action plays a role equivalent to that of the *utility function* in Economics or the *cost function* in Optimal Control. Conversely, the Lagrangian is equivalent to a *running cost* and both are constructed with the same goal in mind. Finally, what is known in the Optimal Control jargon as *control parameter* simply corresponds to the position \vec{q} , and optimizing the cost function (action) yields the optimal solution (dynamics).

The control parameter is the variable over which one has to optimise the cost function. In Physics it usually takes the form of the position, while in Optimal Control, by convention, one chooses rather to control velocity.

2.1.2 Dynamic programming and Hamilton-Jacobi-Bellman equation

While Euler-Lagrange equations can be seen used in the Optimal Control literature, there exists another approach which yields similar results but is better suited to deal with stochastic problems.

Let us consider a system specified by its state variable $\vec{X} \in \mathbb{R}^d$ which evolves according to Langevin dynamics

$$d\vec{X}_t = \vec{a}_t dt + \sigma d\vec{W}_t \quad (2.5)$$

where \vec{a} is the control parameter, σ a constant and \vec{W} a Gaussian white noise of variance one. We want to control (i. e. find the proper dynamics for \vec{a}) so that the following cost function is minimized

$$c[\vec{a}](\vec{X}, t) = \mathbb{E} \left[\int_t^T \left(\frac{\mu}{2} (\vec{a}_\tau)^2 - V(\vec{X}_\tau) \right) d\tau + c_T(\vec{X}_T) \right]. \quad (2.6)$$

Here T is the time at which the game ends, μ is a constant, V can be seen as an environmental gain and c_T a *terminal cost*, that is to say a cost to end the control process in a certain configuration.

In order to find the Optimal Control parameter \vec{a}^* , let us first introduce the *value function* u as the optimal cost function

$$u(\vec{X}, t) \equiv \inf_{\vec{a}} c[\vec{a}](\vec{X}, t). \quad (2.7)$$

To compute u , and ultimately relate the result to \vec{a}^* , we turn to the notion of dynamic programming and more precisely to *Bellman's optimality principle* [14]

"An optimal policy has the property that whatever the initial state and initial decision are, the remaining decisions must constitute an optimal policy with regard to the state resulting from the first decision."

This means the computation of u can be simplified by discretizing the problem and optimizing on infinitesimally small time frames. On the interval $[t, t + dt]$ we then have the relation

$$u(\vec{X}, t) = \inf_{\vec{a}} \mathbb{E} \left[\int_t^{t+dt} \left(\frac{\mu}{2} (\vec{a}_\tau)^2 - V(\vec{X}_\tau) \right) d\tau \right] + u(\vec{X} + d\vec{X}, t + dt), \quad (2.8)$$

which is called Bellman equation. The dynamics of \vec{X} being defined through Langevin equation, $u(\vec{X} + d\vec{X}, t + dt)$ can be expanded to first order in dt using *Itô's Lemma* [48]

$$\begin{aligned} \mathbb{E} \left[u(\vec{X} + d\vec{X}, t + dt) \right] &= u(\vec{X}, t) \\ &+ \left[\partial_t u(\vec{X}, t) + \vec{a} \cdot \vec{\nabla} u(\vec{X}, t) + \frac{\sigma^2}{2} \Delta u(\vec{X}, t) \right] dt' \end{aligned}$$

(2.9)

which, combined with Bellman equation (2.8) yields Hamilton-Jacobi-Bellman (HJB) equation

$$\partial_t u + \frac{\sigma^2}{2} \Delta u + \inf_{\vec{a}} \left[\frac{\mu}{2} (\vec{a})^2 + \vec{a} \cdot \vec{\nabla} u \right] = V, \quad (2.10)$$

that constitutes an alternative to Euler-Lagrange equation (2.4). The optimization of the third term in HJB equation imposes the relation $\vec{a}^* = -\frac{\vec{\nabla} u}{\mu}$ and the equation can be rewritten as

$$\partial_t u + \frac{\sigma^2}{2} \Delta u - \frac{1}{2\mu} \|\vec{\nabla} u\|^2 = V. \quad (2.11)$$

Before going forward, it should be noted that this equation is constructed backward in time, as is hinted by the sign in front of the diffusive term. By definition the boundary condition for the value function is given at time T , the end of the optimization

$$u(\vec{X}, T) = c_T(\vec{X}), \quad (2.12)$$

and solution to HJB equation is then constructed step by step from there.

This concludes my discussion on Optimal Control. In this section I chose to focus on cost functions that only depend on the square of the control parameter, characteristic of the so called *quadratic games*, as those are the ones I will be dealing with in the rest of this manuscript. Of course, the derivation of HJB equation can be easily generalized to more complicated cost functions, I refer you to monograph [18] in this regard. In the next section I will address Game Theory, another important (as the name suggests) aspect of MFG.

2.2 GAME THEORY

Game Theory is a modern label for strategic optimization, "strategic" in the sense that each agent (or player) tries to solve an optimization problem which depends on the others' behaviour (or strategy). Obviously, as interactions are added, complexity escalates quickly, and the need for a new, proper definition of what can be considered a solution of the optimization problem arises.

The emergence of Game Theory as a specific field of research is largely due to J. von Neumann's seminal work [111].

2.2.1 A canonical example

To illustrate what is traditionally called a game and how the notion of solution has to be reinterpreted, we shall consider the seminal *Prisoner's dilemma* as formalized by A. Tucker in 1950 [94].

Imagine two members, A and B, of a same gang are arrested and put in solitary confinement with no means of communicating with

one another. Both are to be convicted for robbery but are also suspected of murder with lack of sufficient evidence. Imagine now that the prosecutors offer both prisoners a bargain based on their suspicion. Here are the possible outcomes of this bargain, as illustrated in Table (1):

- A and B both betray the other and serve 10 years in prison each (convicted for murder with plea bargaining in exchange of a more lenient punishment).
- A betrays B but B stays silent (or vice versa), A is set free and B serves 15 years.
- Both A and B stay silent and serve 4 years (convicted for robbery).

PRISONERS	B BETRAYS	B STAYS SILENT
A BETRAYS	10/10	0/15
A STAYS SILENT	15/0	4/4

Table 1: Prisoner's dilemma pay-off matrix

It is assumed that neither player is loyal to the other and both understand the nature of this game. The dilemma in this situation comes from the fact that mutual betrayal results in a worse outcome than mutual cooperation (20 combined years versus 8) but cooperating is irrational from a self-interested perspective. Framed in this way, betraying always yields better pay-off than staying silent, regardless of what the other decides. If B betrays A, then A should betray B because being convicted for 10 years is better than 15. And if B stays silent, A should still betray B as going free is better than serving 4 years ... Because of this, betraying is called a *dominant strategy* and the situation where both prisoner betray the other is referred to as a *Nash Equilibrium* (see section 2.2.3).

This model is very simplistic and does not aim to describe reality accurately. For example it leaves aside the systematic bias towards cooperative behaviour or the fear of retribution. Its main interest, though, is that it provides a good illustration of what constitutes a game and the issues that come with it, namely the questions of rationality and solution (global vs individual optimum).

2.2.2 Zoology

Because Game Theory is so broad of a discipline, we have to narrow down our field of study before addressing mathematical aspects of the formalism. This section will provide a brief overview of the main

game types and allow me to emphasize what kind of rules I will use to construct the games I will be interested in.

COOPERATION: A game is considered *cooperative* if players can form externally enforced (e.g. through contract law) binding agreements in order to ensure the group will take actions resulting in a collective pay-off. In a *non-cooperative* game, alliances can still form but are self-enforcing and while a collective greater good can be sought within this framework, it still focuses primarily on individual gains.

TIME DEPENDANCE: In *simultaneous* games, players decide on a strategy at the beginning of the game and cannot change it. In *sequential* however, they are able to modify their strategy, for example in reaction to others' behaviour.

INFORMATION: An important aspect in decision making is the amount of information the players have access to before defining their strategy. Do they have *perfect information* as in chess? Do they have *imperfect information* as in poker? Do they have *complete information*, i.e. do they know all the rules and possible pay-offs? And finally, is there some uncertainty resulting in non-deterministic strategies?

RATIONALITY: In Game Theory players are considered *rational* if they are able to solve optimization problems and follow their strategy without psychological bias. Obviously this assumption is generally not realistic but can still be pertinent in some specific cases where it can yield interesting results. Some of the shortcomings of this approach can be accounted for by modifying the players' utility function. For example it could contain a bias towards altruistic behaviours or a penalty towards marginal strategies to represent peer pressure. One of the main difficulties then becomes how to define a proper utility function. The notion of *limited rationality*, where players are not necessarily able or far-sighted enough to solve their problems, is also the subject of extensive research, particularly in the field of *Evolutionary Game Theory* [102].

For the rest of this thesis, I will be focusing on non-cooperative, sequential games with rational but uncertain players, which are typically studied through the lens of Nash Equilibrium.

2.2.3 Nash Equilibrium

In Game Theory, are called *solutions* predictions that describe which strategies players will adopt and, hence, the result of the game. Obviously, depending on how rational (in the game theoretical sense) players are, the result of the game may vary and this led to the emergence

Solution concepts are formal rules for predicting how a game will be played [104].

of the notion of *solution concepts*, the most commonly used being the Nash Equilibrium concept. This concept assumes that players will choose their strategies so as to reach a state called Nash Equilibrium.

Consider a non-cooperative game with N rational players. Let s_i be a strategy adopted by player i from a compact metric space S_i in order to optimize a cost function c_i , continuous and real valued on $\prod_{j=1}^N S_j$. A Nash Equilibrium is then a N -tuple $(\bar{s}_1, \dots, \bar{s}_N) \in \prod_{j=1}^N S_j$ such that, for any $i = 1, \dots, N$

$$c_i(\bar{s}_1, \dots, \bar{s}_N) \leq c_i(s_i, (\bar{s}_j)_{j \neq i}) \quad \forall s_i \in S_i. \quad (2.13)$$

Nash Equilibrium is a state in which for any player i to deviate from their strategy \bar{s}_i would mean to pay a higher cost. Going back to the example of the prisoner's dilemma, the situation where A and B betray each other is a Nash Equilibrium because if either A or B chooses to change strategy (stay silent) it would result in a worst outcome for them (15 years of prison rather than 10).

This solution concept is limited in the sense that even with rational agents a game may not have a Nash Equilibrium or may have several, but is convenient enough (and general enough) that it is a reasonable way to address most games. In the following we will assume the games considered have at least one Nash Equilibrium.

2.2.4 Differential games

Differential games constitute a "gamification" of the optimization problem presented in section 2.1.2. In N -players differential game, the state of player i (assumed rational) is represented by a vector $\vec{X}_t^i \in \mathbb{R}^n$ and their strategy a_t^i is dynamically adjusted as the game progresses. Assuming some uncertainty in the player's decision, one may represent their behaviour through Langevin dynamics

$$d\vec{X}_t^i = \vec{a}_t^i dt + \sigma_i d\vec{W}_t^i, \quad (2.14)$$

where, as in section 2.1.2, \vec{W}_t^i is a Gaussian white noise, independent of $\vec{W}_t^{i \neq i}$ and of amplitude 1. Each player, through the determination of their strategy, aims to optimize a cost functional c_t^i that depends on the behaviour of every other player

$$c_t^i[\vec{a}^1, \dots, \vec{a}^N](\vec{X}_t^1, \dots, \vec{X}_t^N) = \mathbb{E} \left[\int_t^T \left(\frac{\mu^i}{2} (\vec{a}_\tau^i)^2 - V^i(\vec{X}_\tau^1, \dots, \vec{X}_\tau^N) \right) d\tau + c_T^i(\vec{X}_T^1, \dots, \vec{X}_T^N) \right], \quad (2.15)$$

if we postulate all players have quadratic running cost as mentioned at the end of Section 2.1.2. Because we consider rational players, we

look for a Nash Equilibrium $(\vec{a}^1_*, \dots, \vec{a}^N_*)$ as solution of this optimization problem

$$c^i[\vec{a}^1_*, \dots, \vec{a}^N_*] \leq c^i[\vec{a}^1_*, \dots, \vec{a}^i, \dots, \vec{a}^N_*] \quad \forall i = 1, \dots, N \text{ and } \forall \vec{a}^i. \quad (2.16)$$

In this context, the value function u^i_t may be defined as the optimal cost of player i if every other player follows their optimal strategy

$$u^i_t(\vec{X}_t^1, \dots, \vec{X}_t^N) = \inf_{a^i} \mathbb{E} \left[\int_t^T \left(\frac{\mu^i}{2} (\vec{a}_\tau^i)^2 - V^i(\vec{X}_\tau^1, \dots, \vec{X}_\tau^i, \dots, \vec{X}_\tau^N) \right) d\tau + c^i_T(\vec{X}_T^1, \dots, \vec{X}_T^i, \dots, \vec{X}_T^N) \right], \quad (2.17)$$

and evolves according to HJB equation in the following way [78]

$$\partial_t u^i + \frac{\sigma_i^2}{2} \sum_{j=1}^N \Delta_{x^j} u^i - \sum_{j \neq i} \frac{1}{\mu^j} (\vec{\nabla}_{x^j} u^j) \cdot (\vec{\nabla}_{x^j} u^i) - \frac{1}{2\mu^i} \|\vec{\nabla}_{x^i} u^i\|^2 = V, \quad (2.18)$$

with terminal condition

$$u^i_T(\vec{X}_T^1, \dots, \vec{X}_T^N) = c^i_T(\vec{X}_T^1, \dots, \vec{X}_T^N). \quad (2.19)$$

When the number of players increases, differential games become quickly intractable (as the number of coupled stochastic equations increases accordingly) and the need for a new, more adequate, framework, along with its simplifying assumptions, arises.

2.3 MEAN FIELD APPROACH

Mean Field Games were introduced by P.-L. Lions and J.-M. Lasry [77–79], as well as M. Huang, R. P. Malhamé and P. E. Caines [59], to deal with non-atomic differential games involving a large number of identical players. Inspired by the notion of *mean field* developed in Physics [44], they provide a significant simplification when considering that agents are not sensitive to the individual choices of the others but to an averaged quantity aggregating decisions from all players.

Non-atomic games involve only "small" players, such that any set of players of zero measure has no effect on the game (e.g. customers in an economic system) [9].

2.3.1 Mean Field Games equations

In the last few years, many different approaches to MFG have seen the light of day. In this manuscript I will focus on the deterministic Partial Differential Equation (PDE) formulation originally introduced by P.-L. Lions and J.-M. Lasry, but another particular approach of note is the probabilistic view of R. Carmona and F. Delarue [30] that has been an important focus of the mathematical community recently. I refer the interested reader to the following monographs [31, 32] for a more in-depth review.

To construct MFG equations one should start by implementing the aforementioned assumptions in the framework of differential games described section 2.2.4. We consider several identical players, $\{\forall i = 1 \dots N, \sigma_i = \sigma, \mu^i = \mu, V^i = V, c_T^i = c_T\}$, that only differ by their initial state X_0^i and choice of strategy a_t^i . We also choose the potential V and the terminal cost c_T felt by a given player i to depend on the others' behaviour only through the empirical density

$$\tilde{m}(x, t) = \frac{1}{N} \sum_{j=1}^N \delta(x - X_t^j), \quad (2.20)$$

hence $V(\vec{X}_t^1, \dots, \vec{X}_t^N) \approx V[\tilde{m}](X_t^i)$ and $c_T(\vec{X}_T^1, \dots, \vec{X}_T^N) \approx c_T[\tilde{m}](X_T^i)$. As such, in the limit of a large number of players, if we can safely neglect the fluctuations of \tilde{m} (mean field approximation), we may introduce a *mean field* $m(x, t) = \langle \tilde{m}(x, t) \rangle$, average of the empirical density over all realisations of the noise, and define the value function for a given player as [26]

$$u(x, t) = \inf_{\vec{a}} \mathbb{E} \left[\int_t^T \left(\frac{\mu}{2} (\vec{a}_\tau)^2 - V^i[m](\vec{X}_\tau^i) \right) d\tau + c_T^i[m](\vec{X}_T^i) \right], \quad (2.21)$$

where the average is taken over the realisations of the noise to which this player is subjected. This allows to recast the differential game presented in section 2.2.4 into a one-body optimization problem as described in section 2.1.2 while the agents essentially decouple. The value function then verifies HJB equation

$$\begin{cases} \partial_t u + \frac{\sigma^2}{2} \Delta u - \frac{1}{2\mu} \|\vec{\nabla} u\|^2 = V[m], \\ u(x, T) = c_T[m](x) \end{cases}, \quad (2.22)$$

which is the same equation (2.11) of section 2.2.4 except that the potential V now depends on the mean field m .

Now, as is the case in Physics, the use of a mean field allows for a decoupling of the players' dynamics but one still needs to observe self-consistency. This can be ensured by using the fact that, for a large enough number of players following Langevin dynamics (2.14), the density of players m (which also constitutes the mean field) can be accurately described by Fokker-Planck (FP) equation

$$\partial_t m + \vec{\nabla} \cdot [m \vec{a}_*] - \frac{\sigma^2}{2} \Delta m = 0, \quad (2.23)$$

Fokker-Planck equation is obtained by truncating the Kramers-Moyal expansion of the master equation to second order [95].

where $\vec{a}_* = -\frac{1}{\mu}\vec{\nabla}u$ is the optimal control parameter according to [HJB](#) equation. Considering an initial distribution of players $m_0(x)$ the [MFG](#) problem reduces to a system of coupled (deterministic) [PDEs](#)

$$\begin{cases} \partial_t u + \frac{\sigma^2}{2}\Delta u - \frac{1}{2\mu}|\vec{\nabla}u|^2 = V[m] \\ u(\vec{x}, t = T) = c_T[m](\vec{x}) \\ \partial_t m - \frac{1}{\mu}\vec{\nabla} \cdot [m\vec{\nabla}u] - \frac{\sigma^2}{2}\Delta m = 0 \\ m(\vec{x}, t = 0) = m_0(\vec{x}) \end{cases} \quad (2.24)$$

where the unknowns are not the individual strategies anymore but the mean field $m(x, t)$ and the value function $u(x, t)$. One important feature of this system is its unusual forward-backward structure, given that [HJB](#) equation is constructed from the terminal cost at the end of the game while [FP](#) equation describes the evolution of the distribution of players starting from its configuration at the beginning. These mixed initial-final boundary conditions lead to new challenges when trying to characterize, either analytically or numerically, solutions to [MFG](#) equations as they tend to bring forward dynamics that are atypical for physicists.

2.3.2 Long optimization time and ergodic state

For a long enough game, one can imagine that there exists a time, far from both the beginning and the end of the game, at which the solutions of the [MFG](#) equations (2.24) completely decorrelate from the initial and final conditions. It is easy to think of a game where, at one point, players do not (need to) remember their initial state and do (or should) not yet care about the endgame but can still devise an optimal, sometimes stationary, strategy. In this vein P. Cardaliaguet et al. [28] showed that in the limit $T \rightarrow \infty$, if the potential $V[m](x)$ has no explicit time dependence (as we have and will always consider in this manuscript) and if the system is in some way confined (either through V or because of a geometry with fixed spatial extension), there exists an *ergodic state* such that

$$\begin{cases} m(\vec{x}, t) \simeq \bar{m}(\vec{x}) \\ u(\vec{x}, t) \simeq \bar{u}(\vec{x}) + \lambda t \end{cases} \quad (\text{for } 0 \ll t \ll T) \quad , \quad (2.25)$$

with λ a constant that can be determined through the normalisation of m . This result is of paramount importance to get a general overview of how a game will play, even if one is not able to properly solve the

The existence of an ergodic state actually requires a few other conditions to be met. I leave those aside as they will not be the subject of discussion in this manuscript.

system of forward-backward equations (2.24), as it further simplifies the problem by getting rid of the time dependence

$$\begin{cases} \lambda + \frac{\sigma^2}{2} \Delta \bar{u} - \frac{1}{2\mu} \|\bar{\nabla} \bar{u}\|^2 = V[m] \\ \frac{1}{\mu} \bar{\nabla} \cdot [\bar{m} \bar{\nabla} \bar{u}] + \frac{\sigma^2}{2} \Delta \bar{m} = 0 \end{cases} \quad (2.26)$$

An example of ergodic state can be observed on Figure (2) where, for a large portion of the game, the distribution of players is stationary. This notion will be a relevant subject of discussion in chapter 3 and see extensive use in chapter 4.

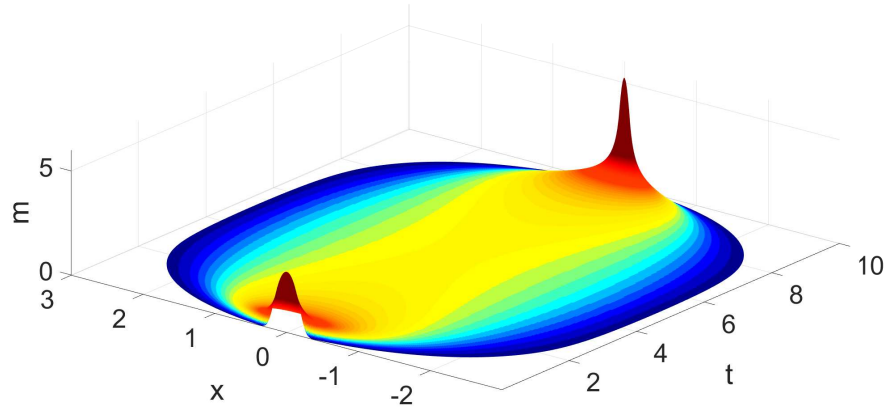


Figure 2: Evolution of the density of players with time. Initially the density is localized around $x = 0$ and then spreads up to the point when the system reaches the ergodic state where it remains for most of the game. Towards the end, players gather once again not to pay too high of a terminal cost. For this simulation we chose a potential featuring repulsive interactions between players and a (confining) environmental gain $V[m] = -2m - 0.1x^2$, with $T = 10$, $\mu = 1$ and $\sigma = 0.4$. The terminal cost $c_T = 10x^2$ is also confining to ensure players effectively gather at the end. All numerical solutions of system (2.24) are obtained using a C++ algorithm described in appendix A.

2.4 CHANGES OF VARIABLES

While the system of MFG equations (2.24) represents a powerful simplification over the differential games presented section 2.2.4 when the number of player is large, solving it still constitutes a challenge. Even if the forward-backward nature of those equations constitute the main difficulty of MFG, the coupling of FP equation with HJB equation is not something physicists are particularly used to dealing with and brings its own set of complications. In the particular case of quadratic

MFG, however, there exists ways to recast the problem into something more familiar to physicists [19, 53, 109]. I shall now discuss these alternative forms of the MFG equations (2.24).

2.4.1 Non-linear Schrödinger formalism

This change of variable was initially introduced by O. Guéant as a way to build a monotonous discretization scheme [53], and then discussed at length, by D. Ullmo, I. Swiecicki and T. Gobron [109], as a gateway into MFG for physicists.

Proceeding as in [109], one can make use of the classic *Cole-Hopf transform* on HJB equation to obtain a standard heat equation [58]

$$\begin{cases} \mu\sigma^2\partial_t\Phi = -\frac{\mu\sigma^4}{2}\Delta\Phi - V[m]\Phi \\ u = -\mu\sigma^2 \log \Phi \end{cases}, \quad (2.27)$$

where this equation is constructed backward in time, similarly to HJB equation, with terminal condition $\Phi(x, t = T) = \exp[-c_T(x)/\mu\sigma^2]$. One can then perform an "hermitization" of equations (2.24)

$$\begin{cases} \mu\sigma^2\partial_t\Gamma = \frac{\mu\sigma^4}{2}\Delta\Gamma + V[m]\Gamma \\ m = \Phi\Gamma \end{cases}, \quad (2.28)$$

this one being forward in time with initial condition $\Gamma(x, t = 0) = m_0(x)/\Phi(x, 0)$. Through these transformations the system of MFG equations (2.24) exhibits a mapping onto the Non-linear Schrödinger (NLS) equation

$$\begin{cases} i\hbar\partial_t\Psi = -\frac{\hbar^2}{2\mu}\Delta\Psi - V[\rho]\Psi \\ i\hbar\partial_t\Psi^* = \frac{\hbar^2}{2\mu}\Delta\Psi^* + V[\rho]\Psi^* \end{cases}, \quad (2.29)$$

under the formal correspondence $\mu\sigma^2 \rightarrow \hbar$, $\Phi(x, t) \rightarrow \Psi(x, it)$, $\Gamma(x, t) \rightarrow [\Psi(x, it)]^*$ and $\rho \equiv \|\Psi\|^2 \rightarrow m \equiv \Phi\Gamma$. The system of equations constituted by (2.27) and (2.28) differ from NLS equation in a few ways. Obviously it retains the forward-backward structure characteristic of MFGs, and, because of how they are constructed, the functional space of which its solutions Φ and Γ are elements is also different than the one we, as physicists, are used to. Because of how they are constructed, Φ and Γ are actually defined as non-periodic, positive functions, while Ψ would be complex valued. Those differences are significant, and their extent will be discussed in chapters 3 and 4, but they are not important enough to undermine the value of this mapping. NLS equation has been studied for decades in the various fields of non-linear optics [66], Bose-Einstein condensation [93] or fluid dynamics [68]. Several methods have been developed along the years to

In this case, as will be for the rest of this thesis, A^ refers to the complex conjugate of A .*

deal with this equation and most can be adapted to [MFG](#) models as was already highlighted in [\[109\]](#).

2.4.2 Hydrodynamic representation

Starting from the [NLS](#) representation of [MFG](#) equations it is possible, through a Madelung-like substitution as described in [\[92\]](#), to make use of the "hermitized" nature of the previous transformations and make yet another change of variables

$$\begin{cases} \Phi(t, x) = \sqrt{m(t, x)} e^{K(t, x)} \\ \Gamma(t, x) = \sqrt{m(t, x)} e^{-K(t, x)} \end{cases}, \quad (2.30)$$

reformulating the problem into a more transparent one. If we define a velocity \vec{v} as

$$\vec{v} = \sigma^2 \vec{\nabla} K = \sigma^2 \frac{\Gamma \vec{\nabla} \Phi - \Phi \vec{\nabla} \Gamma}{2m} = -\frac{\vec{\nabla} u}{\mu} - \sigma^2 \frac{\vec{\nabla} m}{2m}, \quad (2.31)$$

it is easy, from equations [\(2.27\)](#) and [\(2.28\)](#), to obtain a continuity equation along with its associated Euler equation

$$\begin{cases} \partial_t m + \vec{\nabla} \cdot (m \vec{v}) = 0 \\ \partial_t \vec{v} + \vec{\nabla} \left[\frac{\sigma^4}{2\sqrt{m}} \Delta \sqrt{m} + \frac{||\vec{v}||^2}{2} + \frac{V[m]}{\mu} \right] = 0 \end{cases}, \quad (2.32)$$

reminiscent of hydrodynamics. This system closely resembles the original [MFG](#) equations [\(2.24\)](#) but can prove to be more convenient when performing some approximations (small noise limit) or applying some specific methods of resolution.

2.4.3 Action, and conserved quantities

One of the more immediate benefits of those alternative representations is that they enable, in a fairly direct fashion, the introduction of various methods and notions originally developed to study and characterise problems of physics. Most notably, it brings forward the concepts of *action* and *energy* to the context of [MFG](#).

The system of equations [\(2.27\)](#)-[\(2.28\)](#) can be seen as deriving from an action S defined as

$$S[\Gamma, \Phi] \equiv \int_0^T dt \int_{\mathbb{R}} dx \left[\frac{\mu \sigma^2}{2} (\Gamma \partial_t \Phi - \Phi \partial_t \Gamma) - \frac{\mu \sigma^4}{2} \nabla \Gamma \cdot \nabla \Phi + U[m] \right], \quad (2.33)$$

where $U[m]$ represents the functional anti-derivative of $V[m]$, so that its minimisation yields the Schrödinger representation of MFG equations

$$\begin{cases} \frac{\delta S}{\delta \Phi} = 0 \\ \frac{\delta S}{\delta \Gamma} = 0 \end{cases} \Leftrightarrow \begin{cases} \mu\sigma^2\partial_t\Phi = -\frac{\mu\sigma^4}{2}\Delta\Phi - V[m]\Phi \\ \mu\sigma^2\partial_t\Gamma = \frac{\mu\sigma^4}{2}\Delta\Gamma + V[m]\Gamma \end{cases}. \quad (2.34)$$

The existence of an action underlying the dynamics has two major consequences. First, as will be argued in chapter 4, such an action can serve as the basis of a variational approach. Second, because MFG equations (2.24) are time translation invariant, this implies by way of Noether theorem that there exists a corresponding conserved quantity that, by analogy with physical systems, we shall call *energy*.

Depending on the specifics of the considered problem, either the Schrödinger or hydrodynamic representation may prove to be more convenient. As such, I provide the reader with two alternative expressions for the energy of the game

$$\begin{aligned} E &= \int_{\mathbb{R}} dx \left[-\frac{\mu\sigma^4}{2} \nabla\Gamma \cdot \nabla\Phi + U[m] \right] \\ &= \int_{\mathbb{R}} dx \left[\frac{\mu\sigma^2}{2} \left(m \left(\frac{v}{\sigma} \right)^2 - \sigma^2 \frac{(\nabla m)^2}{4m} \right) + U[m] \right]. \end{aligned} \quad (2.35)$$

Continuing on with the analogy with physical systems, the first, σ dependent, term of each integrand can be interpreted as a *kinetic energy*, while the U term would correspond to *potential energy*. Naturally, the way those quantities have to be (concretely) understood, with respect to either social or engineering sciences, differs from the traditional physical interpretation. Those should, above all, be considered abstract quantities: while they can prove useful to formally characterise a problem, as will be shown in chapters 3 and 4, their factual signification (if there is one) depends on the context.

With this I conclude my brief introduction on MFG theory. This chapter should provide the reader with everything they need to know about both optimization and Game Theory as far as this manuscript is concerned. A MFG paradigm of population dynamics along with its constitutive equations have been addressed as well as some interesting changes of variables that will become useful in further developments. The upcoming chapters will deal more closely with my work during my PhD, focusing specifically on one dimensional quadratic games with potential

$$V[m](x) = gm + U_0(x), \quad (2.36)$$

where g is a constant and U_0 an external gain. Potential of this type probably constitute the simplest non-trivial example of explicit (local) interactions between players and, as such, is interesting from the

point of view of developing an intuition of the qualitative behaviours one can expect from [MFG](#) theory.

Part II

KEY FINDINGS

This part showcases the main results of my work as a PhD student. Relying heavily on the Schrödinger representation of Mean Field Games I was able to accommodate methods originating from Physics to study models of Mean Field Games.

INTEGRABILITY OF QUADRATIC MEAN FIELD GAMES

Most of my PhD was dedicated to the (ongoing) study of a class of so-called *integrable quadratic Mean Field Games* that can be solved entirely analytically. The main motivation behind this is to make use of the deep connection between NLS equation (integrable under some conditions) and quadratic MFG in order to develop a formal approach to the forward-backward system of equations (2.24). These integrable games are too specific to be considered toy-models, but, as I shall argue in chapter 4, can be seen as limiting regimes of more general problems. Very few realistic situations can accurately be described by this type of games, but it may serve as a good starting point for more involved discussions.

By *integrable quadratic Mean Field Games* I specifically refer to games described by the system of MFG equations (2.24) in 1+1 dimensions, with potential (2.36) where the external gain is considered zero everywhere

$$\begin{cases} \partial_t u + \frac{\sigma^2}{2} \partial_{xx} u - \frac{1}{2\mu} (\partial_x u)^2 = gm \\ u(x, t = T) = c_T[m](x) \\ \partial_t m - \frac{1}{\mu} \partial_x [m \partial_x u] - \frac{\sigma^2}{2} \partial_{xx} m = 0 \\ m(x, t = 0) = m_0(x) \end{cases}, \quad (3.1)$$

along with its alternative representations. This can be seen as a particular, admittedly very simple, case of the population dynamics model introduced by O. Guéant in 2010 [55], in which players have no preferences whatsoever for a given state x , but only care about the amount of other players in their close vicinity. The sign of the constant g monitors the type of interactions we are interested in. A positive g would correspond to attractive interactions (herding effect, peer pressure, etc.) while negative g would describe repulsive interactions (collective exploration, anti-conformism, etc.). Because the instance of attractive interactions has been the subject of extensive discussions from my predecessor [105, 106, 109] (albeit not through the lens of integrability) I will focus mostly on negative g .

Those games are (completely) integrable in the Liouville sense [81]. By that I mean they can be seen as Hamiltonian systems, albeit of infinite dimensionality, for which one can construct an infinite number of Poisson commuting invariants. Those conserved quantities are said to be in *involution* and are known as *first integrals of motion*. Another,

In this case, x can obviously represent the agents' physical position but may also refer to beliefs, political views etc...

Note that the invariants are not referred to as "constants of motion" to signify that they are not explicitly defined as functions of time. For example, looking at an object of position x moving at constant velocity v , the quantity $x - vt$ is a constant of motion but not an integral of motion.
[16]

more geometrical, way of saying this is that there exists a regular foliation of the phase space by invariant manifolds, such that the Hamiltonian vector fields associated to the invariants of the foliation span the tangent distribution. According to Liouville-Arnold theorem [7], for such systems there exists a canonical transformation (as in preserving Hamilton's equations) to *action-angle variables*. In this system of coordinates, the Hamiltonian only depends upon the action variables (which are equivalent to the first integrals of motion), while the dynamics of angle variables is simply linear. If this canonical transform is explicitly known, one can then solve the system in quadrature, which is what I meant earlier when saying that those games can be "solved entirely analytically".

In this chapter (and in particular in section 3.2), I will argue the existence of those first integrals of motion, the most obvious example of which is the energy (or Hamiltonian) E , as defined by equation (2.35). Two other relevant conserved quantities with a clear physical meaning are the (normalized) number of players

$$N = \int_{\mathbb{R}} m dx = 1 , \quad (3.2)$$

and the momentum

$$P = \int_{\mathbb{R}} (m \partial_x u - u \partial_x m) dx , \quad (3.3)$$

which is also the generator for space translation

$$m(x, t) \rightarrow m(x + x', t) \quad u(x, t) \rightarrow u(x + x', t) , \quad (3.4)$$

under which the system of MFG equations (3.1) is invariant. The other conserved quantities exhibit more complicated expressions and their signification is usually more abstract, this is why I will mostly discuss the first three: N , P and E . I will then try and propose methods to exploit these conserved quantities, either by constructing variational ansätze or by introducing a canonical linearising transform to action-angle variables.

I will start by examining a yet again simplified version of this MFG paradigm where interactions dominate and the effects of noise can be neglected. This allows me to relate the game (3.1) to problems typically found in physics and introduce the notion of integrability in a fairly transparent way. I will then consider the complete problem using quintessential methods of classical integrable systems (namely zero curvature representation and Hamiltonian formalism) and argue the main difficulties (as well as my shortcomings) when trying to adapt these to MFG.

3.1 INTEGRABLE MEAN FIELD GAMES IN THE WEAK NOISE LIMIT

While this section mostly aims to introduce integrability in the realm of MFG theory, it will also provide a good example of what the alter-

native representations described in section 2.4 can bring to the table. Moreover, it should be noted that most of the upcoming discussions can serve as supplementary material to our 2019 letter [19].

3.1.1 Definition and relevance of the weak noise limit

In order to get to why we might be interested in the weak noise limit specifically, we need to take a closer look at the hydrodynamic representation (2.32) which, under the assumptions mentioned earlier that the game is *integrable quadratic*, reads

$$\begin{cases} \partial_t m + \partial_x(mv) = 0 \\ \partial_t v + \partial_x \left[\frac{\sigma^4}{2\sqrt{m}} \partial_{xx} \sqrt{m} + \frac{v^2}{2} + \frac{g}{\mu} m \right] = 0 \end{cases} \quad (3.5)$$

Because the first equation is a simple continuity equation, the meat of the dynamics is contained in the second. Along with the obviously necessary time derivative, the v^2 term is actually mandatory as it is a signature of the quadratic nature of the game we consider (and that is why it does not depend on any parameters). As such, of the 4 terms in the Euler equation we can only fiddle with two: the diffusion term on the one hand and the interaction term on the other. It is precisely the competition of those two effects that dictate the behaviour of the solution.

As was briefly mentioned in section 2.4, this hydrodynamic representation of NLS equation was initially introduced by physicists interested in the expansion of Bose-Einstein condensates [92]. In this context, and to make the investigation of this problem simpler, they were able to make out two limiting regimes by introducing the notion of *healing length* [41]. The healing length, the MFG counterpart of which is $\nu = |\mu\sigma^2/g|$, is the typical length scale on which the interaction energy balances quantum pressure (or diffusion in our case). It is named this way because it is the minimum distance over which the wave function can tend to its bulk value (i.e. "heal") when subjected to a local perturbation. As a corollary, this means that for condensates wider than their healing length, the quantum pressure term can be neglected in the Euler equation, while we may neglect the interactions if the condensate is smaller. This naturally also applies to MFG, and because we are interested in repulsive interactions ($g < 0$) it is fair to assume that, at one point, the player distribution will have expanded enough past ν that the diffusion term can be neglected. Hence the interest for the small noise limit. Because of this I will now, and for the rest of section 3.1, only focus on a simplified version of Eqs (3.5)

Noticeably a similar procedure can be found in study of non-linear waves to decide whether dispersion can be neglected or not [45, 56, 74].

$$\begin{cases} \partial_t m + \partial_x(mv) = 0 \\ \partial_t v + \partial_x \left[\frac{v^2}{2} + \frac{g}{\mu} m \right] = 0 \end{cases} \quad (3.6)$$

3.1.2 Preliminary simulations

In order for the game to be integrable we need the external gain U_0 to be zero everywhere. If we allow the players to spread indefinitely (infinite box) the system is in no way confined and the notion of ergodic state should not apply. Then we may ask ourselves whether there maybe exists a limiting regime that can play a similar role as the ergodic state, even in this particular non confined configuration. This question is of crucial importance as a negative answer would imply that approximation schemes which are completely independent of the initial and final conditions cannot be constructed. To try and answer this question, as well as get a better feeling of the situation, we first turned to numerical simulations. Details concerning the numerical schemes used to produce those can be found in appendix A.

As illustrated on Figure (3), what simulations seem to indicate is that, no matter the initial or final condition, for long enough optimization time and far from both $t = 0$ and $t = T$, the player distribution will end up adopting an almost perfect inverted parabola shape

$$m(t, x) = \begin{cases} \frac{3}{4} \frac{(z(t)^2 - x^2)}{z(t)^3} & \text{if } x \leq z(t) \\ 0 & \text{otherwise} \end{cases}, \quad (3.7)$$

where the prefactor derives from the normalization, and the time dependent scaling factor $z(t)$ grows in time as a power law,

$$z(t) \sim t^{2/3}. \quad (3.8)$$

All of this is made more apparent on Figure (4) where we compared the numerical solution to the scaling form (3.7). The tails of varying length displayed by the rescaled distribution of players on the rightmost figure constitute the last remnants of diffusion ($\sigma = 0.5$ in this simulation) and happen on a distance, when not rescaled, of order the healing length ν .

This scaling solution, while not stationary, can be seen as an extension of the notion of ergodic state. When considering that the forward-backward structure of MFG equations is one of the main challenges posed by the discipline, the fact that there exists a time in the dynamics when the initial and final conditions completely decorrelate (as is the case for the ergodic state) is conceptually, as well as practically (i.e. when trying to describe the solution), extremely important. In a sense this scaling can be considered somewhat universal, even though it is model dependent, because of how important the impact of both the initial and final conditions can be for the overall game. The rest of this section will be mostly dedicated to the characterization of this scaling: where does it come from? what does it mean? what are the conditions for it to be observed?

This should not come to much as a surprise since parabolic solutions have also been observed in other fields where NLS plays an important role, such as non-linear optics [107] or Bose-Einstein condensates [23]. More on that in chapter 4.

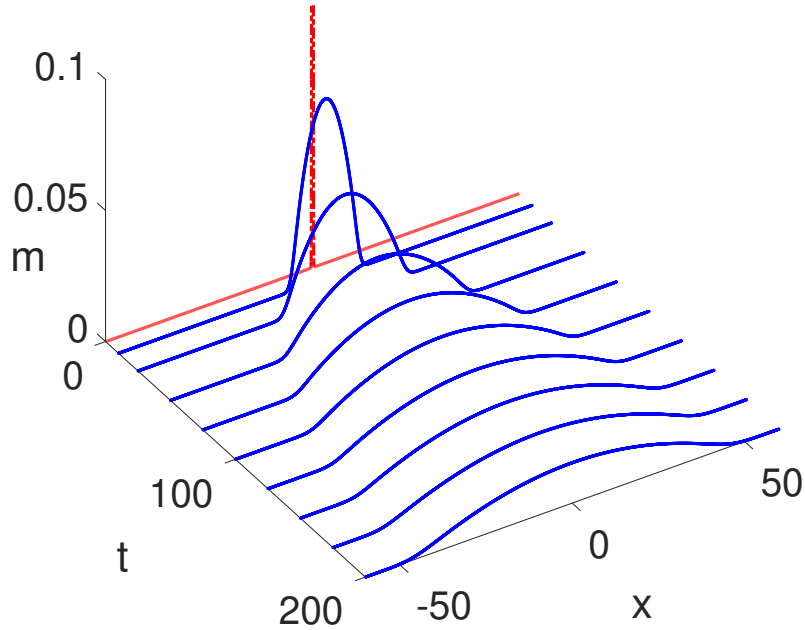


Figure 3: Time evolution of the density of agents. In this case $T = 200$, $g = -2$, $\sigma = 0.5$ and $\mu = 1$. The initial distribution is a Gaussian of variance 0.1, and the terminal cost is flat $c_T(x) = 0$ (for better legibility).

3.1.3 Hodograph transform

In this section we will make use of the hydrodynamic representation of MFG equations (3.6) to design a more transparent and convenient framework through which we can study the scaling solution presented earlier. Because of how similar our problem is to the hydrodynamic representation of NLS equation, this development, at least at first, will closely follow the method presented by A. Kamchatnov in his book [64] and rely heavily on the notions of *Riemann invariants* and *hodograph transform*.

Riemann's method can be considered an extension of the *method of characteristics* presented in appendix B. It amounts to finding curves (characteristics) on which some quantities (Riemann invariants) are conserved. A more detailed discussion of this method, as well as the results it yields, is provided in Appendix C. Essentially we can show

The fact that Φ and Γ are defined as non periodic functions means we cannot use the traditional normal mode decomposition method [92].

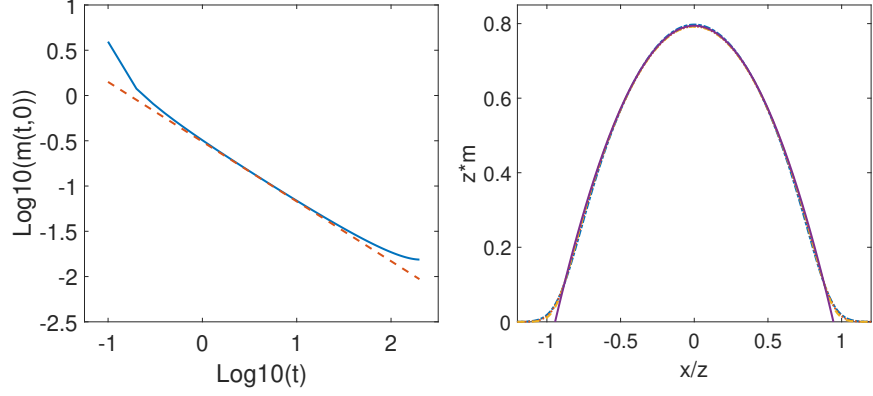


Figure 4: On the left is plotted the evolution of $m(t,0) = 3/4z(t)$ with time (full line) compared to the $t^{2/3}$ scaling behaviour (dashed). On the right are plotted an inverted parabola, and the density $m(x,t)$ rescaled by $z(t)$ for three different times.

that there exists a pair (λ_+, λ_-) of Riemann invariants with the following associated dynamics

$$\begin{cases} \lambda_{\pm} = v \pm 2i\sqrt{\frac{|g|m}{\mu}} \\ \partial_t \lambda_+ + \left(\frac{3}{4}\lambda_+ + \frac{1}{4}\lambda_-\right) \partial_x \lambda_+ = 0 \\ \partial_t \lambda_- + \left(\frac{1}{4}\lambda_+ + \frac{3}{4}\lambda_-\right) \partial_x \lambda_- = 0 \end{cases} \quad (3.9)$$

reducing the hydrodynamic system (3.6) to a simpler one (3.9) that can be linearised through an hodograph transform: by interchanging variables and coordinates. In the region where both λ_+ and λ_- are not constant (when one does not follow a characteristic curve), one may treat them as coordinates in lieu of x and t , which can be, in turn, considered as functions of (λ_+, λ_-) . As will be shown below, this allows to reformulate the problem (3.9) in a more convenient way. To do so, one first needs to express the derivatives with respect to x and t as ones with respect to λ_{\pm}

$$\frac{\partial(x,t)}{\partial(\lambda_+, \lambda_-)} = \left[\frac{\partial(\lambda_+, \lambda_-)}{\partial(x,t)} \right]^{-1} = \frac{1}{J} \begin{pmatrix} \partial_t \lambda_- & -\partial_x \lambda_- \\ -\partial_t \lambda_+ & \partial_x \lambda_+ \end{pmatrix} \quad (3.10)$$

where $J = (\partial_{\lambda_+} x \partial_{\lambda_-} t - \partial_{\lambda_-} x \partial_{\lambda_+} t)$ is the Jacobian of the change of coordinates. The system (3.9) then becomes linear

$$\begin{cases} \partial_{\lambda_-} x - \left(\frac{3}{4}\lambda_+ + \frac{1}{4}\lambda_-\right) \partial_{\lambda_-} t = 0 \\ \partial_{\lambda_+} x - \left(\frac{1}{4}\lambda_+ + \frac{3}{4}\lambda_-\right) \partial_{\lambda_+} t = 0 \end{cases} \quad (3.11)$$

and can readily be integrated once as

$$\begin{cases} x - \beta_+ t = \omega_+ \\ x - \beta_- t = \omega_- \end{cases}, \quad (3.12)$$

where $\beta_{\pm} = \left(\frac{3}{4}\lambda_{\pm} + \frac{1}{4}\lambda_{\mp}\right)$ and ω_{\pm} is solution of

$$\partial_{\lambda_{\pm}} \omega_{\mp} = -(\partial_{\lambda_{\pm}} \beta_{\mp})t = -\frac{1}{4}t, \quad (3.13)$$

so that the functions ω_{\pm} may be presented as derivatives of a potential $\omega_{\pm} = \partial_{\lambda_{\pm}} \chi$. In order to express t in terms of ω_{\pm} (or χ) one can subtract the second equation in system (3.12) to the first and get

$$(\beta_- - \beta_+)t = \omega_+ - \omega_-, \quad (3.14)$$

which, once we used the fact that $\beta_+ - \beta_- = \frac{\lambda_+ - \lambda_-}{2}$, yields

$$\partial_{\lambda_{\pm}} \omega_{\mp} = \frac{\omega_+ - \omega_-}{2(\lambda_+ - \lambda_-)}. \quad (3.15)$$

Substitution of this expression in equation (3.13) gives the potential equation

$$\partial_{\lambda_+, \lambda_-} \chi - \frac{1}{2(\lambda_+ - \lambda_-)} (\partial_{\lambda_+} \chi - \partial_{\lambda_-} \chi) = 0, \quad (3.16)$$

also known as Euler-Poisson-Darboux equation which is the equation one needs to solve when tackling the traditional defocusing NLS equation. The main difference in the present case is that the arguments of χ , namely the Riemann invariants, are complex, sign of the elliptic nature of the problem. Up to this point all we did was to adapt traditional methods to MFG, but we must now deviate from [64]. Fortunately, the fact that λ_+ and λ_- are complex conjugates allows us to reformulate (3.16) into an other well-known equation and show that χ is indeed real. Let $\lambda_{\pm} = \zeta \pm i\eta$, so that

$$\begin{cases} \zeta = v = -\frac{\nabla u}{\mu} - \frac{\sigma^2 \nabla m}{2m} \\ \eta = 2\sqrt{\frac{|g|m}{\mu}} \end{cases}, \quad (3.17)$$

then Euler-Poisson-Darboux equation (3.16) becomes

$$\partial_{\zeta, \zeta} \chi + \partial_{\eta, \eta} \chi + \frac{1}{\eta} \partial_{\eta} \chi = 0, \quad (3.18)$$

which is, if we consider η as a radial distance and ζ as an axial coordinate, Laplace equation in cylindrical coordinates with no angular dependence. What the hodograph transform does is actually reveal a formal correspondence between quadratic MFG (at least in the weak

noise limit) and electrostatics that we can exploit to interpret the scaling solution of section 3.1.2. Equations (3.12) now read

$$\begin{cases} \eta t = -E_\eta \\ 2(x - \zeta t) = -E_\zeta \end{cases} \quad (3.19)$$

with E_η and E_ζ the radial and axial components of an analogous electric field, $\vec{E} = -\vec{\nabla}\chi$. Note that even if Laplace equation (3.18) is technically a two-dimensional problem, because the connection with electrostatics is made clearer when looking at it from the point of view of a three-dimensional problem with axial symmetry, this is the one we will adopt.

3.1.4 Potential representation

Through the hodograph transform we have shown that for any potential χ , solution of Laplace equation (3.18), there is a solution to the hydrodynamic equations (3.6) provided that the relations (3.19) between x , t and the electric field \vec{E} hold. The linear Laplace equation (and the related electrostatic problem) is clearly significantly simpler than the original non-linear hydrodynamic equations. The price to pay for that simplification is that taking into account the boundary conditions becomes highly non trivial since the locus of the curves $t(\zeta, \eta) = 0$ or $t(\zeta, \eta) = T$ on which these conditions are expressed actually depend on the particular potential $\chi(\zeta, \eta)$ considered. This makes the traditional resolution of Laplace equation by means of Green's theorem [103] ill-suited for our mixed-type boundary conditions (more on that in appendix D), but the geometry of the problem in the hodograph space allows for alternative methods.

In the hodograph space, for any given time $t = \tau = \text{const.}$ there exists an associated surface $S_\tau(\zeta(\tau, x); \eta(\tau, x); \theta)$ parametrized by the original space coordinate x and the angular component θ of the cylindrical coordinates with which χ is defined. Since we assumed η goes relatively fast to zero when x goes to infinity (finite extension of the distribution at any given time), we can say that those surfaces are closed. And because the dynamics we are interested in is associated with the spreading of the density of agents, surfaces $S_t(\zeta, \eta, \theta)$ are contracting as t increases, smaller time surfaces including every larger time ones as can be seen on Figure (5).

If we consider χ as generated by a distribution of charge $\rho(\zeta, \eta)$, Laplace equation (3.18) implies that $\rho(\zeta, \eta) = 0$ between the surfaces $S_{t=0}$ and $S_{t=T}$ but can be non-zero either near the origin (for times larger than T) or at large distance (corresponding to negative times). In a sense, the hodograph transform maps the boundary conditions onto a charge distribution. This mapping, once again, is non trivial and while the precise relation between the charge distribution and the boundary conditions is still unclear at the moment, we will see

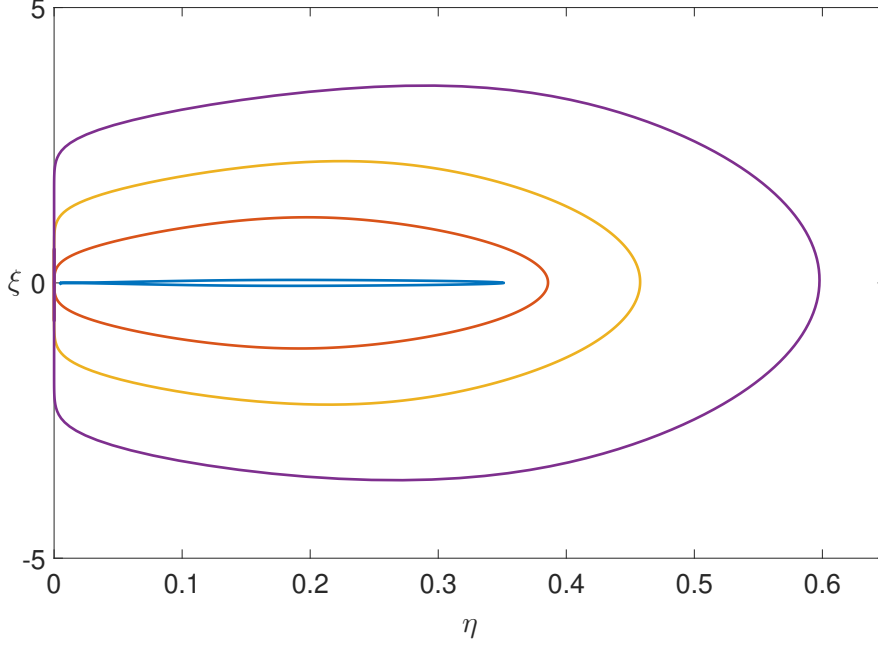


Figure 5: Representation of the contraction of constant-time surfaces S_t in the (η, ξ) plane for the simulation presented in Figure 3. From smallest to largest, $t = 195, 100, 50$ and 20 .

that introducing this notion of "charges" makes the mixed boundary conditions, and by extension the forward-backward structure of MFG equations, considerably more manageable.

Writing $\rho(\xi, \eta)$ as the sum of the charge distribution $\rho_0(\xi, \eta)$ at the origin (representing the final condition) and $\rho_\infty(\xi, \eta)$ at infinity (initial condition), the potential χ takes the form [63]

$$\chi(\eta, \xi) = 2\pi \left(\int \frac{\rho_0(\eta_0, \xi_0)}{|\vec{r} - \vec{r}_0|} \eta_0 d\eta_0 d\xi_0 + \int \frac{\rho_\infty(\eta_\infty, \xi_\infty)}{|\vec{r} - \vec{r}_\infty|} \eta_\infty d\eta_\infty d\xi_\infty \right), \quad (3.20)$$

where $\vec{r} = \eta\vec{e}_\eta + \xi\vec{e}_\xi$ is the point of observation. A feeling of what χ should look like is given Figure (6). This form allows for a multipole expansion assuming that the point of observation is sufficiently far from charges either at the origin or at infinity [63, 80]

$$\chi(\eta, \xi) = \sum_{l=0}^{\infty} \left(\frac{Q_l}{r^{l+1}} + I_l r^l \right) P_l \left(\frac{\xi}{r} \right). \quad (3.21)$$

Here Q_l and I_l are respectively the exterior and interior axial multipole moments and P_l are the Legendre polynomials (spherical harmonics with axial symmetry). This multipole expansion is the most essential tool we will use to characterize the universal scaling solution (3.7).

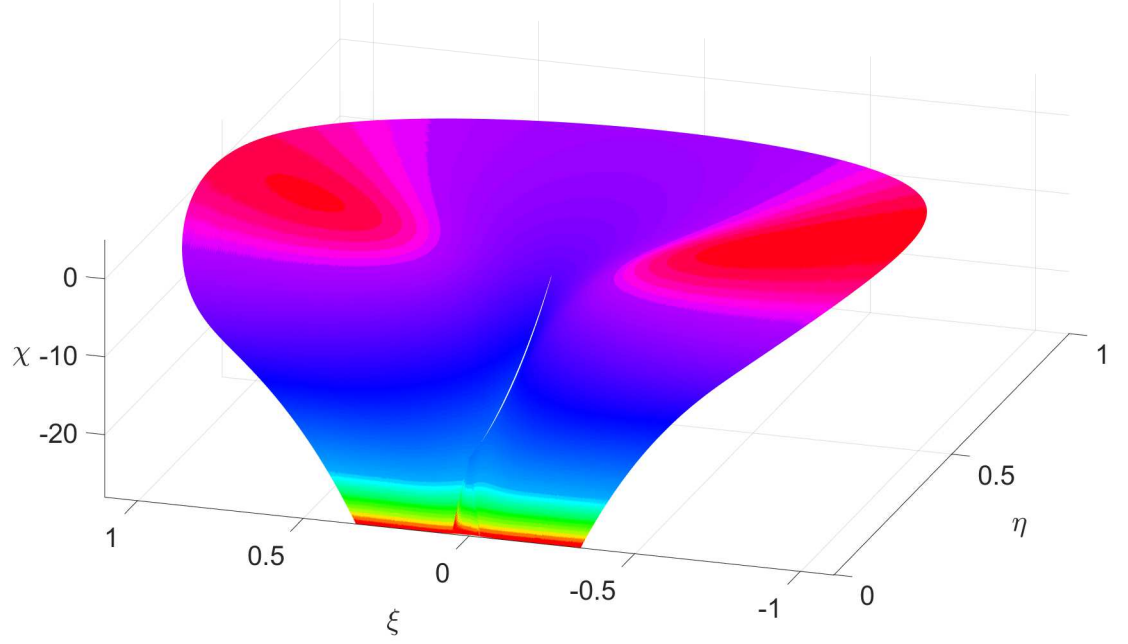


Figure 6: Potential representation in the hodograph space of the simulation illustrated Figure (3). The small slit in the center of the figure represents the terminal condition, that is where charges are located with distribution ρ_0 . As we go further from the origin, the potential seems to flatten indicating the presence of charges at infinity, distributed according to ρ_∞ .

3.1.5 Universal scaling solution in the infinite optimization time limit

If the optimization time is long enough we can assume that there exists a range of times $[\tilde{t}_{\min}, \tilde{t}_{\max}]$, $0 \ll \tilde{t}_{\min}, \tilde{t}_{\max} \ll T$, so that on any surface $S_{t \in [\tilde{t}_{\min}, \tilde{t}_{\max}]}$ we are sufficiently far from the charges at the origin not to be subjected to the details of their distribution and far enough from the charges at infinity so that the effect of each charge is essentially cancelled by its axial symmetric. In that case we should be able to give a satisfactory approximation of χ as the potential created by a point charge Q_0 located at the origin

$$\chi(\eta, \xi) \approx \frac{Q_0}{\sqrt{\eta^2 + \xi^2}}, \quad (3.22)$$

with a relation between Q_0 and the boundary conditions of the problem yet to be determined. The remainder of this section, will then be dedicated to showing that this monopole approximation is perfectly equivalent to the universal parabolic scaling solution (3.7).

Before trying to compute Q_0 , we can start by looking at what equation (3.22) signifies in terms of $m(t, x)$ and $v(t, x)$. Inserting the approximation (3.22) in the compatibility equations (3.19) yields

$$\begin{cases} \partial_\eta \chi = \eta t = -\frac{\eta Q_0}{(\eta^2 + \xi^2)^{3/2}} \\ \partial_\xi \chi = 2(x - \xi t) = -\frac{\xi Q_0}{(\eta^2 + \xi^2)^{3/2}} \end{cases}, \quad (3.23)$$

providing a relation between the original coordinates (x, t) and the hodograph data (ξ, η) . Having recalled the definition of the hodograph coordinates (3.17), this relation can be readily inverted so as to obtain

$$\begin{cases} m(t, x) = \frac{3((\mu Q_0/2g)^{2/3} z(t)^2 - x^2)}{4z(t)^3} \\ v(t, x) = -\frac{z'(t)}{z(t)} x \end{cases}, \quad (3.24)$$

where z takes the form

$$z(t) = 3 \left(\frac{|g|}{4\mu} \right)^{1/3} t^{2/3}. \quad (3.25)$$

This result is very close to the ansatz (3.7), particularly so when considering that the normalization condition imposes that $Q_0 = \frac{2g}{\mu}$. What remains is now to show that the value of Q_0 indeed does not change, no matter the boundary conditions.

Making further use of the electrostatics analogy, since we are not interested in the details of how charges are distributed around the origin (or at infinity for that matter) but only in the total charge, we should be able to compute Q_0 using Gauss's law. As such computing the flow of the field \vec{E} through a surface $S_{\tilde{t}}$ of normal \vec{n} , that includes all charges distributed around the origin, should yield the monopole

Gauss's law is also known as the mean value theorem in potential theory of elliptic PDEs [39].

$$\int_{S_{\tilde{t}}} (\vec{E} \cdot \vec{n}) dS = -4\pi Q_0. \quad (3.26)$$

Because we are working with a particular set of coordinates we need to specify the expressions of dS and \vec{n} . As discussed earlier, at fixed time $t = \tilde{t}$ the surface $S_{\tilde{t}} = (\eta(\tilde{t}, x); \xi(\tilde{t}, x); \theta)$ is parametrized by x and θ . If $\gamma = (\eta(\tilde{t}, x); \xi(\tilde{t}, x))$ is a curve on $S_{\tilde{t}}$ then its surface element dS can be computed as

$$dS = \eta d\theta d\gamma = \eta \sqrt{(\partial_x \xi)^2 + (\partial_x \eta)^2} d\theta dx. \quad (3.27)$$

In the same way we may define the normal \vec{n} to the surface $S_{\tilde{t}}$ as

$$\vec{n} = \frac{1}{\sqrt{(\partial_x \xi)^2 + (\partial_x \eta)^2}} \begin{pmatrix} \partial_x \xi \\ -\partial_x \eta \\ 0 \end{pmatrix}. \quad (3.28)$$

Inserting the two previous results in equation (3.26) finally gives

$$\begin{aligned} Q_0 &= \frac{1}{4\pi} \int_0^{2\pi} \int_{\mathbb{R}} \eta [2(x - \xi\tilde{t})\partial_x\eta - \eta\tilde{t}\partial_x\xi] d\theta dx \\ &= \frac{1}{2} \int_{\mathbb{R}} [-\tilde{t}\partial_x(\eta^2\xi) + 2x\eta\partial_x\eta] dx \end{aligned} \quad (3.29)$$

If we assume η to decrease sufficiently fast with x , the first, time dependent, term integrates to zero. This was to be expected because no matter the time \tilde{t} , as long as $0 < \tilde{t} < T$, the total charge included in $S_{\tilde{t}}$ is the same: Q_0 is by construction a constant. Integrating by part and recalling that $\eta = 2\sqrt{\frac{|g|m}{\mu}}$, equation (3.29) indeed yields

$$Q_0 = \frac{2g}{\mu} \int_{\mathbb{R}} m dx = \frac{2g}{\mu}, \quad (3.30)$$

making use of the normalization condition. This proves the inverted scaling parabola observed numerically is not an artefact of the simulations but something deeper, universal as previously assumed. The hodograph transform provides a very natural interpretation of this scaling solution as the approximation by a simple monopole of a charge distribution creating an electrostatic potential. The condition that the observation point is sufficiently far from both the charges near the origin and the ones near infinity, underlying this approximation, is equivalent to considering times far from both $t = 0$ and $t = T$, which is, of course, only possible in the long optimization time limit $T \rightarrow \infty$. The electrostatic picture even allows for a precise quantification of the conditions of validity of the monopole approximation, making for a complete characterization of this regime. As such we are, in a way, able to extend the notion of ergodic state to a situation where a genuine ergodic state cannot exist.

Of course all of this is only the tip of the iceberg as the scaling parabolic solution is solely due to the contribution of the first non trivial multipole moment (I_0 amounting to an irrelevant additive constant). The next sections will touch on my ongoing work about higher order moments. It will hint at their nature and provide the reader with some leads as how they should be dealt with.

3.1.6 Finite optimization time: impact of higher order multipole moments on the hydrodynamic coordinates

In the case of finite optimization time one cannot only rely on the universal scaling solution (3.7) and needs to account for higher order multipole moments. Naturally the smaller the optimization time (or the closer to either the beginning or the end of the game) the more moments are needed to give an accurate description of the solution.

As is the case in electrostatics, an estimation of which moments should be considered can be easily performed based on the expansion itself (3.21). Particularly if the value of the different moments

are known. But one should note that by construction, as coefficients of the expansion of the potential equation (3.20), interior moments I_l are of order r_∞^{-l} and exterior moments Q_l of order r_0^{l+1} . As such, even not knowing the exact value of moments I_l or Q_l it should be fair to assume that for r big enough in front of r_0 and small enough in front of r_∞ (i.e. for times t , $0 \ll t \ll T$) only lower orders of the multipole expansion matter. Given that, let us compute the impact of the first few moments on the hydrodynamic coordinates, and let us start with I_1 as its contribution is of similar order as Q_0 's. Going back to the compatibility equations (3.19), we may write

$$\begin{cases} \eta t = -\frac{\eta Q_0}{(\eta^2 + \xi^2)^{3/2}} \\ 2(x - \xi t) = -\frac{\xi Q_0}{(\eta^2 + \xi^2)^{3/2}} + I_1 \end{cases}, \quad (3.31)$$

which, recalling $Q_0 = \frac{2g}{\mu}$, can be easily inverted so that

$$\begin{cases} m(t, x) = \frac{3 \left[z(t)^2 - \left(x - \frac{I_1}{2} \right)^2 \right]}{4z(t)^3} \\ v(t, x) = -\frac{z'(t)}{z(t)} \left(x - \frac{I_1}{2} \right) \end{cases}. \quad (3.32)$$

I_1 represents the position of the maximum of the distribution, based on this fact alone it makes perfect sense that its contribution and Q_0 's are of similar importance. Now, let us assume that we are interested in the behaviour of the system at time τ , $0 \ll \tau < T/2$ such that, besides Q_0 and I_1 , only I_2 matters. The compatibility equations (3.19) become

$$\begin{cases} \eta t = -\frac{\eta Q_0}{(\eta^2 + \xi^2)^{3/2}} - \eta I_2 \\ 2(x - \xi t) = -\frac{\xi Q_0}{(\eta^2 + \xi^2)^{3/2}} + I_1 + 2\xi I_2 \end{cases}, \quad (3.33)$$

which can once again be easily inverted to show that I_2 serves as the origin of time (or initial extension of the distribution)

$$\begin{cases} m(t, x) = \frac{3 \left[z(t + I_2)^2 - \left(x - \frac{I_1}{2} \right)^2 \right]}{4z(t + I_2)^3} \\ v(t, x) = -\frac{z'(t + I_2)}{z(t + I_2)} \left(x - \frac{I_1}{2} \right) \end{cases}. \quad (3.34)$$

While these contributions are easily computed, inverting the hodograph transform quickly calls for highly involved calculations. For example, simply adding Q_1 to the equation requires finding the roots of a polynomial of degree 8. Because of this, aiming for anything

but an implicit solution of the problem (3.6) is unrealistic when using purely analytical methods. However the inversion can be made numerically fairly easily [61, 62].

Even if numerics remain involved in this description of the MFG solution, this constitutes a huge improvement over a fully numerical resolution. Numerically implementing the inverse hodograph transform is clearly simpler than the algorithm described in appendix A, and the fact that there is no need for a self-consistency loop means that the program will likely run quicker. Another important aspect of this method is that it allows for a better monitoring of the solution, through the contribution (or lack thereof) of a given multipole moment with physical significance, than a "brute force" numerical resolution, leading to a better understanding of the mechanisms at work.

3.1.7 Physical meaning of the multipole moments

While the physical meaning of a given multipole moment can sometimes be deduced directly from its impact on the hydrodynamic coordinates (like I_1 and I_2), things are usually not that straightforward and one needs to compute the moment itself to obtain more information. For example, it is not clear *a priori* from the compatibility equations (3.19) that Q_0 can be related to the normalization of the player distribution. In this section I will try to provide a method to compute multipole moments and give a sense of what they represent.

To compute the multipole moments we need to go back to their definition as coefficients of the expansion (3.21) of the potential equation (3.20). The equivalence of those equation implies that at any order l

$$\begin{cases} Q_l = 2\pi \int r^l P_l\left(\frac{\tilde{\xi}}{r}\right) \rho_0(\tilde{\xi}, \eta) \eta d\eta d\tilde{\xi} \\ I_l = 2\pi \int r^{-(l+1)} P_l\left(\frac{\tilde{\xi}}{r}\right) \rho_\infty(\eta, \tilde{\xi}) \eta d\eta d\tilde{\xi} \end{cases}, \quad (3.35)$$

corroborating my claim that I_l is of order r_∞^{-l} and Q_l of order r_0^{l+1} . This may not seem particularly helpful at first glance because if we know that the charge distribution ρ is related to the boundary conditions of the game, we do not actually know how they are related. Nonetheless, we will show that we can compute the multipole moments in terms of η and $\tilde{\xi}$ exclusively, using their definition (3.35) and the compatibility equations (3.19).

By considering that the potential χ can be seen as generated by charges distributed either at the origin of the hodograph space or at infinity, we allow ourselves to look both at negative times and times greater than T . This can be represented by rewriting the Laplace equation (3.18) as a Poisson equation

$$\Delta\chi = 4\pi\rho, \quad (3.36)$$

which is equivalent to the integral representation (3.20). As mentioned in section 3.1.3, the compatibility equations (3.19) can serve as definition for an "electric" field $\vec{E} = -\vec{\nabla}\chi$, so that equation (3.36) can be rewritten

$$\vec{\nabla} \cdot \vec{E} = -4\pi\rho. \quad (3.37)$$

We can now replace the charge distribution in the definition of the multipole moments by the divergence of the field which is known through those same compatibility conditions (3.19). However we are still not able to make sense of those moments because $\vec{\nabla} \cdot \vec{E}$ depends on x and t which themselves depend on ξ and η in an unknown way, making the volume integrals involved in the definition (3.35) tricky to compute. A way to (partially) mitigate this problem would be to remove the time dependence by transforming the volume integral in a surface integral (over constant time surface) by way of Stokes theorem. To that end let us introduce \vec{F}^l and \vec{G}^l two vector fields such that

$$\begin{cases} \vec{\nabla} \cdot \vec{F}^l = r^l P_l \left(\frac{\xi}{r} \right) (\vec{\nabla} \cdot \vec{E}) \\ \vec{\nabla} \cdot \vec{G}^l = r^{-(l+1)} P_l \left(\frac{\xi}{r} \right) (\vec{\nabla} \cdot \vec{E}) \end{cases}, \quad (3.38)$$

then we can reformulate the definition of the multipole moments (3.35) in terms of \vec{F}_l and \vec{G}_l as

$$\begin{cases} Q_l = -\frac{1}{2} \oint_{S_{\tilde{t}}} (\vec{F}_l \cdot \vec{n}) dS \\ I_l = -\frac{1}{2} \oint_{S_{\tilde{t}}} (\vec{G}_l \cdot \vec{n}) dS \end{cases}, \quad (3.39)$$

where the integrals are computed over a constant time surface $S_{\tilde{t}}$, $0 < \tilde{t} < T$, so that they include all charges around the origin. In this case, as in section 3.1.5, choosing to integrate over a constant time surface is not necessary but is rather convenient because it explicitly eliminates the time dependence: the surface element dS and the normal \vec{n} are once again defined by equations (3.27) and (3.28). Naturally, the (equally unknown) x dependence remains, but the fact that the multipole moments are by construction constants of motion, and that Q_0 is essentially the normalization constant, hints that they may be equivalent to the first integrals of motion that are traditionally defined as integrals over the position. While this would not help when trying to compute the moments per se, because of the nature of the mixed boundary conditions, it would still help to make sense of what they represent.

The first step to confirming the hypothesis that multipole moments are equivalent to the first integrals of motion is to express \vec{F}^l and \vec{G}^l in terms of ξ and η . Obviously the definition given by equation

(3.38) involves a divergence and multiple solutions would be valid (up to a function of zero divergence), but we choose to go with what can arguably be considered the simplest one: matching the η and ζ components of \vec{F}^l respectively with those of \vec{E}

$$\begin{cases} \vec{F}^l(\eta, \zeta) = F_\eta^l(\eta, \zeta)\vec{e}_\eta + F_\zeta^l(\eta, \zeta)\vec{e}_\zeta \\ \partial_\eta(\eta F_\eta^l) = r^l P_l\left(\frac{\zeta}{r}\right) \partial_\eta(\eta E_\eta) \\ \partial_\zeta F_\zeta^l = r^l P_l\left(\frac{\zeta}{r}\right) \partial_\zeta E_\zeta \end{cases}, \quad (3.40)$$

and the natural equivalent for \vec{G}^l . The first ODE can be integrated over η and the second over ζ , respectively leaving ζ and η (but not t) constant, yielding

$$\begin{cases} F_\eta^l(\eta, \zeta) = \frac{1}{\eta} \left[\int^\eta r^l(\eta', \zeta) P_l\left(\frac{\zeta}{r(\eta', \zeta)}\right) \partial_{\eta'}(\eta'^2 t) d\eta' \right] \Big|_{\zeta=\text{const.}} \\ F_\zeta^l(\eta, \zeta) = \int^\zeta r^l(\eta, \zeta') P_l\left(\frac{\zeta'}{r(\eta, \zeta')}\right) \partial_{\zeta'}(2x - \zeta' t) d\zeta' \Big|_{\eta=\text{const.}} \end{cases}, \quad (3.41)$$

once E_η and E_ζ have been replaced using the compatibility equations (3.19). Inserting this (implicit) expression in equation (3.39) allows to reformulate the definition of the exterior multipole moments

$$\begin{aligned} Q_l = -\frac{1}{2} \int_{\mathbb{R}} \left[\left(\partial_x \zeta \left[\int^\eta r^l(\eta', \zeta) P_l\left(\frac{\zeta}{r(\eta', \zeta)}\right) \partial_{\eta'}(\eta'^2 t) d\eta' \right] \Big|_{\zeta=\text{const.}} \right. \right. \\ \left. \left. + \eta \partial_x \eta \left[\int^\zeta r^l(\eta, \zeta') P_l\left(\frac{\zeta'}{r(\eta, \zeta')}\right) \partial_{\zeta'}(\zeta' t) d\zeta' \right] \Big|_{\eta=\text{const.}} \right) \right. \\ \left. - 2\eta \partial_x \eta \left[\int^\zeta r^l(\eta, \zeta') P_l\left(\frac{\zeta'}{r(\eta, \zeta')}\right) \partial_{\zeta'}(x) d\zeta' \right] \Big|_{\eta=\text{const.}} \right] dx \end{aligned} \quad (3.42)$$

The (time dependent) term in parenthesis integrates to zero because Q_l is a constant, while the other can be rewritten as an integral over the position x at constant η

$$Q_l = \int_{\mathbb{R}} \eta \partial_x \eta \left[\int^x r^l P_l\left(\frac{\zeta}{r}\right) dx' \right] \Big|_{\eta=\text{const.}} dx, \quad (3.43)$$

leaving us with a fairly compact expression. Obviously the same treatment can be applied to I_l , hence

$$I_l = \int_{\mathbb{R}} \eta \partial_x \eta \left[\int^x r^{-(l+1)} P_l\left(\frac{\zeta}{r}\right) dx' \right] \Big|_{\eta=\text{const.}} dx. \quad (3.44)$$

We can deal with the integral over x' by integration by part and take a look at the first multipole moments

$$\begin{aligned}
 Q_0 &= -\frac{1}{2} \int_{\mathbb{R}} \eta^2 dx = \frac{2g}{\mu} \int_{\mathbb{R}} m dx \\
 Q_1 &= -\frac{1}{2} \int_{\mathbb{R}} \eta^2 \zeta dx = -\frac{2g}{\mu^2} \int_{\mathbb{R}} m \nabla u dx = -\frac{2g}{\mu^2} \int_{\mathbb{R}} \left(\frac{m \nabla u - u \nabla m}{2} \right) dx . \\
 Q_2 &= \int_{\mathbb{R}} \frac{\eta^4}{4} - \zeta^2 \eta^2 dx = \frac{8g}{\mu^2} \int_{\mathbb{R}} \frac{g}{2} m^2 + \frac{1}{2\mu} m (\nabla u)^2 dx
 \end{aligned} \tag{3.45}$$

First, we can fortunately check that equation (3.43) gives the same result we found in section 3.1.5 when applied to Q_0 . Now, Q_1 and Q_2 are interesting because they are respectively proportional to the momentum and Hamiltonian of the MFG equations (2.24) in their weak noise limit. Form definitions (3.3) and (2.35), we can indeed check that

$$Q_1 = -\frac{g}{\mu^2} P, \tag{3.46}$$

and

$$Q_2 = \lim_{\sigma \rightarrow 0} \left[\frac{8g}{\mu^2} E \right]. \tag{3.47}$$

This tends to confirm our hypothesis, and while we lack rigorous proof, it would not be too far-fetched to conjecture that the (exterior) multipole moments are equivalent to the first integrals of motion. For the interior moments I_l , however, equation (3.44) does not yield particularly exploitable results (at least to my understanding). But we already have a feeling of what role the interior multipole moments play thanks to section 3.1.6. It seems that the interior moments help define the initial condition while the exterior moments describe how it will evolve, which is coherent with their respective location in the hodograph space. As such, the mapping between the boundary conditions and the distribution of charges turns into an equally non trivial, albeit less abstract, mapping between the boundary conditions and the first integrals of motion. Given that, I also want to stress how the forward-backward structure of MFG equations (2.24) affect how we should deal with their resolution on a fundamental level. Were it an initial value problem we would be able to compute an arbitrary large number of multipole moments (or even directly compute χ through Green's theorem, c.f. Appendix D) and solve it completely. But the mixed boundary conditions does not give such an opportunity.

The existence of the potential χ underlies the integrable character of the hydrodynamic equations (3.6). In a sense it can be seen as the generating functional of the canonical linearising transforms, which the hodograph transform would be part of. This is important because

it means that, as we were able to adapt Riemann's method, usually employed to deal with dispersionless hydrodynamics, to MFG in the weak noise limit, we may also be able to adapt more complex tools like the Inverse Scattering Transform (IST) or even Witham theories to a more general problem like the quadratic integrable MFG equations (3.1).

3.1.8 Multipole expansion and the boundary conditions: constructing a numerical ansatz

Before I conclude this discussion on the weak noise limit of integrable MFG, I would like to say a few words about the value of the potential representation and its multipole expansion as a way to numerically approximate solutions of hydrodynamic equations (3.6). This is something I mentioned briefly at the end of section 3.1.7, the multipole expansion allows for the construction of a variational ansatz, with an arbitrary number of physically meaningful parameters to fit.

Multipole coefficients are not arbitrary fitting parameters, they have physical significance. If one were to compute every last one, they would be able to reconstruct the exact solution of Laplace equation [65].

This ansatz can be used in a very simple way to obtain a reasonable (arbitrarily precise) approximation of m and v . Denoting by $\bar{\cdot}$ the discretized version of \cdot , the most straightforward method maybe is to compute a truncated version of the multipole expansion (3.21)

$$\bar{\chi}(\eta, \zeta) = \sum_{l=0}^N \left(\frac{Q_l}{\bar{r}^{l+1}} + I_l \bar{r}^l \right) P_l \left(\frac{\bar{\zeta}}{\bar{r}} \right), \quad (3.48)$$

along with the compatibility conditions (3.19)

$$\begin{cases} \partial_{\bar{\eta}} \bar{\chi} = \bar{\eta} \bar{t} \\ \partial_{\bar{\zeta}} \bar{\chi} = 2(\bar{x} - \bar{\zeta} \bar{t}) \end{cases}. \quad (3.49)$$

We may then define a cost function

$$c = \sum_{\langle \bar{i}=0 \rangle} |\bar{m} - m_0(\bar{x})| + \sum_{\langle \bar{i}=T \rangle} |\bar{v} - v_T(\bar{x})|, \quad (3.50)$$

where $\langle \bar{i} = 0 \rangle$ and $\langle \bar{i} = T \rangle$ refer to the sum over all the values taken by \bar{m} and \bar{x} so that $\bar{t} = 0$ and $\bar{t} = T$ respectively. Finding the best approximation of m and v , solutions of hydrodynamic equations (3.6) with boundary conditions $m(0, x) = m_0(x)$ and $v(T, x) = v_T(x)$, amounts to finding the ensemble of multipole coefficients $\{Q_0, \dots, Q_N; I_0, \dots, I_N\}$ that minimizes c . This can be done using standard optimization techniques and can prove (for a reasonable number of fitting parameters) significantly faster than a brute force resolution like the one presented in Appendix A. These two approaches are philosophically distinct and have different purpose. This section's method provides a quick way to obtain a qualitative, easy to interpret and physically significant solution. It is particularly pertinent at the early, exploratory stage that this thesis is written. Alternatively, a (longer, more time consuming)

brute force resolution would yield quantitatively exact results better suited to applications oriented studies. Unfortunately, this exact solution would come with little insight (because of its high complexity) about the underlying MFG mechanisms. To briefly discuss the efficiency of the present method I shall provide a few examples.

First I will consider equations (3.6) with parabolic initial condition $m_0(x)$ and linear terminal condition v_T , and try to approximate the solutions via an expansion (3.48) truncated at order $N = 2$. On Figure (7) are represented the numerical solutions of $m(0, x)$ and $v(T, x)$ obtained through the optimization of c over $\{Q_0, Q_1, Q_2; I_0, I_1, I_2\}$ compared to m_0 and v_T . Because m_0 and v_T are part of the family of solutions generated by $N = 2$, we can see that the approximation and the boundary condition are essentially indistinguishable, and it remains the case throughout the rest of the game.

If I depart from initial conditions that belong to the family of solutions described by $N = 2$, for example m_0 Gaussian, I can still obtain acceptable results, as illustrated Figure (8a), at $t = 0$. As we can expect from the electrostatics analogy, the system then relaxes towards an inverted parabola as we move away from the charges at infinity. This is exemplified Figure (8b) where the tails of the numerical distribution only come from the fact that the program described in Appendix A cannot deal with $\sigma = 0$.

The next step would now be to consider both initial and final conditions that do not belong to the $N = 2$ family, for example m_0 Gaussian and v_T cubic. A comparison between those two initial / final conditions and the best fit using a $N = 2$ multipole expansion is shown Figure (9). However, contrary to the previous case, the system will not relax towards the inverted parabola solution as (especially for such a short game) moving away from charges at infinity means coming closer to charges at the origin. In particular, the curvature of the terminal cost has the distribution of players split into three parts, all of which are smaller inverted parabolas. This can be observed Figure (10) where the distribution of player is shown at the middle of the game, $t = T/2$. At this point, all the $N = 2$ approximation can provide is an idea about the extension of the distribution of players. A more precise, quantitative description would require using higher order moments.

With this I conclude this section on integrable MFG in the weak noise limit. Making use of notions originating from hydrodynamics, namely Riemann invariants and the hodograph transform, I was able to introduce a powerful analogy between electrostatics and MFG through the potential representation (3.18). The main benefit of this alternative representation is to allow for an admittedly non-trivial mapping between first integrals of motion and boundary conditions thanks to a multipole expansion. Because of this mapping I was able to highlight the existence of a universal scaling solution, an extension

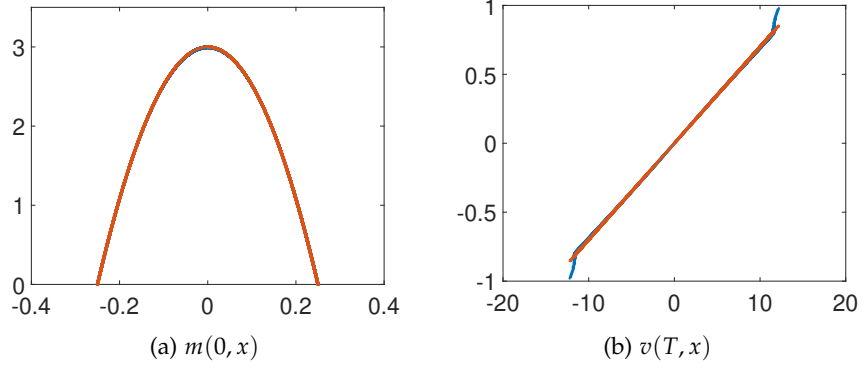


Figure 7: Comparison between the $N = 2$ approximation (blue) and the boundary conditions (red). For this Figure I chose $T = 10$, $g = -2$, $\mu = 1$, $m_0(x) = \frac{3(0.25^2 - x^2)}{4(0.25)^3}$ and $v_T(x) = 0.07x$, while the optimization of c yields $Q_0 = -2$, $Q_1 = 0$, $Q_2 = -0.12$, $I_0 = 0$, $I_1 = 0$, $I_2 = 0.034$.

of the notion of ergodic state in a context where the ergodic state should not exist, as well as develop ansätze of various degrees of complexity. While the forward-backward structure still constitutes a major challenge, these tools make it more manageable and bring a better understanding of the processes at work.

The next section will deal with the "complete" integrability of the more general problem described by the quadratic integrable MFG equations (3.1). Following a similar procedure of trying to adapt and implement proven methods developed by physicists in the context of MFG, the next section will provide some elements on how to accommodate the Inverse Scattering Transform (IST) to the problem at hand.

3.2 COMPLETE INTEGRABILITY OF MEAN FIELD GAMES EQUATIONS

The last section hinted to the fact that the fundamental reason why we were able to construct this potential representation was in fact the integrable nature of hydrodynamic equations (3.6), property they share with the more general equations (3.1) we will now consider. This was to be expected and can obviously be traced back to the Schrödinger representation of MFG equations (3.1)

$$\begin{cases} \mu\sigma^2\partial_t\Phi = -\frac{\mu\sigma^4}{2}\Delta\Phi - gm\Phi \\ \mu\sigma^2\partial_t\Gamma = \frac{\mu\sigma^4}{2}\Delta\Gamma + gm\Gamma \end{cases} \quad (3.51)$$

NLS equation being integrable in the absence of external potential, it is natural to assume that equations (3.51), its MFG counterpart, are

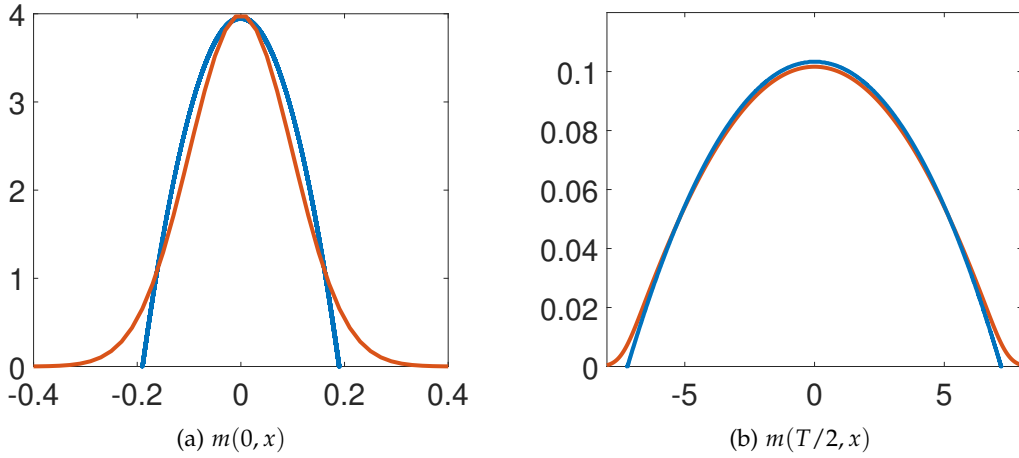


Figure 8: Comparison between the $N = 2$ approximation (blue) and the results of the brute force resolution described in Appendix A (red). For this Figure I chose $T = 10$, $g = -2$, $\mu = 1$, a Gaussian of variance 0.1 as initial distribution $m_0(x)$ and $v_T(x) = 0.07x$, while the optimization of c yields $Q_0 = -2$, $Q_1 = 0$, $Q_2 = -0.12$, $I_0 = 0$, $I_1 = 0$, $I_2 = 0.0225$. Simulations have been made with non-zero noise, $\sigma = 0.4$.

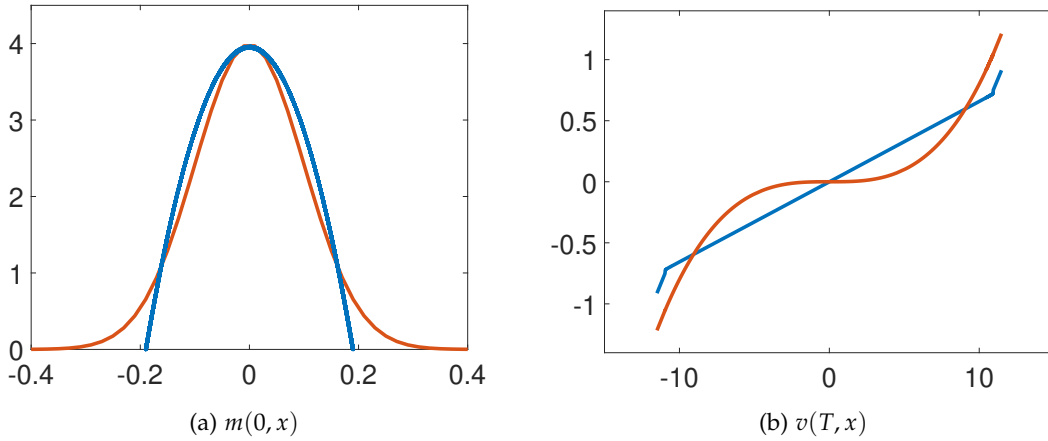


Figure 9: Comparison between the $N = 2$ approximation (blue) and the boundary conditions (red). For this Figure I chose $T = 10$, $g = -2$, $\mu = 1$, a Gaussian of variance 0.1 as initial distribution $m_0(x)$ and $v_T(x) = 8 \cdot 10^{-4} x^3$, while the optimization of c yields $Q_0 = -2$, $Q_1 = 0$, $Q_2 = 0.025$, $I_0 = 0$, $I_1 = 0$, $I_2 = 0.0225$.

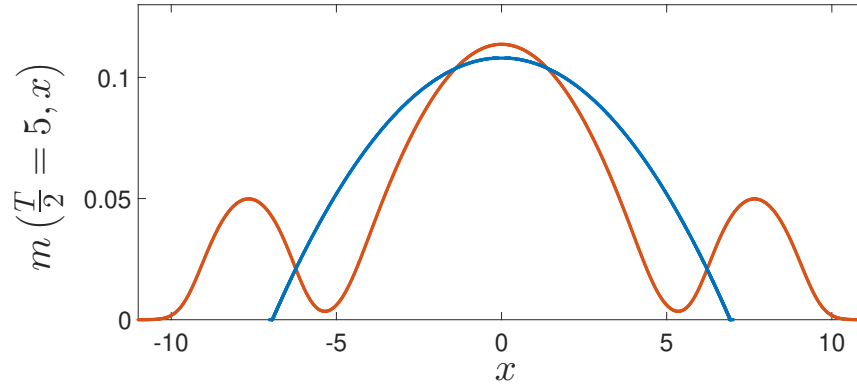


Figure 10: Comparison between the $N = 2$ approximation (blue) and the results of the brute force resolution described in Appendix A (red). For this Figure I chose $T = 10$, $g = -2$, $\mu = 1$, a Gaussian of variance 0.1 as initial distribution $m_0(x)$ and $v_T(x) = 8 \cdot 10^{-4} x^3$, while the optimization of c yields $Q_0 = -2$, $Q_1 = 0$, $Q_2 = 0.025$, $I_0 = 0$, $I_1 = 0$, $I_2 = 0.0225$. Simulations have been made with non-zero noise, $\sigma = 0.4$.

An example of such caveat is the fact that Φ and Γ are defined positive, rendering the traditional dark soliton [92] solution invalid.

too. NLS equation has been studied extensively for the past 60 years and we should be able to make use, with a few caveats, of the tools developed during this period to, in turn, study MFG.

One of the most powerful methods when it comes to exploiting the integrability of NLS equation was first introduced by V. Zakharov and A. Shabat in their seminal paper of 1972 [99]. It presents what would later be known as the Inverse Scattering Transform (IST) and constitutes the basis of soliton theory [89]. In this section I will try to adapt this method, in its modern acceptance, to MFG and, to that end, will rely heavily on a book written by L. Faddeev and L. Takhtajan [46].

This section deals with unfinished work. It presents the IST formalism and how it can be applied to MFG, but does not provide a solution to the system of equations (3.51). Instead it examines intermediate results, such as a way to generate first integrals of motion, and discusses issues with this method (when it comes to MFG) that will need to be addressed.

3.2.1 Nondimensionalization

As is often the case when dealing with non-linear PDEs, it will prove convenient to parametrize the system of equations (3.51) using dimensionless units. This is particularly true now that we are interested in the complete problem rather than its weak noise limit, and that the effects carried by the different parameters μ , σ and g are actually competing with one another.

We have already introduced the healing length $\nu = |\mu\sigma^4/g|$ in section 3.1.1 as a typical length scale of the problem and, in a similar fashion, we can now introduce $\tau = 2\mu^2\sigma^6/g^2$ as its typical time scale. Denoting both $t' = t/\tau$ and $x' = x/\nu$ we can then write equations (3.51) in their dimensionless form

$$\begin{cases} \partial_{t'}\Phi = -\partial_{x'x'}\Phi + 2\nu m\Phi \\ \partial_{t'}\Gamma = +\partial_{x'x'}\Gamma - 2\nu m\Gamma \end{cases}, \quad (3.52)$$

making it even clearer that ν is essentially the only relevant parameter.

I should stress that m has dimension inverse length and is of order $1/L$, where L is the typical extension of the distribution of players. This system of dimensionless equations tends to confirm my earlier claim that one can safely neglect diffusion as long as players are typically distributed over a distance larger than the healing length ν .

Dropping the "prime", this is the representation I will use for the rest of this section as it makes tracing the impact of the different parameters all that easier. Especially when one takes into account the several transformations required by the IST method.

3.2.2 Zero curvature representation

The foundation of the IST method lies in the fact that dimensionless equations (3.52) can be seen as compatibility conditions for an auxiliary, overdetermined, linear system. Let $F = (f_1, f_2)$ be a vector function of (x, t) defined by

$$\begin{cases} \partial_x F = U(x, t, \lambda)F \\ \partial_t F = V(x, t, \lambda)F \end{cases}, \quad (3.53)$$

where U and V are 2×2 matrix functions depending unsurprisingly on (x, t) but also on a *spectral parameter* λ , the importance of which will be made clear later. By computing the cross derivative of F in different ways, it is easy to check that in order for it to verify Schwartz's theorem and the problem to be well-defined, one needs to impose

$$\partial_t U - \partial_x V + [U, V] = 0, \quad (3.54)$$

and this relation to hold no matter the value taken by λ . If we assume that

$$U = \sqrt{\nu} \begin{pmatrix} 0 & \Phi \\ \Gamma & 0 \end{pmatrix} + \begin{pmatrix} \frac{\lambda}{2} & 0 \\ 0 & -\frac{\lambda}{2} \end{pmatrix}, \quad (3.55)$$

and

$$V = \sqrt{\nu} \begin{pmatrix} \sqrt{\nu}\Phi\Gamma & -\partial_x\Phi \\ \partial_x\Gamma & -\sqrt{\nu}\Phi\Gamma \end{pmatrix} - \lambda U, \quad (3.56)$$

then equations (3.52) are perfectly equivalent to the compatibility condition (3.54). What this representation brings to the table is a fairly natural geometric interpretation. The matrices U and V can be seen as the x and t components of a connection (or gauge field) in the vector bundle $\mathbb{R}^2 \times \mathbb{R}^{+2}$, while the left hand side of compatibility condition (3.54) can be seen as the curvature (or strength field) of this connection according to the Ambrose-Singer theorem [6]. Hence the name *zero-curvature representation*. In the field of classical integrable systems this is known as Lax connection and the compatibility equation (3.54) is equivalent to Lax equation when the number of degrees of freedom becomes infinite [11].

A reasonable progression, once we interpret (U, V) as a connection, is to consider the parallel transport it induces. Let γ be a curve in \mathbb{R}^2 partitioned into N adjacent segments $\gamma_1 \dots \gamma_N$. We define the parallel transport along γ as

$$\Omega_\gamma = \lim_{N \rightarrow \infty} \left[\mathcal{P} \prod_{n=1}^N \left(\mathbb{1} + \int_{\gamma_n} (Udx + Vdt) \right) \right] \quad (3.57)$$

where \mathcal{P} denotes the path ordering (because the connection is non-Abelian) and $\mathbb{1}$ the identity. A physicist's (and more compact) notation for this expression would be

$$\Omega_\gamma = \mathcal{P} \exp \int_\gamma (Udx + Vdt), \quad (3.58)$$

and this is the one we will use from now on. This last expression is particularly convenient for two reasons. The first one is that it makes it clear that if γ represents a path from the origin (x_0, t_0) to the point of observation (x, t) , the parallel transport along this path is simply F , solution of the auxiliary problem (3.53) with initial condition $F(x_0, t_0) = (1, 1)$. More generally, given initial data $F(x_0, t_0)$, solution of equations (3.53) is given by the covariantly constant vector field

$$F(x, t) = \Omega_\gamma F(x_0, t_0). \quad (3.59)$$

The second, and maybe more important, reason is that it makes computing the parallel transport over a closed curve γ_0 (holonomy of the connection) trivial by way of the non-Abelian Stokes theorem (cf appendix E). Indeed

$$\Omega_{\gamma_0} = \mathbb{1}, \quad (3.60)$$

no matter the starting point thanks to the vanishing of the curvature. This property is akin to that of Lagrangian manifolds in Hamiltonian mechanics and will prove to play a fundamental role in the computations of integrals of motion.

More generally those conventions and this nomenclature come from the path integrals representation of propagators in quantum mechanics [113]. Path integrals have become more and more pervasive in physics since the 50s, for a primer on the subject I refer the reader to [98].

3.2.3 Monodromy matrix

The main characteristics of the problem are the *monodromy matrices* defined as the propagators in the two directions x and t

$$\begin{cases} T(x, y, \lambda; t) = \mathcal{P} \exp \int_x^y U(z, t, \lambda) dz \\ S(t_1, t_2, \lambda; x) = \mathcal{P} \exp \int_{t_1}^{t_2} V(x, t, \lambda) dt \end{cases} . \quad (3.61)$$

These "global" objects will turn out to be easier to manipulate than their local counterparts U and V , notably thanks to the non-Abelian Stokes theorem. To illustrate this, I shall consider a closed rectangular loop γ_R as represented Figure (11). Because of its geometry, the

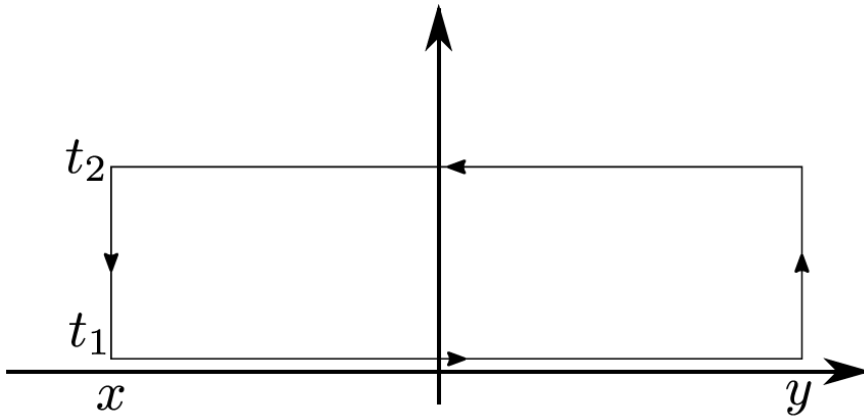


Figure 11: A rectangular loop γ_R in the (x, t) plane. The vanishing of the curvature imposes that the parallel transport along it is the identity.

parallel transport along γ_R can be readily expressed in terms of the monodromy matrices

$$\Omega_{\gamma_R} = S(t_2, t_1, \lambda; x) T(y, x, \lambda; t_2) S(t_1, t_2, \lambda; y) T(x, y, \lambda; t_1) = \mathbb{1} . \quad (3.62)$$

By construction, the monodromy matrices exhibit the following inversion property

$$\begin{cases} T(x, y, \lambda; t) = T^{-1}(y, x, \lambda; t) \\ S(t_1, t_2, \lambda; x) = S^{-1}(t_2, t_1, \lambda; x) \end{cases} ' \quad (3.63)$$

which one can use to write the parallel transport equation (3.62) as

$$T(x, y, \lambda; t_1) = S^{-1}(t_1, t_2, \lambda; y) T(x, y, \lambda; t_2) S(t_1, t_2, \lambda; x) . \quad (3.64)$$

Now, if one can find two points x and y (for example $x \rightarrow -\infty$ and $y \rightarrow \infty$) so that for all times t

$$V(x, t, \lambda) = V(y, t, \lambda) , \quad (3.65)$$

then the time evolution of the monodromy matrix T given by equation (3.64) can be seen as equivalent to a gauge transformation. This implies that the (gauge invariant) Wilson line that constitutes $\text{Tr}[T]$ is a constant in time

$$\begin{aligned} \text{Tr}[T(x, y, \lambda; t_1)] &= \text{Tr}\left[S^{-1}(t_1, t_2, \lambda; x)T(x, y, \lambda; t_2)S(t_1, t_2, \lambda; x)\right] \\ &= \text{Tr}[T(x, y, \lambda; t_2)] , \end{aligned} \quad (3.66)$$

and this for any λ . I will now show that $\text{Tr}[T]$ can be used as generating function for the constants of motion.

3.2.4 Computing conserved quantities

The monodromy matrix contains all the information we need about the system of equations (3.52), most notably, its trace can be used as generating functions for the first integrals of motion. To extract those conserved quantities one first needs to write the monodromy matrix as a Poincaré expansion in terms of λ . I will not discuss how this upcoming expansion came to be, for a complete derivation I refer the interested reader to the aforementioned monograph [46].

We start by introducing $E(y - x, \lambda)$, the monodromy matrix of equations (3.52) for the trivial constant solutions $\Phi(x, t) = \Gamma(x, t) = 0$

$$\begin{aligned} E(y - x, \lambda) &= \lim_{\Phi \rightarrow 0} \lim_{\Gamma \rightarrow 0} \left[\mathcal{P} \exp \int_x^y U(z, t, \lambda) dz \right] \\ &= \exp \left[\frac{\lambda}{2} (y - x) \sigma_3 \right] , \end{aligned} \quad (3.67)$$

where σ_3 is the Pauli matrix

$$\sigma_3 = \begin{pmatrix} 1 & 0 \\ 0 & -1 \end{pmatrix} . \quad (3.68)$$

The monodromy matrix can then be written as

$$\begin{aligned} T(x, y, \lambda; t) &= E(y - x, \lambda) + \sum_{n=1}^{\infty} \frac{T_n(x, y; t) E(y - x, \lambda)}{\lambda^n} \\ &\quad + \sum_{n=1}^{\infty} \frac{\tilde{T}_n(x, y; t) E(x - y, \lambda)}{\lambda^n} + o(\lambda^{-\infty}) . \end{aligned} \quad (3.69)$$

This expansion will allow us to associate a conserved quantity to each and every order in λ .

To get a more explicit expression of the coefficients T_n and \tilde{T}_n we turn to an alternative definition of the monodromy matrix T . The integral definition (3.61) is perfectly equivalent to the differential equation

$$\partial_y T(x, y, \lambda; t) = U(y, t, \lambda) T(x, y, \lambda; t) , \quad (3.70)$$

with initial condition

$$T(x, y, \lambda; t)|_{x=y} = \mathbb{1}. \quad (3.71)$$

To solve equation (3.70) at every order in λ , because we are eventually interested in taking the trace of T , it is convenient to write the monodromy matrix as the gauge transformation of a diagonal matrix, a process sometimes called *abelianization* [11]. If condition (3.65) is satisfied, one can write

$$T(x, y, \lambda; t) = (\mathbb{1} + W(x, \lambda; t)) \exp Z(x, y, \lambda; t) (\mathbb{1} + W(y, \lambda; t))^{-1}, \quad (3.72)$$

where W and Z are respectively an off-diagonal and a diagonal matrix, shown to be uniquely defined, of Poincaré expansion [46]

$$W(y, \lambda; t) = \sum_n \frac{W_n(y; t)}{\lambda^n}, \quad (3.73)$$

and

$$Z(x, y, \lambda; t) = E(y - x, \lambda) + \sum_n \frac{Z_n(x, y; t)}{\lambda^n}. \quad (3.74)$$

Inserting the expression (3.72) in equation (3.70), and separating diagonal and off-diagonal parts, one obtains

$$\begin{cases} \partial_y Z(x, y, \lambda; t) = \lambda \sigma_3 + \underline{U}(y, t) W(y, \lambda; t) \\ \partial_y W(y, \lambda; t) + W(y, \lambda; t) \partial_y Z(x, y, \lambda; t) = \underline{U}(y, t) + \frac{\lambda}{2} \sigma_3 W(y, \lambda; t) \end{cases}, \quad (3.75)$$

by denoting $\underline{U}(y, t) \equiv U(y, t, \lambda = 0)$. The implicit expression of $\partial_y Z$ given by the diagonal part of equations (3.75) can be used to write the off-diagonal part as a Riccati equation

$$\partial_y W - \lambda \sigma_3 W + W \underline{U} W - \underline{U} = 0. \quad (3.76)$$

Using the expansion (3.73) and focusing on the n th order in λ yields the recursion relation

$$W_{n+1} = \sigma_3 \left[\partial_y W_n + \sum_{k=1}^{n-1} W_k \underline{U} W_{n-k} \right], \quad (3.77)$$

with initial condition

$$W_1 = -\sigma_3 \underline{U}. \quad (3.78)$$

More explicitly, if we write

$$W = \sqrt{V} \begin{pmatrix} 0 & -\sum_n \frac{\bar{w}_n}{\lambda^n} \\ \sum_n \frac{w_n}{\lambda^n} & 0 \end{pmatrix}, \quad (3.79)$$

the recursion relation (3.77) becomes

$$\begin{cases} w_{n+1} = \partial_y w_n + \nu \Phi \sum_{k=1}^{n-1} w_k w_{n-k} \\ \tilde{w}_{n+1} = -\partial_y \tilde{w}_n - \nu \Gamma \sum_{k=1}^{n-1} \tilde{w}_k \tilde{w}_{n-k} \end{cases}, \quad (3.80)$$

with

$$\begin{cases} w_1 = \Gamma \\ \tilde{w}_1 = -\Phi \end{cases}. \quad (3.81)$$

Now, let us go back to the diagonal part of equations (3.75), which can be readily integrated as

$$Z(x, y, \lambda; t) = \frac{\lambda(y-x)\sigma_3}{2} + \int_x^y U_0(z, t) W(z, \lambda; t) dz. \quad (3.82)$$

If we expand W in the integral this last expression becomes

$$\begin{aligned} Z(x, y, \lambda; t) = & \frac{\lambda(y-x)}{2} \begin{pmatrix} 1 & 0 \\ 0 & -1 \end{pmatrix} \\ & + \begin{pmatrix} \sum_{n=0}^{\infty} \frac{1}{\lambda^n} \int_x^y w_n \Phi dz & 0 \\ 0 & -\sum_{n=0}^{\infty} \frac{1}{\lambda^n} \int_x^y \tilde{w}_n \Gamma dz \end{pmatrix}. \end{aligned} \quad (3.83)$$

By way of equations (3.80) and (3.81), it is easy to check that

$$\int_x^y w_n(x, t) \Phi(x, t) dz = \int_x^y \tilde{w}_n(x, t) \Gamma(x, t) dz, \quad (3.84)$$

for all n . Like $\text{Tr}[T]$, $\text{Tr}[\exp Z]$ constitutes a Wilson line and is intrinsically gauge invariant. As such, by exponentiating equation (3.83) and taking the trace, we obtain from the abelianization equation (3.72)

$$\begin{aligned} \text{Tr}[T] &= \text{Tr}[\exp Z] \\ &= 2 \text{ch} \left[\lambda(y-x) + \sum_{n=0}^{\infty} \frac{1}{\lambda^n} \int_x^y w_n(x, t) \Phi(x, t) dz \right], \end{aligned} \quad (3.85)$$

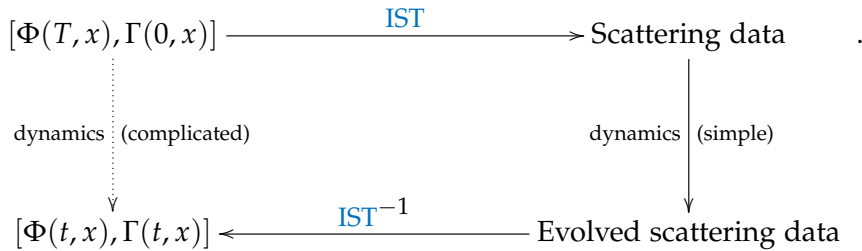
meaning that for all n the integral (3.84) has to be constant in time. By looking at the first three orders and computing the monodromy matrix over the whole domain we are interested in (letting $x \rightarrow -\infty$ while $y \rightarrow \infty$)

$$\begin{aligned} Q_0 &= \int_{\mathbb{R}} w_1 \Phi dx = \int_{\mathbb{R}} \Gamma \Phi dx \propto N \\ Q_1 &= \int_{\mathbb{R}} w_2 \Phi dx = \frac{1}{2} \int_{\mathbb{R}} (\Gamma \partial_x \phi - \Phi \partial_x \Gamma) dx \propto P. \\ Q_2 &= \int_{\mathbb{R}} w_3 \Phi dx = \int_{\mathbb{R}} (\nu m^2 + \partial_x \Phi \partial_x \Gamma) dx \propto E \end{aligned} \quad (3.86)$$

One can check that these are indeed equivalent to the conserved quantities N, P and E introduced at the beginning of the chapter. Higher order terms correspond to more abstract quantities I will not discuss but are still, by construction, invariant. To prove that those invariants are actually first integrals of motion, and to recover the definition of Liouville integrability, one simply needs to show that they all are in involution, something that is done in appendix F.

3.2.5 Inverse scattering transform and its application to Mean Field Games

The IST can be seen as a more complicated Fourier transform (and a generalization in some sense) for non-linear equations. Its implementation as a method for solving NLS equation can be summarized in three major steps, just like Fourier transform for translational invariant systems, presented as a commutative diagram



First, one needs to relate the fields Φ and Γ to their associated scattering data, namely the transition coefficients and the discrete spectrum for the first equation of the auxiliary problem (3.53), all of which can be extracted from the monodromy matrix T . This done, one can now compute the time evolution of this scattering data, which is significantly simpler than the original equations (3.51): as we shall see, the dynamics of T is actually linear. The last step is also the most arduous one. It consists in reconstructing the fields from the evolved scattering data, and this usually amounts to solving some flavour of the Riemann problem or Gelfand-Levitan-Marchenko integral equation. In this section I will discuss the steps I was able to take in order to accommodate the IST to MFG and the difficulties I faced trying to fully implement the method.

In terms of Hamiltonian mechanics, the IST defines a canonical transformation to action-angle variables.

Scattering data and relation to scattering theory

To extract the scattering data, let us go back to the auxiliary problem (3.53) and focus on its x -component

$$\partial_x F(x, t) = U(x, t, \lambda) F(x, t), \tag{3.87}$$

where the solution $F = (f_1, f_2)$ is a vector function and, given initial data at point (x_0, t) , can be computed as

$$F(x, t) = T(x_0, x, \lambda; t) F(x_0, t). \tag{3.88}$$

The problem (3.87) consists in a first order, linear, 2-dimensional system: its space of solution is 2-dimensional as well and it can prove useful to fix a basis of solutions by looking at their asymptotic behaviour when $x \rightarrow \pm\infty$. From the definition of Lax connection (3.55), if one assumes that Φ and Γ decrease sufficiently fast, one can write

$$\mathcal{U}(\lambda) = \lim_{x \rightarrow \pm\infty} U(x, t, \lambda) = \frac{\lambda}{2} \sigma_3, \quad (3.89)$$

from which one can deduce a basis of asymptotic solutions

$$\Psi_1(x) = \begin{pmatrix} 1 \\ 0 \end{pmatrix} \exp\left[\frac{\lambda}{2}x\right] \quad \Psi_2(x) = \begin{pmatrix} 0 \\ 1 \end{pmatrix} \exp\left[-\frac{\lambda}{2}x\right]. \quad (3.90)$$

One can now identify two bases of solutions ℓ_i and g_i , $i = 1, 2$, known in the context of scattering theory as *Jost solutions*, according to their asymptotic behaviour either when $x \rightarrow \infty$ or $x \rightarrow -\infty$

$$\begin{aligned} \ell_i(x, t) &\xrightarrow{x \rightarrow +\infty} \Psi_i(x) \\ g_i(x, t) &\xrightarrow{x \rightarrow -\infty} \Psi_i(x) \end{aligned} \quad (3.91)$$

For compactness, the two vectors of each of those bases can be arranged as the columns of 2×2 matrices

$$\begin{aligned} \mathcal{F}(x, t) &= (\ell_1(x, t), \ell_2(x, t)) \\ \mathcal{G}(x, t) &= (g_1(x, t), g_2(x, t))' \end{aligned} \quad (3.92)$$

which can be explicitly computed as

$$\begin{aligned} \mathcal{F}(x, t) &= \lim_{x_0 \rightarrow \infty} T(x_0, x, \lambda; t) E(x_0) \\ \mathcal{G}(x, t) &= \lim_{x_0 \rightarrow -\infty} T(x_0, x, \lambda; t) E(x_0)' \end{aligned} \quad (3.93)$$

by noting that the previously defined matrix E , equation (3.67), can actually be written $E = (\Psi_1, \Psi_2)$. Because both \mathcal{F} and \mathcal{G} are basis for the space of solutions of the auxiliary problem (3.87), one can perform a change of basis

$$\mathcal{F}(x, t) = \mathcal{G}(x, t) \mathcal{T}(\lambda, t), \quad (3.94)$$

where

$$\begin{aligned} \mathcal{T}(\lambda, t) &= \mathcal{G}^{-1}(x, t) \mathcal{F}(x, t) \\ &= \lim_{x \rightarrow \infty} \lim_{y \rightarrow -\infty} E(-x, \lambda) T(x, y, \lambda; t) E(y, \lambda). \end{aligned} \quad (3.95)$$

The transformation matrix \mathcal{T} is called the *reduced monodromy matrix*. Because it converts one Jost solution into the other it can be interpreted as a classical equivalent to the S-matrix of scattering theory and its elements are called *transition coefficients* by analogy. In the most general case

$$\mathcal{T}(\lambda, t) = \begin{pmatrix} a(\lambda, t) & b(\lambda, t) \\ c(\lambda, t) & d(\lambda, t) \end{pmatrix}, \quad (3.96)$$

and a, b, c, d constitute the scattering data.

Evolution of the reduced monodromy matrix

To compute the time evolution of the reduced monodromy matrix \mathcal{T} one should first consider the regular monodromy matrix T . To that end let us take the time derivative of equation (3.70)

$$\partial_{t,y}T = \partial_t UT - U\partial_t T . \quad (3.97)$$

Using the compatibility conditions (3.54) to express $\partial_t U$ in terms of V yields

$$\partial_y(\partial_t T - VT) = U(\partial_t T - VT) , \quad (3.98)$$

from which we can infer

$$\partial_t T(x, y, \lambda; t) = V(y, t, \lambda)T(x, y, \lambda; t) + T(x, y, \lambda; t)V(x, t, \lambda) , \quad (3.99)$$

by making use of the initial condition (3.71). Now, to get the evolution of the reduced monodromy matrix one has to consider the asymptotic behaviour

$$\lim_{x \rightarrow \pm\infty} V(x, t, \lambda)E(x) = \frac{\lambda^2}{2}\sigma_3 E(x) \quad (3.100)$$

leading to a remarkably simple dynamics

$$\partial_t \mathcal{T}(\lambda, t) = \frac{\lambda^2}{2}[\sigma_3, \mathcal{T}] . \quad (3.101)$$

Another interesting aspect of this equation is that the dependence on Φ and Γ has completely disappeared, making for a trivial resolution. In terms of the transition coefficients this means that a and d on the diagonal are constants

$$\begin{aligned} a(\lambda, t) &= a(\lambda, 0) \\ d(\lambda, t) &= d(\lambda, 0) \end{aligned} \quad (3.102)$$

which was to be expected because of equation (3.66), and that b and c on the off-diagonal can be expressed as

$$\begin{aligned} b(\lambda, t) &= b(\lambda, 0)e^{\lambda^2 t} \\ c(\lambda, t) &= c(\lambda, 0)e^{-\lambda^2 t} \end{aligned} \quad (3.103)$$

This simplification comes from the fact that the IST can be interpreted, from the Hamiltonian standpoint, as a transformation to action-angle variables. The trace of \mathcal{T} can be used as a generating function of the conserved quantities and, hence, of the action variables, while elements on the off-diagonal serve as angle variables.

Of note, one can use relations (3.102) and (3.103) to further the analogy with scattering theory. The matrix U being trace-less, the

monodromy matrix T , and by extension its reduced counterpart \mathcal{T} , are by construction uni-modular

$$ad - bc = 1 . \quad (3.104)$$

Because the products ad and bc are both constant in time, this previous relation can be understood as a normalization condition. Moreover, by dividing equation (3.104) by ad , one can recover an equation akin to the 1D optical theorem

$$\frac{1}{ad} + \frac{bc}{ad} = 1 \quad (3.105)$$

where one can define $t(\lambda) = 1/a(\lambda)d(\lambda)$ and $r(\lambda) = b(\lambda)c(\lambda)/a(\lambda)d(\lambda)$, respectively the *transmission* and *reflection* coefficients of scattering theory associated to the auxiliary problem (3.87).

Inverse transform and difficulties with Mean Field Games

To perform the inverse transform, one would have to solve the Riemann problem that constitutes equation (3.95)

$$\mathcal{T} = \mathcal{G}^{-1} \mathcal{F} , \quad (3.106)$$

but would also need to address certain issues that come with MFGs.

The most pressing issue probably comes from the fact that, contrary to their NLS counterpart, the fields Φ and Γ are not complex conjugates. The main consequence of this manifests when dealing with the reduced monodromy matrix \mathcal{T} which has to be expressed in the more general way equation (3.96), rather than the traditional

$$\mathcal{T}_{NLS}(\lambda, t) = \begin{pmatrix} a(\lambda, t) & b(\lambda, t) \\ b^*(\lambda, t) & a^*(\lambda, t) \end{pmatrix} , \quad (3.107)$$

\bar{a} and \bar{b} denoting the complex conjugates of a and b . This symmetry simplifies the Riemann problem (3.106) greatly but also makes the practical computations of the scattering data undoubtedly easier. In this configuration, a direct and explicit relation between a and the conserved quantities can be obtained using equation (3.85) and another one, between a and b , can be derived through the normalization condition

$$|a(\lambda)|^2 - |b(\lambda)|^2 = 1 . \quad (3.108)$$

Moreover, one can actually extract a lot of information from this simple relation, in particular concerning the analytic properties of the scattering data. Notably this implies that the transition coefficient a has no zeros for real λ but, in general, these definitions can be extended in the complex λ upper-half plane where a is analytic except

for simple zeros that correspond to bound states of the auxiliary problem (3.87) (poles of the reflection and transmission coefficients, and hence of the S-matrix). Those poles can be found by noticing that equation (3.87) reduces to an eigenvalue problem when multiplied by σ_3 on the left

$$\mathcal{L}F = \frac{\lambda}{2}F, \quad (3.109)$$

for the first order differential operator

$$\mathcal{L} = \sigma_3 \partial_x - U_0. \quad (3.110)$$

The new-found operator \mathcal{L} has continuous spectrum of multiplicity two on the whole real line - two linearly independent bounded solutions of equation (3.87) - associated with the transition coefficients a and b . It also admits the set $\lambda_j, j = 1 \dots n$, which is the complete list of zeros of a , as discrete spectrum. Both the continuous and discrete (if it exists) part of the spectrum are needed to solve the Riemann problem [46]. I assume a simplification similar to equation (3.107) exists in the context of MFG, because it seems too fundamental not to, but still have not found it.

Another issue lies in the fact that, depending on the type of utility function u considered, the assumption that Φ and Γ decrease sufficiently fast, necessary for asymptotic equation (3.89), may not be legitimate. This is particularly true for repulsive interactions where utility function translates to no confining effect whatsoever: u goes to zero at infinity where it is minimal, which means that

$$\lim_{x \rightarrow \pm\infty} \Phi = \lim_{x \rightarrow \pm\infty} \exp \left[-\frac{u}{\mu\sigma^2} \right] = 1. \quad (3.111)$$

One would then have to find a way to regularize the problem, which should be doable (see *The case of finite density* [46]), by modifying the time component V of the Lax connection, but would require some additional work.

Finally, as always, remains the issue of the forward-backward structure of equations (3.51). It is not yet clear how this will affect the IST but I can see two avenues to attempt and solve the problem. The first one would be to add a self-consistency equation, on top of the IST, which may prove to be highly non-trivial to solve. Another solution would be to try and study the reduced monodromy matrix in time along with \mathcal{T} and use the notion of duality of Lax pairs as discussed by J. Avan and V. Caudrelier in [10]. Both those approaches seem reasonable and may shed some new light on the forward-backward structure, but they would require a good understanding of the problem at hand and one should first focus on the two other aforementioned issues.

The IST is a powerful tool to solve non-linear PDEs and, just like the potential representation, being able to devise a MFG equivalent of

such a method would prove to be a useful step towards a better understanding of the mechanisms at hand in equations (3.51) but also of the forward-backward structure. Even if I have not been able, during my PhD, to fully accommodate the IST to the problem (3.51), the fact that there exists a zero-curvature representation is nonetheless sufficient to say that this is feasible. This is because the vanishing curvature of the Lax connection underlies a Poisson structure for the scattering data: equations (3.51) constitute an infinite-dimensional Hamiltonian system while the IST can be seen as the transform to the action-angle variables that compose the scattering data. Then, even if it differs slightly from the traditional IST, such a transform should exist in the context of MFG, and, in order to try and find it, I have identified three main issues that need to be addressed and will be the subject of further research.

With this I conclude this chapter on the integrability of MFG. In the next chapter I will discuss methods on how to handle the MFG problem (2.24) with non-zero external potential on the heuristic level, making use of results obtained through the study of its integrable limit.

HEURISTIC APPROACH TO 1D QUADRATIC MEAN FIELD GAMES

This chapter follows a different philosophical path than the previous one and is largely based on a not yet published article [21]. Its main aim is to provide a discussion on a small set of "paradigm" MFG problems, which, in the spirit of the Ising problem of statistical mechanics, are simple enough to be analysed and understood (at least from the physicist's point of view) but complex and rich enough to shed some light on a set of mechanisms that will characterize a much larger class of MFG models. The way this chapter differs from chapter 3, though, is a practical one. While the previous chapter was focused on finding exact results in some (very) limiting regimes, chapter 4 will outline a strategy, that takes its root from those aforementioned results, to examine more general problems, this time, in a more qualitative fashion.

This "more general" class of problems I will now consider still falls under the category of quadratic MFG, described by the 1+1 dimension system of equations (2.24) with potential (2.36) featuring, contrary to chapter 3 potential, a non-zero external gain

$$\begin{cases} \partial_t u + \frac{\sigma^2}{2} \partial_{xx} u - \frac{1}{2\mu} (\partial_x u)^2 = gm + U_0(x) \\ u(x, t = T) = c_T[m](x) \\ \partial_t m - \frac{1}{\mu} \partial_x [m \partial_x u] - \frac{\sigma^2}{2} \partial_{xx} m = 0 \\ m(x, t = 0) = m_0(x) \end{cases} \quad (4.1)$$

A potential of the type $V[m] = gm + U_0(x)$ displays short-range interactions, the strength of which is monitored by the constant g , and an external gain $U_0(x)$ representing the intrinsic interest for a player to be in state x (proximity to various facilities or resources, trending market, uncontroversial opinion, etc.). Of important note is that, because the potential V has to be interpreted as a gain (by opposition to a cost) according to the chosen sign convention, positive and negative g respectively imply attractive and repulsive interactions, while, for it to have a confining effect, U_0 has to be negative at large distance.

Similar problems have been already studied in the regime of strong positive interactions [106, 108]. Consequently, this chapter proposes an extension of these previous studies by considering in details the negative coordination regime. In particular, it will tackle in depth one of the conceptual difficulties presented by MFG theory, namely the one associated with the forward-backward structure of equations (4.1),

which, in some sense, makes the problem non-local in time. Since a forward equation, specified by its past, is coupled to a backward equation, specified by its future, the behaviour at any given time appears, a priori, affected by what is going on during the entire duration of the MFG process. In order to exacerbate this issue of *time non-locality*, this chapter will focus on the long optimization time limit, and on configurations such that the considered system goes through different regimes in which the weight of disorder, interactions between players, and personal preferences on the location have different relative importance. As such, those different regimes will be characterized by the balance between the various components of the energy

This typically refers to problems that involve a very narrow initial distribution of agents.

$$\begin{aligned} E &= \int_{\mathbb{R}} dx \left[-\frac{\mu\sigma^4}{2} \partial_x \Gamma \cdot \partial_x \Phi + \left[U_0 + \frac{g}{2} \Gamma \Phi \right] \Gamma \Phi \right] \\ &= \int_{\mathbb{R}} dx \left[\frac{\mu\sigma^2}{2} \left(m \left(\frac{v}{\sigma} \right)^2 - \sigma^2 \frac{(\partial_x m)^2}{4m} \right) + \left[U_0 + \frac{g}{2} m \right] m \right]. \end{aligned} \quad (4.2)$$

Just as in section 2.4.3, the first, σ dependent, term of the integrand can be interpreted as *kinetic energy*, the U_0 term as *potential energy* and the g term as *interaction energy*. The conservation of total energy, and the fact that transitioning from one regime to another implies a transfer between one "kind" of energy to another, will help in providing a global picture, across various regimes, of the MFG dynamics.

Because long optimisation times are considered, the first aspect of MFG equations (4.1) one should address is the corresponding ergodic state. As will be argued in section 4.1, the (static) ergodic state characterises a significant part of the agents dynamics and its existence even provides a major simplification for the transient dynamics as it effectively decouples the initial and terminal boundary conditions of the problem. Section 4.2 will then introduce, in some details, two relevant limiting regimes which will serve as starting points to describe the early stages of the game. Finally, in section 4.3, the full dynamics of the problem will be examined, and in particular, the essential question of matching the different regimes will be addressed.

4.1 STATIC MEAN FIELD GAME : THE ERGODIC STATE

The notion of ergodic state is crucial in MFG theory, and its importance is twofold. To start with, it corresponds to a simpler, static problem, which, for the vast majority of the game, provides a good approximation of the exact behaviour of equations (4.1). But it also allows for the short time and long time dynamics (leading to or leaving the ergodic state) to essentially decouple. Rather than having to find a solution of equations (4.1) for perfectly arbitrary boundary conditions $m_0(x)$ and $c_T(x)$, the beginning of the game can be described by solving those equations with the same arbitrary initial condition $m_0(x)$ but a generic terminal condition : the ergodic state. Conversely, the

end of the game can be described using the ergodic state as initial condition and $c_T(x)$ as terminal. As such, this notion of ergodic state reduces the problem (4.1) to two relatively simpler ones and it therefore makes sense to address it first. The aim of this section will be to discuss the ergodic solution, the approximation schemes used to describe this regime, and its stability.

4.1.1 Alternative representations in the ergodic state

In the strong interaction regime we focus on, the ergodic state can be approached equivalently within either the Schrödinger or hydrodynamic representations. The two approaches lead to a very simple analysis and both are presented below.

During the ergodic state, strategies become essentially stationary, as established by equations (2.25). As such, it is appropriate to introduce $\bar{\Psi}(x)$, solution of the stationary NLS equation

$$-\lambda \bar{\Psi}(x) = \frac{\mu \sigma^4}{2} \partial_{xx} \bar{\Psi}(x) + U_0(x) \bar{\Psi}(x) + g |\bar{\Psi}(x)|^2 \bar{\Psi}(x), \quad (4.3)$$

to describe $\bar{\Phi} = \exp[-\bar{u}/\mu\sigma^2]$ and $\bar{\Gamma} = \bar{m}/\bar{\Phi}$, ergodic solutions in the Schrödinger representation. Indeed, one can easily check from the definition of the ergodic state, equations (2.26), that both $\bar{\Phi}$ and $\bar{\Gamma}$ follow the same equation (4.3). Under the ergodic state, the system of time-dependent coupled PDEs (2.29) reduces to the one, time-independent, ODE (4.3), and the connection with NLS equation is made even clearer. One can then check that

$$\begin{cases} \Phi(t, x) = \exp\left(+\frac{\lambda}{\mu\sigma^2}t\right) \bar{\Phi}(x) \\ \Gamma(t, x) = \exp\left(-\frac{\lambda}{\mu\sigma^2}t\right) \bar{\Gamma}(x) \end{cases}, \quad (4.4)$$

are solutions of the time-dependent equation (2.29) and that $\Phi(t, x)\Gamma(t, x) = \bar{\Phi}(x)\bar{\Gamma}(x) = \bar{m}(x)$ corresponds to the static ergodic density.

Similarly, one can introduce the ergodic equations of the hydrodynamic representation. Introducing \bar{v} as the ergodic velocity, equations (2.32) readily become

$$\begin{cases} \bar{v} = 0 \\ \frac{\lambda}{\mu} + \frac{\sigma^4}{2\sqrt{\bar{m}}} \partial_{xx} \sqrt{\bar{m}} + \frac{g\bar{m} + U_0}{\mu} = 0 \end{cases}, \quad (4.5)$$

once again simplifying greatly the problem by getting rid of the time dependence but also of the coupling between the two functions \bar{v} and \bar{m} .

Of note, $\bar{\Psi}$ is not to be confused with the complex conjugate of Ψ , denoted Ψ^ .*

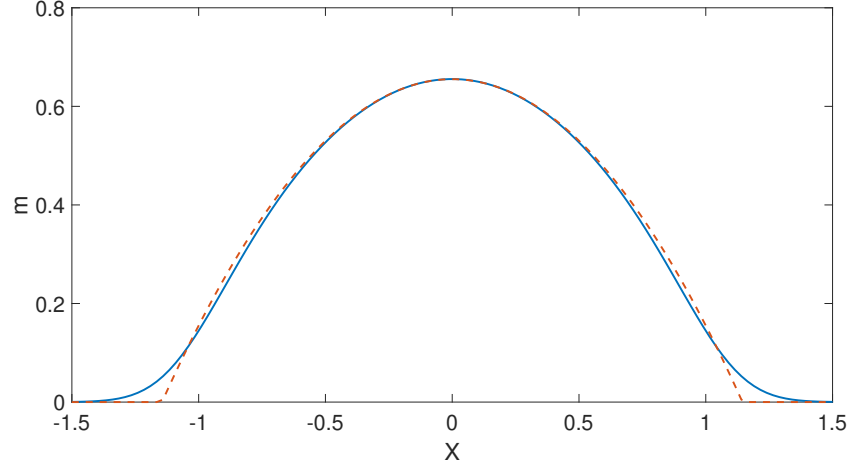


Figure 12: Computational solution of the Gross-Pitaevskii equation (full) and Thomas-Fermi approximation (dashed). In this case $g = -2$, $\sigma = 0.4$, $\mu = 1$ and $U_0(x) = -x^2$.

4.1.2 Bulk of the distribution: Thomas-Fermi approximation

One of the many interests of the Schrödinger representation is that one can exploit the large literature surrounding this equation. In the strong interaction regime, a particularly popular way of tackling the stationary NLS (or Gross-Pitaevskii) equation is through the use of Thomas-Fermi approximation, as described in [40].

Introducing L , the typical extension of the distribution of players, one can check that the *kinetic* term of energy (4.2) behaves as

$$E_{\text{kin}} = - \int_{\mathbb{R}} dx \frac{\mu \sigma^4}{2} \partial_x \Gamma \cdot \partial_x \Phi \sim \frac{\mu \sigma^4}{L^2}, \quad (4.6)$$

while the *interaction* term scales as

$$E_{\text{int}} = \int_{\mathbb{R}} dx \frac{g}{2} (\Phi \Gamma)^2 \sim \frac{g}{L}. \quad (4.7)$$

The ratio between kinetic and interaction energies constitutes a good representation of the relative importance of diffusion and interaction processes and can be estimated by

$$\left| \frac{E_{\text{kin}}}{E_{\text{int}}} \right| \sim \frac{\nu}{L}, \quad (4.8)$$

where

$$\nu \equiv \frac{\mu \sigma^4}{|g|} \quad (4.9)$$

is the *healing length*, already introduced in chapter 3.

In the limiting case where kinetic energy is negligible in the bulk of the distribution, i.e. when the typical extension of the distribution

is large in front of the healing length ν , equation (4.3) loses its differential status and becomes a simple algebraic equation

$$-\lambda \approx U_0(x) + g|\bar{\Psi}(x)|^2, \quad (4.10)$$

which is easily solved as

$$\Psi_{\text{TF}}(x) = \begin{cases} \left(\frac{\lambda + U_0(x)}{|g|} \right)^{1/2} & \text{if } \lambda > -U_0(x) \\ 0 & \text{otherwise} \end{cases}, \quad (4.11)$$

where the constant λ is then computed using the normalisation condition

$$\int_{\mathbb{R}} \bar{m}(x) dx = 1. \quad (4.12)$$

The exact same approximation can also be obtained by neglecting the $o(\sigma^4)$ term in the system of hydrodynamic equations (4.5), which yields

$$\begin{cases} \bar{v} = 0 \\ \bar{m} = \frac{\lambda + U_0}{|g|} \end{cases}, \quad (4.13)$$

an expression that is perfectly equivalent to equation (4.11).

Such an approximation may seem naive at first but actually yields rather good results. Looking at the example of quadratic external potential $U_0(x) = -\mu\omega_0^2 x^2/2$, one can infer, through the normalisation of the distribution of players, that

$$\lambda = \left[\frac{3|g|}{4} \sqrt{\frac{\mu\omega_0^2}{2}} \right]^{2/3}, \quad (4.14)$$

and check that in the bulk of the distribution, as illustrated on Figure (12), the approximation agrees perfectly with the exact result.

The tails of the distribution, for which player density is low, and thus where interactions effects are small, constitute the only place where diffusion has to be taken into account. As such, they cannot be properly described by Thomas-Fermi approximation and call for a specific treatment.

4.1.3 Tails of the distribution: semi-classical approximation

Thomas-Fermi approximation yields good results in the bulk of the distribution, i.e. for $\lambda > -U_0(x)$, but fails to describe regions where

Such configurations are bound to happen as long as one assumes (strong) repulsive interactions will cause agents to spread despite the confining effect of U_0 .

Note that, as mentioned above, $U_0(x)$ has to be understood as a gain and, to have a confining effect, it has to reach its maximum value for a finite value of x , thus the negative sign.

the density of agents is small. If this density is sufficiently small however, for example in the tails of the distribution where $\lambda + U_0$ is sufficiently negative, the problem simplifies once again because the non-linear term that represents interactions becomes negligible. In this context equation (4.3) now reads

$$-\lambda \bar{\Psi}(x) \approx \frac{\mu\sigma^4}{2} \partial_{xx} \bar{\Psi}(x) + U_0(x) \bar{\Psi}(x), \quad (4.15)$$

and we will address it here through a semi-classical approximation. More specifically, we look for solutions of equation (4.15) in the form $\Psi_{\text{SC}}(x) = \psi(x) \exp\left(S(x)/\sqrt{\mu\sigma^4}\right)$ up to the second order in σ^2 . As an example, we will once again look at the case of quadratic external potential $U_0(x) = -\mu\omega_0^2 x^2/2$, and compare the approximation to numerical results. In order to keep the core of the text concise, details of the computation are provided in appendix G. The semi-classical approximation yields

$$\Psi_{\text{SC}}(x) = \left[\frac{C}{\mu\omega_0^2 x^2 - 2\lambda} \right]^{1/4} \exp \left\{ \frac{\lambda}{\mu\omega_0 \sigma^2} \left[x \sqrt{\frac{\mu\omega_0^2}{2\lambda}} \sqrt{x^2 \frac{\mu\omega_0^2}{2\lambda} - 1} - \operatorname{argcosh} \left(x \sqrt{\frac{\mu\omega_0^2}{2\lambda}} \right) \right] \right\}, \quad (4.16)$$

where C is a constant numerically determined to match with the bulk of the distribution. As illustrated Figure (13), results provided by this approximation are in very good agreement with the actual solution of equation (4.3) for $x > \sqrt{\frac{2\lambda}{\mu\omega^2}}$.

However, one can note that, for this approximation scheme, the (so-called) turning point $x = X$, where the Thomas-Fermi solution Ψ_{TF} vanishes, is singular. This can be easily avoided by way of a uniform approximation [76]

$$\Psi_{\text{SC}} = \begin{cases} C_{\text{left}} \left(\frac{8\pi S_{\text{left}}}{3U_0} \right)^{1/2} \cos\left(\frac{\pi}{3}\right) [J_{1/3}(S_{\text{left}}) + J_{1/3}(S_{\text{left}})] & \text{if } x < X \\ 2C_{\text{right}} \left(\frac{8S_{\text{right}}}{\pi |U_0|} \right)^{1/2} \cos\left(\frac{\pi}{3}\right) K_{1/3}(S_{\text{right}}) & \text{if } x > X \end{cases}, \quad (4.17)$$

where C_{left} and C_{right} are constants to be numerically determined, J_γ stands for the Bessel function of the first kind of order γ and K_γ for the modified Bessel function of the second kind. Explicit expressions for the actions S_{left} and S_{right} , in the case of the quadratic gain $U_0(x) = -\mu\omega_0^2 x^2/2$, are provided in Appendix G. Figure (14) illustrates how this uniform approximation, equation (4.17), constitutes an improvement over the previous one, equation (4.16).

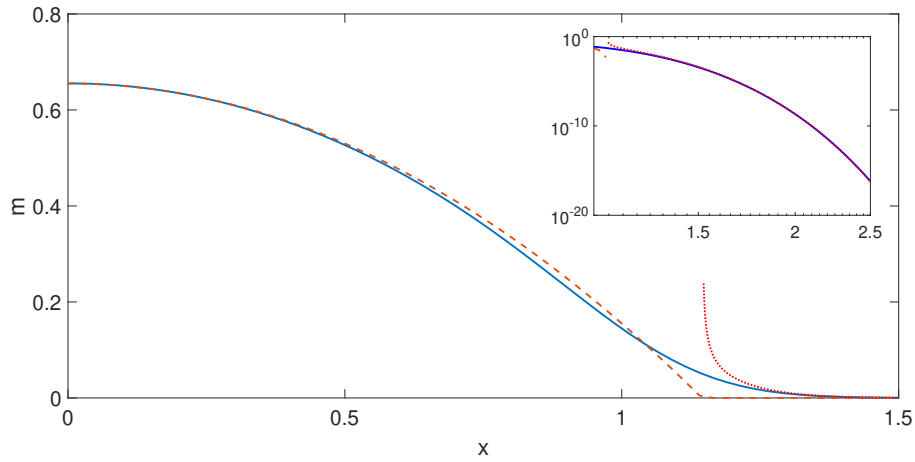


Figure 13: Computational solution of the Gross-Pitaevskii equation (full), Thomas-Fermi approximation (dashed) and semi-classical approximation (dot). The inset shows the same curves in Log-Linear plot focusing on the tail of the distribution. Parameters for this figure are $g = -2, \sigma = 0.4, \mu = 1, U_0(x) = -x^2$ and $C = 8 \cdot 10^{-4}$.

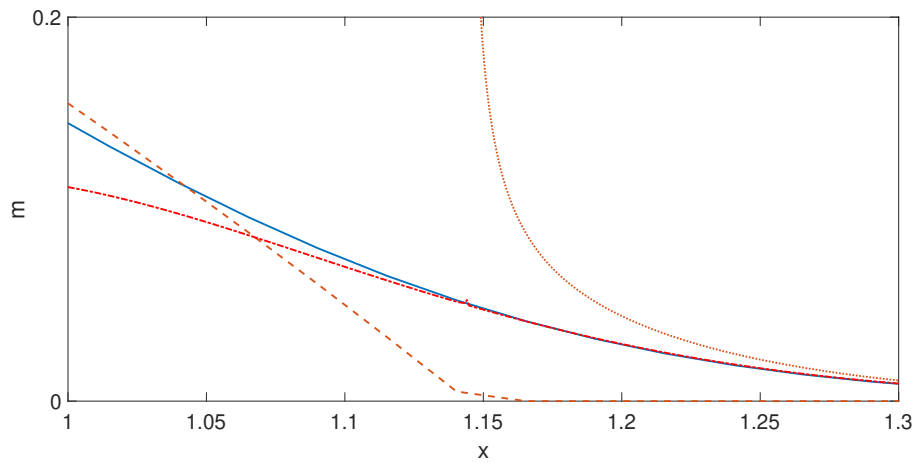


Figure 14: Computational solution of the Gross-Pitaevskii equation (full), Thomas-Fermi approximation (dashed), semi-classical approximation (dot) and uniform approximation (dash-dot). Parameters for this figure are to $g = -2, \sigma = 0.4, \mu = 1, U_0(x) = -x^2, C_{\text{left}} = 0.14$ and $C_{\text{right}} = 0.07$.

Depending on the specifics of $U_0(x)$, computing this approximation may become somewhat involved. If so, the tails of the distribution can still be described by an Airy function, as discussed in [40], using the consistently simpler, albeit less accurate, approximation method of linearising the external gain around the turning point $x \approx X$ and looking at the asymptotic behaviour.

4.1.4 Some properties of the ergodic state

To conclude this section on the ergodic state, I shall describe here some of its properties that will prove to be essential when trying to connect it to the beginning (or end) of the game.

4.1.4.1 Final cost and energy

Something that may not appear clearly from the original definition of the ergodic state, equations (2.26), but becomes obvious when looking at its hydrodynamic counterpart, equations (4.13), is that, for quadratic MFG in the strong repulsive interactions regime, the value function u becomes essentially flat during the ergodic state

$$\bar{v} = 0 \quad \Leftrightarrow \quad \bar{u} = \bar{K} + o(\sigma^2), \quad (4.18)$$

where the $o(\sigma^2)$ term represents corrections to the Thomas-Fermi approximation and \bar{K} is a constant. MFG equations (4.1) being invariant by translation of u , I will choose this constant \bar{K} to be zero for the remainder of this chapter. In the upcoming sections, this characteristic $\bar{u} = 0$ will be used as an *effective* terminal condition when discussing the beginning of the game.

Another interesting aspect of the ergodic state is that it provides an easy access to the (conserved) energy $E = \bar{E}$ of the system

$$\bar{E} = \int_{\mathbb{R}} dx \left[\frac{g}{2} \bar{m}^2 + \bar{m} U_0 dx \right] < 0, \quad (4.19)$$

neglecting $o(\sigma^4)$ terms of the *kinetic* energy. By definition, because interactions are chosen to be repulsive and the external gain to be confining (which implies it can be chosen negative for all x), the energy has to be negative.

What those two properties allow is for one to restrict their analysis of the transient states to games of negative energy and flat cost terminal conditions, making for a simpler discussion of the time-dependent problem.

4.1.4.2 Approaching the ergodic state : stability analysis

To conclude this section, I discuss the stability of the ergodic state. Focusing mainly on the bulk of the distribution, I will use the hydrodynamic representation as it is the better framework to deal with the

small σ limit. Recalling equations (4.13), the expression of the ergodic state under this representation

$$\begin{cases} \bar{v} = 0 \\ \bar{m} = -\frac{\lambda + U_0}{g} \end{cases}, \quad (4.20)$$

one can then apply small perturbations δm and δv to this stationary state and compute their evolution. Near the ergodic state equations (2.32) become

$$\begin{cases} \delta \dot{m} = -\partial_x(\bar{m}\delta v) \\ \delta \dot{v} = -\frac{g}{\mu}\partial_x\delta m \end{cases}, \quad (4.21)$$

implying

$$\delta \ddot{m} = \frac{g}{\mu}\partial_x(\bar{m}\partial_x\delta m). \quad (4.22)$$

Assuming that $\delta m = \delta m_0 e^{\omega t}$, equation (4.22) amounts to the eigenvalue problem

$$\hat{D}\delta m_0 = -\frac{\mu}{g}\omega^2\delta m_0, \quad (4.23)$$

with

$$\hat{D} \equiv -\partial_x(\bar{m}(\bar{x})\partial_x). \quad (4.24)$$

It is relatively straightforward to show that \hat{D} is a real symmetric operator, implying its eigenvalues are real, and furthermore that all these eigenvalues are positive (cf Appendix. H). Denoting by ϵ_i these real eigenvalues and by $\varphi_i(x)$ the corresponding eigenvector, the *linear modes* in the vicinity of (\bar{m}, \bar{v}) take the form

$$\mathcal{Q}_{(i)}^\pm = \left(\delta m_{(i)}, \delta v_{(i)}^\pm \right) \equiv \left(\varphi_i(x), \pm \sqrt{-g/\mu\epsilon_i}\partial_x\varphi_i(x) \right), \quad (4.25)$$

One should be reminded that g is negative in this context.

and follow an exponential time dependence

$$\begin{cases} \mathcal{Q}_{(i)}^\pm(t) = e^{\pm\omega_i t}\mathcal{Q}_{(i)}^\pm(0) \\ \omega_i = \sqrt{\frac{-g\epsilon_i}{\mu}} \end{cases}. \quad (4.26)$$

This exponential behaviour highlights the fact that, as discussed in [108] in a simpler (variational) context, the ergodic state should be understood as a *unstable / hyperbolic* fixed point, which is approached exponentially fast at small times, and departed from similarly quickly near the end of the game T .

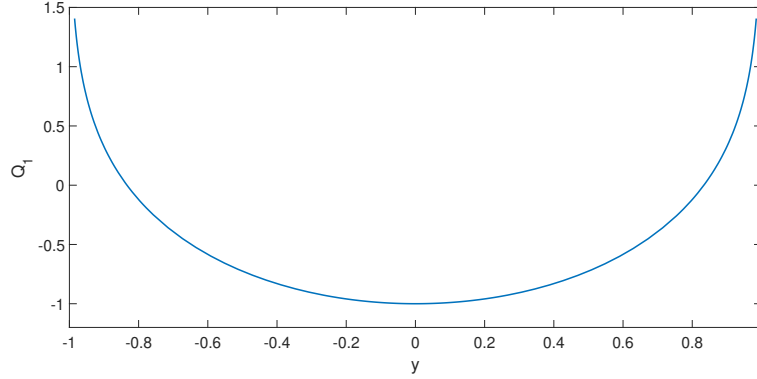


Figure 15: First order Legendre polynomial of the second kind. Its effect on the ergodic state would be to add feet to the distribution.

Returning to the particular case of quadratic external gain $U_0 = -\mu\omega_0^2 x^2/2$, and assuming, as is the case above, that $\delta m \propto e^{\pm\omega t}$, one obtains

$$\begin{cases} -2 \left(\frac{\omega}{\omega_0} \right)^2 \delta m = \partial_y [(1-y^2)\partial_y \delta m] \\ y = x \sqrt{\frac{\mu\omega_0^2}{2\lambda}} \end{cases}, \quad (4.27)$$

a Legendre equation defined for $0 \leq y \leq 1$. Dismissing odd ones, the solution with smallest eigenvalue (for $\omega = \omega_0$) is the first order Legendre polynomial of the second kind, hence

$$\delta m \sim Q_1(y) e^{\pm\omega_0 t}. \quad (4.28)$$

As shown on Figure (15), the effect of this perturbation is simply to add tails to the distribution of agents, which is qualitatively in good agreement with simulations.

4.2 TIME DEPENDENT PROBLEM: THE BEGINNING OF THE GAME

As was previously argued, different length scales are associated with different dynamical regimes: very short distances $L \ll \nu$ are dominated by diffusion, while, for longer ones $L \gg \nu$, interactions take over. As the typical size of the distribution of agents further increases, however, interaction effects become weaker (although the effects of diffusion decrease even more rapidly) and, even in the large $|g|$ limit, the ergodic state is eventually characterized by a balance between interaction energy E_{int} and potential energy E_{pot} . The fact that this balance has to be reached is precisely what fixes the extension of the ergodic state distribution.

To consider a system which traverses all dynamical regimes, one then has to assume that the initial distribution is extremely narrow.

The large interaction limit considered in this chapter essentially implies that the healing length ν is much smaller than any characteristic feature of the individual (external) gain $U_0(x)$.

As such, the beginning of the game will mainly consist in an expansion of this initial distribution, expansion that will go on until the balance between E_{int} and E_{pot} is reached. During that expansion, under the assumption that $|g|$ is sufficiently large [109], one may neglect the effects of the external potential. To describe the earlier stages of the game it is, hence, sufficient to study the set of equations (2.29) in the particular case of $U_0(x) = 0$

$$\begin{cases} -\mu\sigma^2\partial_t\Phi(t,x) = \frac{\mu\sigma^4}{2}\partial_{xx}\Phi(t,x) + g\Phi^2(t,x)\Gamma(t,x) \\ +\mu\sigma^2\partial_t\Gamma(t,x) = \frac{\mu\sigma^4}{2}\partial_{xx}\Gamma(t,x) + g\Phi(t,x)\Gamma^2(t,x) \end{cases}. \quad (4.29)$$

While it can be shown that this system is integrable (in the sense that there exists a canonical transform from (Φ, Γ) to action-angle variables), with this section I do not aim to explicitly make use of this property. Rather, I will argue that those various limiting regimes can be efficiently investigated through the use of variational ansätze. Finally, to simplify the analysis even further, based on results from section 4.1.4 on the ergodic value function (which can here be interpreted as a final cost for the beginning of the game), upcoming discussions will be made under the assumption that the terminal cost is essentially flat.

4.2.1 Large ν regime : Gaussian ansatz

When the extension of the distribution of agents is small in front of ν , the effects of diffusion become dominant, and equations (4.29) become simple heat equations, for which the Green's function has a Gaussian shape. It is therefore natural to tackle this regime using Gaussian variational approach [91], already applied to MFG models featuring large attractive interactions [108].

4.2.1.1 Preambular definitions

Variational approximation amounts to minimizing the action (2.33) on a small subclass of functions (here chosen so that the distribution of agents is Gaussian), effectively reducing a problem with an infinite number of degrees of freedom to one with a finite, easily manageable, number. As in [108] I consider the following ansatz

$$\begin{cases} \Phi(x,t) = \exp\left[\frac{(-\Lambda_t/4 + P_t \cdot x)}{\mu\sigma^2}\right] \frac{1}{(2\pi\Sigma_t)^{1/4}} \exp\left[-\frac{(x - X_t)^2}{(2\Sigma_t)^2} \left(1 - \frac{\Lambda_t}{\mu\sigma^2}\right)\right] \\ \Gamma(x,t) = \exp\left[\frac{(+\Lambda_t/4 - P_t \cdot x)}{\mu\sigma^2}\right] \frac{1}{(2\pi\Sigma_t)^{1/4}} \exp\left[-\frac{(x - X_t)^2}{(2\Sigma_t)^2} \left(1 + \frac{\Lambda_t}{\mu\sigma^2}\right)\right] \end{cases}, \quad (4.30)$$

which indeed yields a Gaussian distribution centered in X_t with standard deviation Σ_t

$$m(t, x) = \Gamma(t, x)\Phi(t, x) = \frac{1}{\sqrt{2\pi\Sigma_t^2}} \exp\left[-\frac{(x - X_t)^2}{2(\Sigma_t)^2}\right], \quad (4.31)$$

and where P_t and Λ_t respectively are the momentum and the position-momentum correlator of the system. Inserting this variational ansatz in the action (2.33) one gets

$$\tilde{S} = \int_0^T \tilde{L}(t) dt \quad (4.32)$$

where the Lagrangian $\tilde{L} = \tilde{L}_\tau + \tilde{E}_{\text{kin}} + \tilde{E}_{\text{int}} + \tilde{E}_{\text{pot}}$ only depends on X_t , P_t , Σ_t , Λ_t and their time derivatives. This yields

$$\begin{cases} \tilde{L}_\tau = \dot{P}_t X_t - \frac{\Lambda_t}{2\Sigma_t} \dot{\Sigma}_t & \tilde{E}_{\text{kin}} = \frac{P_t^2}{2\mu} + \frac{\Lambda_t^2 - \mu^2\sigma^4}{8\mu\Sigma_t^2} \\ \tilde{E}_{\text{int}} = \frac{g}{4\sqrt{\pi}\Sigma_t} & \tilde{E}_{\text{pot}} = \int_{\mathbb{R}} U_0(x)m(t, x) dx \end{cases} \quad (4.33)$$

As long as the density of players $m(t, x)$ remains narrow enough that $U_0(x)$ can be linearised on the distance Σ_t , one may assume that $\tilde{E}_{\text{pot}} \approx U_0(X_t)$ and that the variables (X_t, P_t) and (Σ_t, Λ_t) decouple. As discussed in [108], (X_t, P_t) then follows the dynamics of a point particle of mass μ subjected to the external potential $U_0(x)$. The discussion below, in which the approximation $U_0(x) = 0$ is considered, could therefore be generalized straightforwardly to this aforementioned situation (by simply adding the motion of the center of mass).

4.2.1.2 Evolution of the reduced system $(X_t, \Sigma_t; P_t, \Lambda_t)$ for $U_0(x) = 0$

Minimizing the action with respect to each parameter yields the evolution equations

$$\begin{cases} \dot{X}_t = \frac{P_t}{\mu} & \dot{P}_t = 0 \\ \dot{\Sigma}_t = \frac{\Lambda_t}{2\mu\Sigma_t} & \dot{\Lambda}_t = \frac{\Lambda_t^2 - \mu^2\sigma^4}{2\mu\Sigma_t^2} + \frac{g}{2\sqrt{\pi}\Sigma_t} \end{cases} \quad (4.34)$$

Under the assumption that $U_0(x) = 0$, P_t is a constant and is essentially a measure of the asymmetry of $\Phi(t, x)$ and $\Gamma(t, x)$ as well as the drift of the center of mass of the distribution of players. If $\Phi(t, x)$ and $\Gamma(t, x)$ are symmetric with respect to $x = x_0$, $P_t = 0$ and the center of mass does not move. For the sake of simplicity, let us focus on this configuration and let $X_t = x_0 = 0$. The equations concerning $(\Sigma_t; \Lambda_t)$ are more complicated but can be decoupled using the fact that the total energy of the system $\tilde{E}_{\text{tot}} = \tilde{E}_{\text{kin}} + \tilde{E}_{\text{int}} + \tilde{E}_{\text{pot}}$ is conserved, hence

$$\tilde{E}_{\text{tot}} = \frac{\mu\dot{\Sigma}^2}{2} - \frac{\mu\sigma^4}{8\Sigma_t^2} + \frac{g}{4\sqrt{\pi}\Sigma_t}. \quad (4.35)$$

4.2.1.3 *Zero-energy solution*

In the limiting case where $U_0(x)$ is negligible for all times (not just the initial expansion we consider here), and assuming an infinitely long game, the distribution of agents will spread indefinitely, tending towards a perfectly diluted state $m(t, x) \approx 0$. This would correspond to an (asymptotic) ergodic state $\bar{\Sigma} \rightarrow \infty$ of energy $\tilde{E}_{\text{tot}} \rightarrow 0$. In that case the the evolution equation (4.35) reads

$$\dot{\Sigma}_t = \frac{1}{\Sigma_t} \sqrt{\frac{\mu\sigma^4\sqrt{\pi} - 2g\Sigma_t}{4\mu\sqrt{\pi}}}, \quad (4.36)$$

which can be integrated as

$$\sqrt{1 - \frac{2\Sigma_t}{\sqrt{\pi}\eta}} \left(1 + \frac{\Sigma_t}{\sqrt{\pi}\eta}\right) - \sqrt{1 - \frac{2\Sigma_0}{\sqrt{\pi}\eta}} \left(1 + \frac{\Sigma_0}{\sqrt{\pi}\eta}\right) = -\frac{3t}{2\pi\tau}, \quad (4.37)$$

Σ_0 being the initial width of the distribution.

 4.2.1.4 *Finite-energy solutions*

In practice, according to section 4.1.4, the energy of the ergodic state is known to be negative and, as such, one should mainly be interested in negative energy solutions. In that case, it is important to note that Σ_t cannot grow past a certain value $\Sigma^* = \frac{g\sqrt{\pi} + \sqrt{g^2/\sqrt{\pi} - 8\mu\sigma^4 \tilde{E}_{\text{tot}}}}{8\tilde{E}_{\text{tot}}}$ otherwise $\dot{\Sigma}_t$ would become complex valued. If $\tilde{E}_{\text{tot}} < 0$, equation (4.35) can be integrated as

$$F(8E_{\text{tot}}, -2g/\sqrt{\pi}, \mu\sigma^4; \Sigma_t) - F(8E_{\text{tot}}, -2g/\sqrt{\pi}, \mu\sigma^4; \Sigma_0) = \frac{t}{2\sqrt{\mu}}, \quad (4.38)$$

where $F(a, b, c; x)$ is defined as

$$\begin{aligned} F(a, b, c; x) &= \int \frac{xdx}{\sqrt{ax^2 + bx + c}} \\ &= \frac{b}{2|a|^{3/2}} \arcsin \left[\sqrt{\frac{4a^2}{b^2 - 4ac}} \left(x + \frac{b}{2a}\right) \right] + \frac{\sqrt{ax^2 + bx + c}}{a}. \end{aligned} \quad (4.39)$$

For completeness, I also provide solution of equation (4.35) in the case of positive energy

$$\begin{aligned} G(8\sqrt{\pi}E_{\text{tot}}, -2g, \mu\sigma^4\sqrt{\pi}; \Sigma_t) \\ - G(8\sqrt{\pi}E_{\text{tot}}, -2g, \mu\sigma^4\sqrt{\pi}; \Sigma_0) &= \frac{t}{2\sqrt{\mu\sqrt{\pi}}}, \end{aligned} \quad (4.40)$$

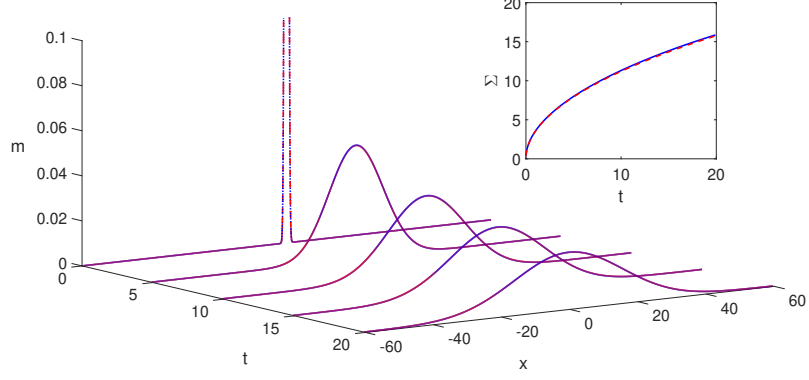


Figure 16: Computational solution of the Gross-Pitaevskii equation with Gaussian initial condition (blue dot) and variational ansatz (red dashed). The inset shows the time evolution of the numerical variance (blue full) and Σ_t (red dashed) as defined in equation (4.38). In this case $g = -2$, $\sigma = 3.5$, $\mu = 1$, $\Sigma_0 = 0.2$ and $T = 20$.

where $G(a, b, c; x)$ is defined as

$$G(a, b, c; x) = \begin{cases} \frac{\sqrt{ax^2 + bx + c}}{a} \\ -\frac{b}{2|a|^{3/2}} \operatorname{argsinh} \left[\sqrt{\frac{4a^2}{b^2 - 4ac}} \left(x + \frac{b}{2a} \right) \right] & \text{if } \frac{b^2}{4ac} > 1 \\ \frac{\sqrt{ax^2 + bx + c}}{a} \\ -\frac{b}{2|a|^{3/2}} \operatorname{argcosh} \left[\sqrt{\frac{4a^2}{4ac - b^2}} \left(x + \frac{b}{2a} \right) \right] & \text{if } \frac{b^2}{4ac} < 1 \end{cases} \quad (4.41)$$

It can be worth noting that in the $t \rightarrow 0$ limit, equations (4.36), (4.38) and (4.40) yield similar behaviour for Σ_t , scaling as $t^{2/3}$. This type of variational approach yields quantitatively accurate results, illustrated Figure (16), as long as $\Sigma_t \ll \nu$. With that, I conclude my discussion of the large ν regime, next I will address the small ν one.

4.2.2 Small ν regime : Parabolic ansatz

As was shown in a previous paper [19], and argued at length in chapter 3, in the weak noise, infinite optimization time limit of the potential-free negative coordination MFG, the distribution of players quickly deforms to take the shape of an inverted parabola that scales with time. These parabolic solutions can be interpreted as arising from a low order approximation of a multipolar expansion (3.21) in an electrostatic representation of the problem [19]. Furthermore, simulations indicate that, under the assumption that the variations of the

terminal cost are small compared to $\tilde{u} = \mu\sigma^2$, (non scaling) inverted parabolas are still stable solutions of equations (4.29) with finite optimization time.

Imposing the normalisation condition $\{\int_{\mathbb{R}} m(t, x) dx = 1 \ \forall t\}$ one can thus consider the ansatz

$$m(t, x) = \begin{cases} \frac{3(z(t)^2 - x^2)}{4z(t)^3} & \text{if } z(t) > x \\ 0 & \text{otherwise} \end{cases}, \quad (4.42)$$

already introduced in chapter 3, and look for a formal solution outside the singularities in the derivative at $x = \pm z(t)$. It is worth mentioning that such an approach already exists in the realm of cold atoms [41] [23]. However, differences arise from the fact that, contrary to NLS equation, equations (4.29) do not feature complex time dynamics, and from the quintessential forward-backward structure of MFG.

In practice, in this subsection, I shall examine (as an independent problem) an effective potential-free (i.e. $U_0(x) = 0$) game in the small ν regime. Once again, I shall assume that the final condition, at $t = \tilde{T}$, is that of a flat terminal cost $\tilde{c}_{\tilde{T}}(x) = 0$. Moreover, I will consider that the initial density of agents, at $t = 0$, is essentially a Dirac delta function, or in other words, an inverted parabola of the form (4.42) with $z(t=0) = z_0 = 0$. Note that, as I will still assume that the healing length ν is the smallest length size of the problem, this implies that I actually consider in this section the limit $\nu, z_0 \rightarrow 0$ with $z_0 \gg \nu$. In the context of the original game, this effective game will correspond to the expansion phase beyond the healing scale ν . How it will be coupled to the ergodic state or to the small ν regime will be examined subsequently, but as the conserved energy of the ergodic state is negative, I will consider more specifically this regime.

4.2.2.1 Preambular definitions

While the Schrödinger representation of MFG equations (4.1), along with the Gaussian variational ansatz, were well-suited to describe a large ν regime, the hydrodynamic representation is actually more convenient to deal with the small noise limit. In the context of cold atoms, the equivalent of the $o(\sigma^4)$ term in hydrodynamic equations (2.32) is considered to be safely negligible as long as the extension of the condensate is large in front of the healing length ν . Focusing on this weak noise regime (Thomas-Fermi approximation) here amounts to studying the system

$$\begin{cases} \partial_t m + \partial_x(mv) = 0 \\ \partial_t v + \partial_x \left[\frac{v^2}{2} + \frac{g}{\mu} m + \frac{U_0}{\mu} \right] = 0 \end{cases}. \quad (4.43)$$

Going through Madelung substitution shows that we can get away with only neglecting $o(\sigma^4)$ terms while absorbing $o(\sigma^2)$ contributions in the definition of v equation (2.31), which is not as transparent from equations (4.1).

As will be argued below, one can find exact solutions of equations (4.43) assuming the parabolic form (4.42), and, therefore, one does not need to resort to the action (2.33) to derive the corresponding dynamics.

4.2.2.2 Elementary integration of the hydrodynamic representation

In the $U_0(x) = 0$ limit, the expression of the velocity associated to a parabolic distribution, ansatz (4.42), can easily be extracted from the continuity equation in (4.43). Integrating over $[-\infty; x]$ and taking into account that m vanishes at infinity, one obtains

$$v(t, x) = \frac{z'(t)}{z(t)} x. \quad (4.44)$$

To derive the time evolution of $z(t)$, one can insert the explicit forms of $m(t, x)$ and $v(t, x)$ in the second equation of equations (4.43), yielding

$$z''(t) = \frac{3g}{2\mu z(t)^2}. \quad (4.45)$$

This closely resembles what can be found when dealing with expanding Bose Einstein condensates [23], one main difference lying in the fact that the multiplicative constant in front of $1/z^2$ is negative in the context of MFG but positive in the context of Bose Einstein condensates. This last equation (4.45) can be integrated as

$$z'(t)^2 = -\frac{3g}{\mu} \left[\frac{1}{z(t)} + \frac{\epsilon}{z_*} \right]. \quad (4.46)$$

For commodity the integration constant has been written as $3|g|\epsilon/\mu z_*$ where ϵ can take the values $-1, 0$ or 1 , and z_* is a constant of same dimension as z (in this case a length). As will be discussed below, the values $-1, 0$ or 1 of ϵ correspond to negative, zero or positive energies. Furthermore, it will be shown that, in the particular case of $\epsilon = -1$, $z_*(> 0)$ can be interpreted as the final extension $z(\tilde{T})$ of the distribution of players in the effective game. In the context Bose Einstein condensates, only the positive ϵ case is relevant [23], and the fact that, here, zero or negative ϵ may be considered as well, which allows for new sets of solutions, constitutes another important difference.

4.2.2.3 Characterisation of $z(t)$

To solve this equation, let us introduce two functions $\zeta^+(y) > 0$ and $\zeta^-(y) \in [0; 1]$, associated with $+1$ and -1 values of ϵ , implicitly defined through the relations

$$\sqrt{\zeta^+(y)(1 + \zeta^+(y))} - \operatorname{argsinh} \sqrt{\zeta^+(y)} = y \quad \forall y > 0, \quad (4.47)$$

and

$$\arcsin \sqrt{\zeta^-(y)} - \sqrt{\zeta^-(y)(1 - \zeta^-(y))} = y \quad \forall y \in [0, \frac{\pi}{2}]. \quad (4.48)$$

One should also define a third function $\zeta^0(t)$ given explicitly as

$$\zeta^0(y) = \left(\frac{3y}{2}\right)^{2/3} \quad \forall y > 0, \quad (4.49)$$

which corresponds to the $\epsilon = 0$ solution discussed in chapter 3. It is worth noting that all three functions are monotonous, increasing functions of time and have the following properties

$$\begin{cases} \zeta^+(0) = \zeta^-(0) = \zeta^0(0) = 0 \\ \zeta^+(y) > \zeta^0(y) \quad \forall y \\ \zeta^0(y) > \zeta^-(y) \quad \forall y \in]0, \frac{\pi}{2}] \\ \zeta^+(y) \approx \zeta^0(y) \approx \zeta^-(y) \quad \text{as } y \rightarrow 0 \end{cases}.$$

One can now write the different solutions of equation (4.46) in terms of the above functions. Even if only repulsive interactions are considered, because of the square power in equation (4.46), its solutions can either be increasing or decreasing. There are three families of increasing solutions

$$z(t) = \begin{cases} z_* \zeta^+(\alpha z_*^{-3/2} t) & \text{if } \epsilon = 1 \\ \zeta^0(\alpha t) & \text{if } \epsilon = 0 \\ z_* \zeta^-(\alpha z_*^{-3/2} t) & \text{if } \epsilon = -1 \end{cases}, \quad (4.50)$$

where $\alpha = \sqrt{-3g/\mu}$. The reciprocal three families of decreasing solutions are irrelevant to this chapter's discussion as they will not ultimately lead to the ergodic state introduced section 4.1. Still, a succinct analysis of those solutions are provided in appendix I for the sake of completeness.

One should now wonder how the boundary conditions of the effective game constrain solutions within the family (4.50). The aforementioned initial condition that the density of agents starts as a Dirac delta function, which imposes that $z(t=0) = 0$, is actually already implemented in equation (4.50). One, then, only has to consider the

terminal boundary condition, i.e. the fact that at \tilde{T} the terminal cost is flat. Recalling the definition of the velocity

$$v = -\frac{\partial_x u}{\mu} + o(\sigma^2), \quad (4.51)$$

its expression (4.44) in the small ν regime implies that the terminal cost $c_{\tilde{T}}(x) = u(\tilde{T}, x)$ can be constant only if the time derivative of $z(t)$ is zero. According to equation (4.46), this is only possible if $\epsilon = -1$ and $z(t) = z_*$. Hence, the study of the effective game considered in this section can be reduced to that of "-" type solutions and one can infer that $z_* = z(\tilde{T})$. Now, one can check easily from equation (4.48) that $\xi^-(\pi/2) = 1$ (which is compatible with the fact that $\xi^-(y) \in [0; 1]$ is an increasing monotonous function defined for $y \in [0, \pi/2]$). From equation (4.50) one can then deduce

$$z(\tilde{T}) = z_* \quad \Rightarrow \quad \alpha z_*^{-3/2}(\tilde{T}) = \frac{\pi}{2}. \quad (4.52)$$

This yields a relation between the final time of the effective game \tilde{T} and the final extension of the distribution of players

$$\tilde{T} = \frac{\pi z_*^{3/2}}{2\alpha}. \quad (4.53)$$

The duration of the effective game, i.e. the time it takes to go from a narrow, delta-like, initial distribution of agents to a flat terminal cost, thus determines the parameter z_* , and therefore fixes which member of the family equation (4.50) has to be considered.

Inserting equation (4.50) in the ansätze (4.42) and (4.44), directly yields explicit expressions for m and v , which, as illustrated on Figure (17), provide excellent approximations, even when the noise σ , and thus the healing length ν , is not strictly zero (see captions for details).

4.2.2.4 Energy of the system

The energy plays a crucial role in the dynamics of the spreading of players and its conservation is a key property one can use to match different regimes of approximation. Because the ultimate goal of this chapter is to propose a method to link this regime, representing early stages of the game, to the ergodic state described in section (4.1), this section will focus on negative energy only. In the potential-free regime, the energy contains two terms, one represents kinetic energy (associated with the diffusion term), while the other comes from the interactions. Dropping the $o(\sigma^4)$ term in the definition equation (4.2) of the kinetic energy, we thus have $E = E_{\text{kin}} + E_{\text{int}}$, with

$$\begin{cases} E_{\text{kin}} = \frac{\mu}{2} \int_{-z}^z m v^2 dx \\ E_{\text{int}} = \int_{-z}^z \frac{g m^2}{2} dx \end{cases}. \quad (4.54)$$

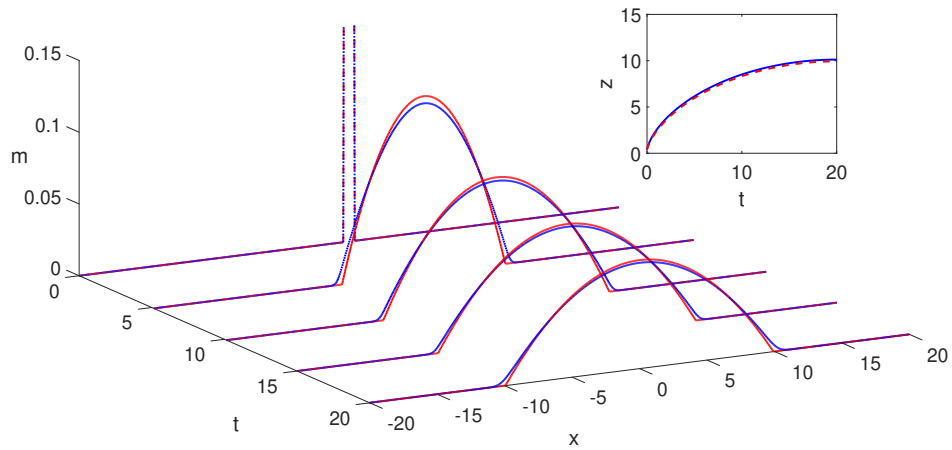


Figure 17: Computational solution of the Gross-Pitaevskii equation (blue dot) and parabolic ansatz (red dashed). The inset shows the time evolution of z numerically (blue full) and analytically (red dashed). In this case, parameters are chosen to be $g = -2$, $\sigma = 0.45$ and $\mu = 1$, meaning $\nu \approx 0.02$. The actual (numerical) game takes place from $t = 0$, when it starts as an inverted parabola of extension 0.4, to $t = T = 20$ when the terminal cost is flat. The effective game essentially starts at time $t \approx -0.07$ as a Dirac delta function and its effective duration is $\tilde{T} \approx 20.07$. The only difference between the numerical results and the parabolic ansatz comes from the fact that σ is non-zero in the simulation. This figure also illustrates how the Thomas-Fermi approximation becomes more and more effective as the typical extension of the density becomes larger in front of ν .

As the energy is conserved, it can be evaluated at any time, and particularly at the end of the effective game. If $\epsilon = 0$, $z \rightarrow \infty$ as $t \rightarrow \infty$ and it becomes clear that, in this case, $E = 0$. A similar reasoning would show that, asymptotically if $\epsilon = +1$, $E \sim 1/z_*^2 > 0$. When $\epsilon = -1$, however, we can evaluate the energy at $t = \tilde{T}$, when $z = z_*$ and $v = 0$, which trivially implies that, at that point and within the Thomas-Fermi approximation, kinetic energy is zero. Inserting equation (4.42) with $z(t) = z_*$ into the second equation (interaction energy) of system (4.54) one obtains

$$\begin{cases} E_{\text{kin}}^-(\tilde{T}) = 0 + o(\sigma^4) \\ E_{\text{int}}(\tilde{T}) = \frac{3g}{10z_*} \end{cases}, \quad (4.55)$$

which, using equation (4.53) implies

$$E = \frac{3g}{10z_*} = \frac{3g}{10} \left(\frac{2\alpha\tilde{T}}{\pi} \right)^{-2/3}. \quad (4.56)$$

For the effective game considered here – narrow initial density, flat terminal cost $v(\tilde{T}) = 0$, small ν regime and individual gain $U_0(x) = 0$ – there is a strong link between the duration of the game \tilde{T} and the energy E . In some sense \tilde{T} monitors the dynamics of the spreading of the players completely, and takes the same role as \tilde{E}_{tot} did in the large ν regime. As such, finite games with flat terminal cost correspond to non-zero energy and there is a one-to-one relation between \tilde{T} and E .

This closes the analysis of the small ν regime, and more generally of the expansion regime. The next section will now address ways to relate those transient times to the ergodic state.

4.3 THE ENTIRE GAME

In this section will be examined how the previously discussed regimes of approximation couple with one another. Section 4.3.1 will first address, once again, an effective game, in the vein of the one studied in section 4.2.2, but assuming a finite value of healing length so that players are initially distributed on a distance much smaller than ν . This allows to focus on the transition from a large to a small ν regime during the initial stages of the game. Then, in section 4.3.2 will be considered the matching of the expansion phase, described by the effective game, with the ergodic state.

4.3.1 Matching small and large ν regimes

As mentioned above, this section, just as section 4.2.2, will feature an effective potential-free game of duration \tilde{T}_4 , with flat terminal cost and an initial distribution of agents which width Σ_0 is much smaller

that the healing length ν . Furthermore, it will be assumed that the optimization time is large enough so that, at the end of the game, the distribution of players has spread on a distance much larger than the healing length ν .

Under those assumptions, one can distinguish two main phases the effective game will go through: an initial phase which can be described by the Gaussian ansatz introduced section 4.2.1 and, at the end of the game, a terminal phase for which the density of agents will evolve according to the parabolic ansatz of section 4.2.2. Between those two phases, the density will transition from a Gaussian-like distribution to an inverted parabola. The precise shape of the density during the crossover is complicated to describe, and will not be addressed here, but, as will soon be argued, one can still estimate the dynamics of the spreading of players across the two regimes.

To proceed, let us introduce a couple of quantities that will characterise the dynamics. The first one is the total energy E of the system, a conserved quantity, which is common to both regimes. The second is the time t_{tr} at which the system will transition from the Gaussian regime to the parabolic one.

Seen from the Gaussian side of the transition, the transition time t_{tr}^{G} is defined by the condition

$$\Sigma(t_{\text{tr}}^{\text{G}}) = \nu, \quad (4.57)$$

which, through equation (4.38), provides a relation between E and t_{tr}^{G}

$$F(8E, -2g/\sqrt{\pi}, \mu\sigma^4; \nu) - F(8E, -2g/\sqrt{\pi}, \mu\sigma^4; \Sigma_0) = \frac{t_{\text{tr}}^{\text{G}}}{2\sqrt{\mu}}. \quad (4.58)$$

But, seen from the parabolic side of the transition, the energy E fixes the duration \tilde{T}_3 of the effective game of section 4.2.2 through equation (4.56). On this side of the transition, the transition time $t_{\text{tr}}^{\text{para}}$ is defined by the condition

$$\frac{z(t_{\text{tr}}^{\text{para}} - t_0^{\text{para}})}{\sqrt{5}} = \nu, \quad (4.59)$$

where $z/\sqrt{5}$ is the standard deviation of the parabolic distribution equation (4.42), and $t_0^{\text{para}} = \tilde{T}_4 - \tilde{T}_3$ the time at which the parabolic evolution appears to have started (from an initial Dirac delta shape) seen from the small ν side of the transition. Based on equation (4.50), this implies that

$$\frac{\sqrt{5}\nu}{z_*} = \zeta^- \left(\alpha z_*^{-3/2} (t_{\text{tr}}^{\text{para}} - t_0^{\text{para}}) \right). \quad (4.60)$$

Using this last result along with equation (4.48), one obtains now a relation between $t_{\text{tr}}^{\text{para}}$ and z_*

$$\frac{\alpha}{z_*^{3/2}} (t_{\text{tr}}^{\text{para}} - t_0^{\text{para}}) = \arcsin \sqrt{\frac{\sqrt{5}\nu}{z_*}} - \sqrt{\frac{\sqrt{5}\nu}{z_*} \left(1 - \frac{\sqrt{5}\nu}{z_*} \right)}, \quad (4.61)$$

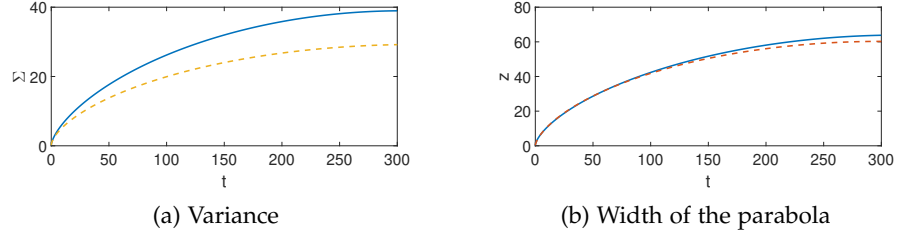


Figure 18: Time evolution of the variance (left) and the width of the parabola (right). The numerical solution for the density of players has been numerically fitted with a Gaussian and an inverted parabola, full curves are obtained through the extraction of the fitting parameters. Dashed curves are obtained using either the Gaussian or parabolic ansatz with energy $E = -9.95 \times 10^{-3}$ computed through the self-consistent condition. Parameters for this figure are $g = -2$, $\sigma = 1.2$, $\mu = 1$, $\nu = 1$, $\Sigma_0 = 0.2$ and $T = 300$.

which, given the fact that z_* and E are linked through equation (4.56) is actually a relation between $t_{\text{tr}}^{\text{para}}$ and E .

The self-consistent condition $t_{\text{tr}}^{\text{para}} = t_{\text{tr}}^{\text{G}}$ then implies that equations (4.58)-(4.61) fix both the energy E and the transition time t_{tr} , and thus solve the game we are considering in this subsection.

Knowing the energy, as illustrated in Figure (18), one can reconstruct the evolution of the variance of the Gaussian distribution at small times using equation (4.38) and, then, of the width of the inverted parabola using equation (4.50). Figure (19) gives further indication that both the Gaussian and parabolic ansätze yield good results to evaluate not only the spreading of the players but also the shape of the distribution in this configuration. The two regimes overlap when Σ_t is of order ν and either approximation regime gives a fairly accurate description of the phenomenon. However, as we near the end of the game both approximations become less and less accurate due to the proximity of the terminal condition, which, because σ is non-zero, is not perfectly flat

$$v_T(x) = 0 + o(\sigma^2). \quad (4.62)$$

Another reason for this would be the presence of higher order multipole coefficients Q_n , $n > 2$, that we (implicitly) neglected when constructing the parabolic ansatz, but can be shown to be non-zero nonetheless.

4.3.2 Matching transient and ergodic states

With this section I now turn back to the complete game, of equations (4.1), or, more specifically, to the first half of that game linking the initial distribution of agents to the ergodic state. I will focus on the case of a narrow initial condition, of width $\Sigma_0 \ll \nu$, for the distri-

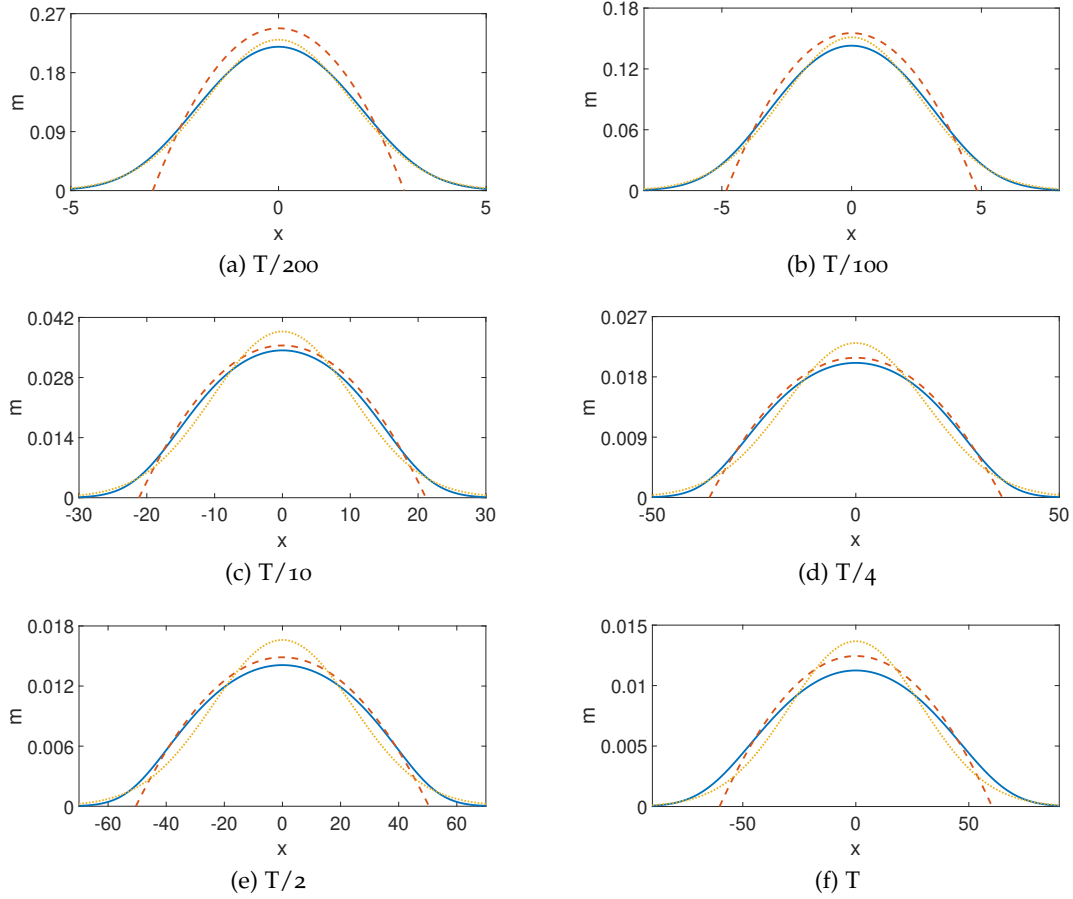


Figure 19: Density of players at different times, numerical results are plotted (solid line) along with the Gaussian (dotted line) and the parabolic ansatz (dashed line). At the beginning of the game, Figs (19a) and (19b), the Gaussian ansatz is the most accurate. Then in the middle of the game, Figs (19c) and (19d), the parabolic constitutes a better approximation. At the end of the game, Figs (19e) and (19f), the parabolic ansatz becomes less and less accurate as we near the terminal condition. Here $g = -2$, $\sigma = 1.2$, $\mu = 1$, $\nu = 1$, $\Sigma_0 = 0.2$ and $T = 300$, while $E = -9.95 \times 10^{-3}$ has been computed through the self-consistent condition.

It should also be noted that I will assume that the maximum of the external gain U_0 coincides with the center of mass of the initial distribution, so that I do not have to take its motion into account.

bution of agents, so that it includes the three regimes of approximation examined in this chapter. The system will, therefore, initially go through an expansion phase, during which one can neglect the individual gain / potential $U_0(x)$, and will successively traverse the large ν and the small ν regimes before reaching the ergodic state. The goal of this section then is to provide ways to understand how to connect those three regimes.

In this configuration, the energy E is completely fixed by the ergodic state

$$E = \bar{E} = \frac{g}{2} \int_{\mathbb{R}} \bar{m}^2 dx + \int_{\mathbb{R}} \bar{m} U_0 dx . \quad (4.63)$$

The initial large ν expansion phase is therefore completely fixed by E and Σ_0 through equation (4.38), which in turn fixes the transition time t_{tr} between the large and the small ν regimes through equation (4.58).

Once in the small ν regime, the energy E again fixes the duration \tilde{T}_3 of the effective game of section 4.2.2. The only parameter that remains to be fixed is the effective beginning time t_0^{para} of that effective game which is given by equation (4.61) with, according to equation (4.56), $z_* = 3g/10E$.

Naturally, because one has to take the external gain into account when nearing the ergodic state, the final extension of the effective game z_* does not correspond to the extension the ergodic state \bar{z} and its duration \tilde{T}_3 does not correspond to typical duration $\bar{\tau}$ of the transient time leading to the ergodic state. However, those respective quantities are of same order as long as, in the ergodic state, interaction energy and potential energy are comparable. No matter the external gain, as mentioned in section 4.1.2

$$\bar{E}_{\text{int}} \sim \frac{g}{\bar{z}} . \quad (4.64)$$

Hence, if interaction energy represents a set proportion p of the total energy, $\bar{E}_{\text{int}} = p\bar{E}$, \bar{z} should be of order z_*/p . And, noting that $\tilde{T}_3 \sim z_*^{3/2}$, we can infer that $\bar{\tau}$ should not be too far-off from $\tilde{T}_3/p^{3/2}$. In the particular case of a quadratic external gain $U_0(x) = -\mu\omega_0^2 x^2/2$, we can easily compute the ratio between \bar{E}_{int} and \bar{E}_{pot}

$$\frac{\bar{E}_{\text{int}}}{\bar{E}_{\text{pot}}} = 2 \quad \Rightarrow \quad \bar{E}_{\text{int}} = \frac{2}{3}E , \quad (4.65)$$

result which is completely independent of the values of g , μ or ω_0 . The ergodic density is then an inverted parabola of width $\bar{z} = 3z_*/2$ and $\bar{\tau}$ is of order $\tilde{T}_3(3/2)^{3/2}$. This is illustrated Figure (20).

What the effective game provides, in this context, is not a quantitatively precise description but a good qualitative estimation of what actually happens during the beginning of the game.

Mean Field Games constitute a challenge because of their unusual forward-backward structure. In this chapter I presented a simple,

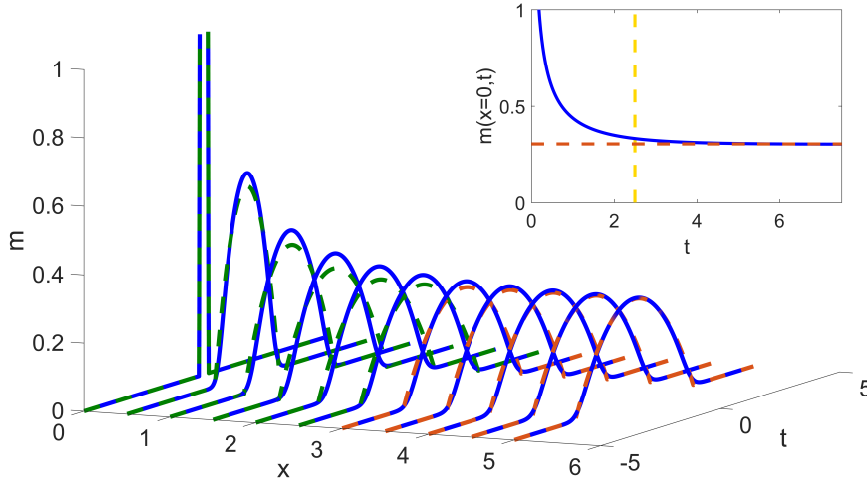


Figure 20: The full blue line represents the numerical density of players, the dashed green line is obtained through a parabolic ansatz of intrinsic time $\bar{\tau} = \tilde{T}_{IV}(3/2)^{3/2} = 2.5$ and the dashed red line corresponds to the ergodic density. In the inset the full line shows the time evolution of the maximum of the player density $m(x=0,t)$, while the dashed horizontal line is set at $\bar{m}(0)$, maximum of the density during the ergodic state, and the dotted vertical at $t = \bar{\tau} = 2.5$. Here $g = -2$, $\sigma = 0.4$, $\mu = 1$, $\omega_0^2 = 0.2$, $E = -0.36$ and $T = 15$.

heuristic, yet efficient method to describe negatively coordinated MFG in one dimension, leaning heavily on the notion of ergodic state introduced by P. Cardaliaguet [28]. The existence of this ergodic state proves to be of paramount importance as it allows the initial and final conditions to essentially decouple. The problem of finding a way to link initial and final conditions, both arbitrary, simplifies as it becomes a problem of finding a way to link either to a generic ergodic state. Making first use of the mapping to the non-linear Schrödinger equation as introduced in [108], and then of the hydrodynamic representation from [19], we were able to identify different regimes of approximation and put forward adequate ansätze to reconstruct the whole game. Results from those ansätze have been compared to numerical solutions, for parameters in their domain of application, and are highly satisfactory as well as easily computed.

SEMI-CLASSICAL ANALYSIS OF FOKKER-PLANCK EQUATION : WEAK NOISE LIMIT OF THE SEMINAR PROBLEM

This chapter is largely based on a 2019 paper [20] and constitutes, in some way, a departure from the previous two. By that I mean that it will not deal with a potential of the type (2.36) or even with interacting players for that matter. At least not interacting in a sense that would be traditionally admitted in physics. In fact, in this chapter, I will argue the Wentzel-Kramers-Brillouin (WKB) approximation in the context of the weak noise limit of FP equation and examine its application to a MFG toy-model. As such, this chapter has, in a sense, more to do with FP equation than with MFG per se. But, on a more global scale, it can also be seen as the first steps towards an alternative approach to the small noise limit of MFG I've been discussing in the past two chapters.

The idea behind this work originates from a paper [60] written by my predecessor, I. Swiecicki, and supervisors, T. Gobron and D. Ullmo, discussing in some details a specific MFG toy-model, the *seminar problem*, introduced by O. Guéant and co-workers [55]. This MFG problem consists in finding the effective starting time of a seminar, fixed by a quorum condition, when all the participants try to optimize their behaviour to avoid arriving too late or too early. The *state variable* x is therefore one dimensional, and corresponds simply to the physical space in which the motion of the agents takes place (the corridor leading to the seminar room) modelled as the negative real line $x \in]-\infty, 0]$. Absorbing boundary conditions $\{\forall t, m(t, x = 0) = 0\}$ are assumed since no one is expected to exit the seminar room before the beginning of the talk. Furthermore, the functional $V[m_t](x)$ is taken to be uniformly zero, and the coupling between the HJB equation and the density of agents is just provided by a quorum condition on the number of agents in the room at the beginning of the seminar. In other words the seminar is initially planned to begin at time $t = \bar{t}$ but actually starts at $t = T$ defined as

$$T = \inf \left\{ t \geq \bar{t} : \int_{-\infty}^0 m(x, t) \leq 1 - \theta \right\} , \quad (5.1)$$

where θ is a (known) acceptable proportion of the expected number of attendees: the seminar does not start if the room is empty, but waiting for it to be completely full would be a waste of time. As such one can define a terminal cost

$$c(t) = \alpha[t - \bar{t}]_+ + \beta[t - T]_+ + \gamma[T - t]_+ , \quad (5.2)$$

where α , β and γ respectively quantify the susceptibility to social pressure, the desire not to be late and the reluctance to pointless waiting. In this context, the quadratic MFG equations (2.24) would read

$$\partial_t m(x, t) + \partial_x(m(x, t)a(x, t)) - \frac{\sigma^2}{2} \partial_{xx} m(x, t) = 0 \quad \text{FP}, \quad (5.3)$$

$$\partial_t u(x, t) - \frac{1}{2\mu} [\partial_x u(x, t)]^2 + \frac{\sigma^2}{2} \partial_{xx} u(x, t) = 0 \quad \text{HJB}, \quad (5.4)$$

with initial and final conditions $m(x, t=0) = m_0(x)$, $u(x, t=T) = c_T(x)$. The coupling between these two PDEs here only comes from the fact that the drift velocity in equation (5.3) is given in term of the gradient of the utility function as $a(x, t) = -\partial_x u(x, t)/\mu$, and interactions are implicitly hidden in the definition of T .

In the noiseless limit $\sigma = 0$, this system of equations reduces to a transport equation coupled to a Hamilton-Jacobi equation, both of which we associate with the classical dynamics of point particles. This limit is therefore rather intuitive, and in some respects simpler to analyse than the noisy regime. It turns out however that in many circumstances this limit is ill-defined, which implies that it is mandatory to include a small but non zero noise. In that case, what one needs to analyse is the small (but non-zero) σ limit of the system MFG equations (5.3)-(5.4), which quite naturally one would wish to study in terms of *classical trajectories* to make contact with the intuitive description one has in mind for the $\sigma = 0$ limit.

In the weak noise regime, it has been shown in [60] that this problem is associated with the drift field depicted Figure (21), and reading to leading order

$$a(t, x) = \begin{cases} a^{(0)} & \text{for } x \leq -a^{(0)}(T-t) \\ \frac{-x}{(T-t)} & \text{for } -a^{(0)}(T-t) \leq x \leq -a^{(2)}(T-t) \\ a^{(2)} & \text{for } -a^{(2)}(T-t) \leq x \leq 0 \end{cases}, \quad (5.5)$$

where $a^{(0)} > a^{(2)}$ are two constant drift velocities.

In this chapter I will therefore analyse the Fokker-Planck equation for this velocity field in the small σ regime, and try to show that we can provide a very precise solution of this problem based solely on the *classical trajectories* for a dynamics closely related to (but slightly different from) the $\sigma = 0$ limit of equation (5.3).

The fact that this can be achieved for the FP equation can be seen readily by multiplying equation (5.3) by σ^2 , and noting that it then has the structure of what Maslov has termed a λ -pseudo differential operator [83], in the sense that each partial derivative is associated with a factor $\lambda^{-1} \equiv \sigma^2$. This implies that a *semi-classical approximation* scheme can be applied to this equation in small σ^2 limit. This fact has of course been recognized for many years, and led to some publications [43, 96, 100]. Most of them, however, use a rather indirect

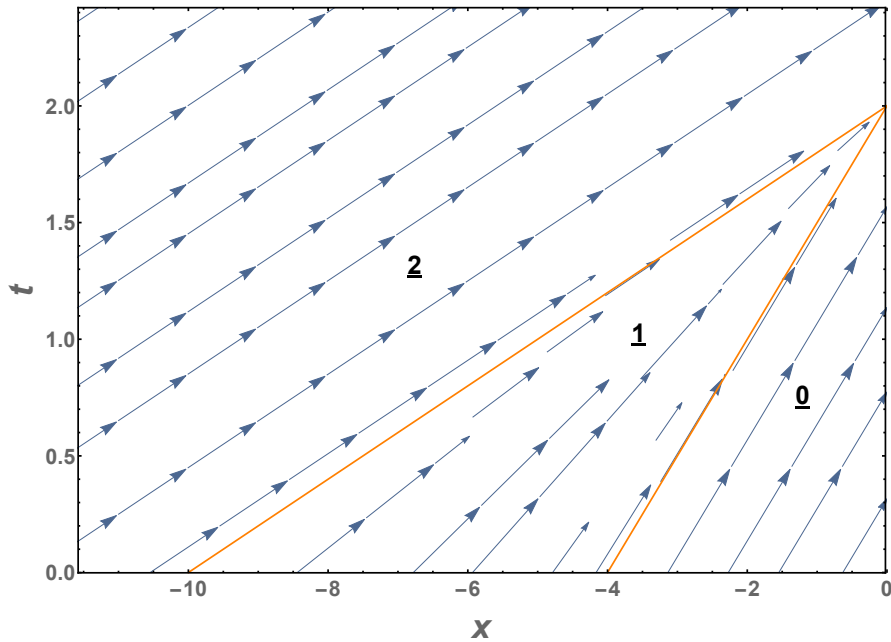


Figure 21: Regions of the (t, \vec{x}) space, where $T = 2$ is the time when the semimartingale effectively begins, and their associated optimal drift $a(t, \vec{x})$. In regions (0) and (2) the drift stays constant and is denoted respectively $a^{(0)}$ and $a^{(2)}$ (here 5 and 2). In region (1), the drift is linear in x .

approach, for example making use of transformation of variables to a form more directly related to the Schrödinger equation and then applying normal mode decomposition (c.f. [35] on the example of a diffusion in bi-stable potentials). Here, I instead choose to adopt the philosophy of the ray method introduced in [38].

The goal of this chapter will thus be to show that a straightforward approach, where the time-dependent WKB approximation is applied directly on equation (5.3), can be used effectively to obtain an extremely good approximation for the solution of FP equation (5.3) with the drift field (5.5). As such, I will only address the first (and maybe simplest) step in the analysis of the coupled MFG equations system, and furthermore do this on a specific illustrative case. But I will take this as an opportunity to discuss the application of the WKB approach in the perspective developed by Maslov [83], which is, in a way, more transparent than what can be found in the literature [38], and leads to a rather intuitive interpretation.

The chapter will be organized as follows. In section 5.1, I will give, without justification, the recipe for the construction of the WKB approximation. For the sake of clarity this will be done for a one dimensional problem, and I will assume that the initial density $m_0(x)$ is a Gaussian. Section 5.2 will then provide a derivation of these WKB expressions, together with a generalization to higher dimensionality and to a larger class of initial densities. Readers with little interest

in these formal issues may skip that section and go directly to section 5.3 where the WKB approximation is applied to two simple examples, where it turns out to provide the exact solution, as well as to the case corresponding to the drift field equations (5.5).

5.1 WKB APPROXIMATION OF A 1D FOKKER-PLANCK EQUATION

This section aims to provide, without any demonstration, the prescription for the construction of the WKB solution of the FP equation (5.3) in the small σ regime. We limit ourselves here to the one-dimensional case and to Gaussian initial densities

$$m_0(x) = \mathcal{N} \exp \left[-\frac{\mu(x - \underline{x}_0)^2}{2\sigma^2} \right], \quad (5.6)$$

where \underline{x}_0 is the center of the Gaussian and $\mathcal{N} = \sqrt{\mu/2\pi\sigma^2}$ is a normalization factor. More general $m_0(x)$ could easily be considered (see section 5.2), but Gaussians have an intrinsic interest, and, in addition, this also allows us to get the Green's function of the equation by reducing the width of the Gaussian to zero.

The semi-classical scheme follows three steps. The first one consists in constructing a Lagrangian symplectic manifold on which we can define an action. The second step uses this input to build the WKB approximation. Finally, we address how absorbing boundary conditions can be implemented in the semi-classical scheme.

5.1.1 Symplectic manifold and classical action

Introducing the λ -pseudo differential operator

$$\hat{L} \equiv [\lambda^{-1}\partial_t \cdot + \lambda^{-1}\partial_x(a \cdot) - \frac{1}{2}(\lambda^{-1}\partial_x)^2 \cdot], \quad (5.7)$$

with, once again, $\lambda \equiv \sigma^{-2}$ assumed large, FP equation (5.3) can be written as

$$\hat{L}m = 0. \quad (5.8)$$

Using the usual mapping $\lambda^{-1}\partial_x \rightarrow p$, $\lambda^{-1}\partial_t \rightarrow E$, \hat{L} can be associated with the *classical symbol*

$$L(x, t; p, E) = E + pa(x, t) - \frac{p^2}{2}, \quad (5.9)$$

which, if understood as a classical Hamiltonian leads to the canonical equations

$$\begin{cases} \dot{t} = \partial_E L = 1 & \dot{E} = -\partial_t L = -p\partial_t a \\ \dot{x} = \partial_p L = a(t, x) - p & \dot{p} = -\partial_x L = -p\partial_x a \end{cases}. \quad (5.10)$$

Now, consider the initial Gaussian distribution (5.6) for \underline{x}_0 and μ given. It can be written in the semi-classical form

$$m_0(x_0) = \mathcal{N} \exp [\lambda S_0(x_0)] , \quad (5.11)$$

with

$$S_0(x_0) \equiv -\mu \frac{(x_0 - \underline{x}_0)^2}{2} . \quad (5.12)$$

At any point of space x_0 , one can therefore initiate a classical trajectory at $t = t_0$ with an initial momentum

$$p_0(x_0) = \nabla S_0(x_0) = -\mu(x_0 - \underline{x}_0) , \quad (5.13)$$

and fulfilling the *compatibility condition*

$$L(x, t; p, E) \equiv 0 . \quad (5.14)$$

The reunion of all these trajectories obtained from these initial conditions and the canonical equations (5.10) form a 2-dimensional manifold $\mathcal{M} = \{(t, x(t, x_0), \mathcal{E}(t, x_0), \mathcal{P}(t, x_0))\}$ where \mathcal{P} , x and \mathcal{E} respectively represent the value taken by p , x and E after evolving on this manifold from $\vec{r}_0 = (t_0, x_0; E_0(x_0), p_0(x_0))$ for a time $t - t_0$. An example of such a manifold is illustrated in Figure (22).

To the manifold \mathcal{M} , we can now associate a classical action

$$S(t, x) \equiv \int_{[\mathcal{L}: \vec{r}_0 \rightarrow \vec{r}] \subset \mathcal{M}} p dx + E dt \quad (5.15)$$

where $\vec{r}_0 = (t_0, x_0; E=0, p=0)$ is the point on \mathcal{M} above $\vec{X}_0 = (t_0, x_0)$, and $\vec{r} \in \mathcal{M}$ is the point above $\vec{X} = (t, x)$.

Of note is that, since \mathcal{M} is a Lagrangian manifold, the integral in equation (5.15) can be taken on *any path* on \mathcal{M} joining \vec{r}_0 to \vec{r} . For instance, the action $S(t, x)$ can be computed either as

$$S_1(t, x) = \underbrace{\int_{\underline{x}_0}^{x_0(t, x)} p_0(x') dx'}_{S_0(x_0)} + \int_{t_0}^t (\mathcal{P}(s, x_0) \dot{x}(s, x_0) + \mathcal{E}(s, x_0)) ds , \quad (5.16)$$

in which $x_0(t, x)$ is the initial position of the trajectory arriving at x at time t , or as

$$S_2(t, x) = \int_{t_0}^t (\mathcal{P}(s, \underline{x}_0) \dot{x}(s, \underline{x}_0) + \mathcal{E}(s, \underline{x}_0)) ds + \int_{x(t, \underline{x}_0)}^x p(x', t) dx' , \quad (5.17)$$

with $p(x, t)$ the momentum coordinate of the point of \mathcal{M} above (t, x) . Both expressions lead to the same result (i.e. $S_1(t, x) = S_2(t, x) = S(t, x)$). This is illustrated on Figure (23).

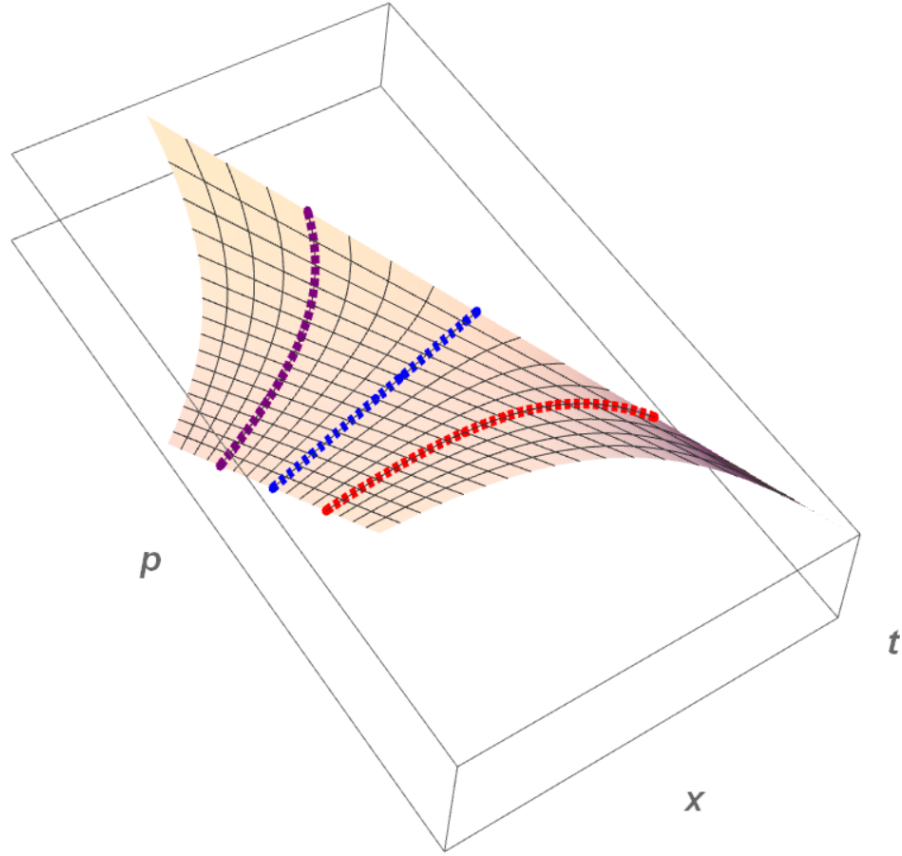


Figure 22: A typical manifold generated by the classical trajectories in region (1) of the drift field. In this case $a = \frac{-x}{T-t}$, $\mu = 1.5$, $\sigma = 0.4$, $T = 2$ and $\underline{x}_0 = -5$. The dashed curves represent specific trajectories beginning at $x_0 = -5.5$, -5 and -4.5 from left to right.

For the Gaussian initial density considered here, the definition of the initial momentum given by Eq. (5.13) and the compatibility condition $L \equiv 0$ imposes that $\rho(t, \underline{x}_0) = 0$ and $\mathcal{E}(t, \underline{x}_0) = 0$ for all time, yielding

$$S(t, x) = S_2(t, x) = \int_{x(t, \underline{x}_0)}^x p(t, x') dx', \quad (5.18)$$

where the path of integration on the manifold is taken at *constant time* t from the point above $\underline{x} \equiv x(t, \underline{x}_0)$ (evolution of the center of the distribution \underline{x}_0) to the point above x .

As a final comment, it is worth mentioning that, for more general initial conditions, $S_0(\underline{x}_0)$ can be non-zero and should be added to the right-hand side of equation (5.15).

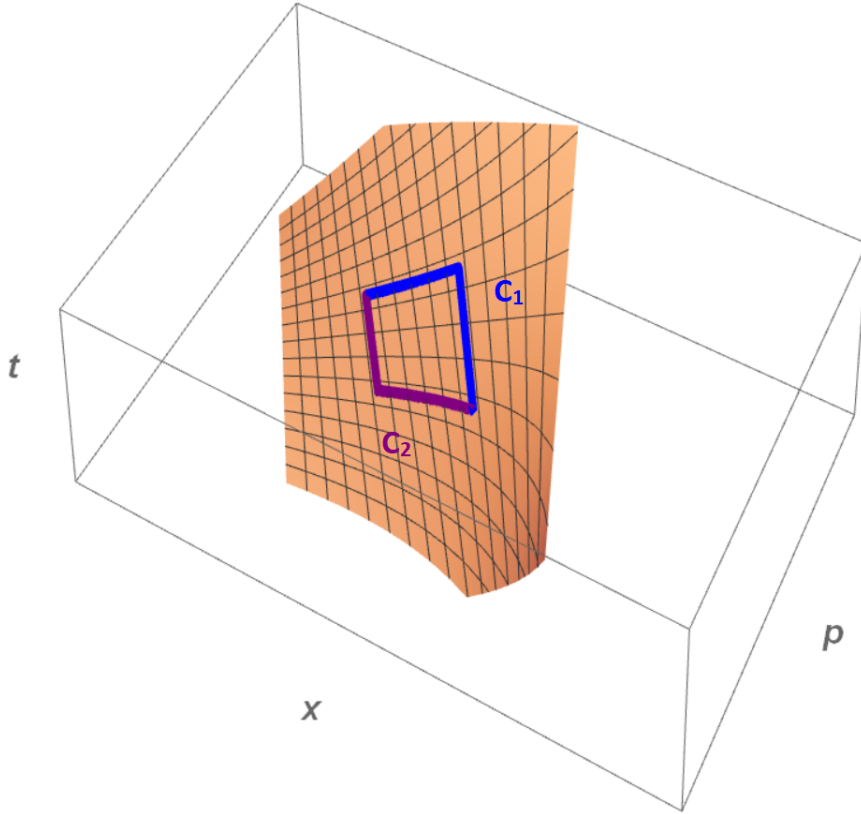


Figure 23: Same manifold as in Figure (22) where are highlighted two paths with same beginning and end. Because of the Lagrangian nature of the manifold we can write $\int_{C_1} (E\dot{t} + p\dot{x})dt = \int_{C_2} (E\dot{t} + p\dot{x})dt$.

5.1.2 Semi-classical approximation for $m(t, x)$

With the aforementioned definition of the action, the WKB approximation for the density of probability is expressed as

$$m_{\text{s.c.}}(t, x) = \frac{\mathcal{N}}{\sqrt{\partial_{x_0} x(t, x_0)}} \exp \left[\lambda S(t, x) - \frac{1}{2} \int_{t_0}^t (\partial_x a) d\tau \right], \quad (5.19)$$

where, in the pre-factor, $x(t, x_0)$ is the position of a trajectory started at x_0 at time $t = t_0$ (thus with an initial momentum $p_0(x_0)$ given by equation (5.13)), and the integral in the exponential is taken along this trajectory. Except for the fact that the exponent is real rather than complex, the only difference with respect to the traditional WKB expressions derived in optics or in the context of Schrödinger equation is the extra term $\frac{1}{2} \int_{t_0}^t (\partial_x a) d\tau$ in the exponent. This additional term can be traced back to the non-symmetric ordering of the operators $\hat{p} \equiv \lambda^{-1} \partial_x$ and $\hat{x} \equiv \times x$ in FP equation which makes, in particular, the operator \hat{L} non hermitian. Introducing \hat{L}_0 the hermitian approximation of \hat{L} in which the term $\lambda^{-1} \partial_x(a \cdot)$ has been replaced by its symmetric counterpart $(1/2)[\lambda^{-1} \partial_x(a \cdot) + a \lambda^{-1} \partial_x(\cdot)]$, and $\hat{L}_1 = \hat{L} - \hat{L}_0$, the

additional term in the semi-classical form (5.19) can be understood as arising from the perturbative effect of \hat{L}_1 on \hat{L}_0 (c.f. Appendix J).

5.1.3 Absorbing boundary conditions

In section 5.3, we shall illustrate this WKB approach with the problem corresponding to the drift velocity field (5.5), problem for which we assume an absorbing boundary condition at $x = 0$. Because such absorbing boundary conditions are rather common, I shall now discuss how they can be implemented in the semi-classical scheme.

Let us consider the semi-classical solution of the free problem (i.e. without absorbing boundary condition)

$$m_{\text{free}}(t, x) = \frac{\mathcal{N}}{\sqrt{\partial_{x_0} x(t, x_0)}} \exp \left[\lambda S(t, x) - \frac{1}{2} \int_{t_0}^t (\partial_x a) d\tau \right]. \quad (5.20)$$

For sake of simplicity, I assume that (as will be the case in the examples we are going to consider), the trajectories on which $S(t, x)$ is constructed are reaching $x = 0$ with positive velocity.

Consider now the compatibility condition (5.14) at $x = 0$, for an arbitrary time t , and with the choice $E = \partial_t S$

$$L(0, t; p, \partial_t S) = 0.$$

It admits two solutions

$$\dot{x} = a(x, t) - p = \pm \sqrt{a^2 + 2\partial_t S}. \quad (5.21)$$

The one corresponding to a positive velocity is simply

$$p_+(t) = \partial_x S(t, x=0), \quad (5.22)$$

but another set of trajectories initiated at time t and position $x = 0$ can be generated with momentum

$$p_-(t) = a + \sqrt{a^2(t, 0) + 2\partial_t S(t, 0)} \quad (5.23)$$

and energy

$$E(t) = \partial_t S(t, 0). \quad (5.24)$$

These trajectories have negative velocities and thus “bounce” off the boundary point $x = 0$. A *reflected density*

$$m_{\text{ref}}(t, x) = \frac{\mathcal{N}}{\sqrt{\partial_{x_0} \tilde{x}(t, x_0)}} \exp \left[\lambda \tilde{S}(t, x) - \frac{1}{2} \int_{t_0}^t (\partial_x a) d\tau \right], \quad (5.25)$$

can therefore be constructed in exactly the same way as before using the reflected trajectories \tilde{x} and reflected action \tilde{S} . At $x = 0$, $m_{\text{ref}}(t, 0) = m_{\text{free}}(t, 0)$ since the time derivative of the incident or

*One should only
impose
 $S(t_0, 0) = \tilde{S}(t_0, 0)$
for an arbitrary time
 t_0 .*

reflected action are identical $\partial_t S(t, 0) = \partial_t \tilde{S}(t, 0) = E(t, 0)$, and the same is true for the pre-factors $\partial_{x_0} \tilde{x}(t, x_0) = \partial_{x_0} x(t, x_0)$ as at $x = 0$ only the momentum has changed but not the position. Therefore, the total density

$$m_{\text{tot}}(t, x) = m_{\text{free}}(t, x) - m_{\text{ref}}(t, x) \quad (5.26)$$

is a semi-classical solution to FP equation (5.3) which fulfils the absorbing boundary condition $m_{\text{tot}}(t, 0) = 0$.

5.2 DERIVATION AND GENERALIZATION

I will now provide a derivation (and some generalization) of the semi-classical solution (5.19). This approach is very similar in spirit to the *ray method* developed by Cohen and Lewis [38], but follows more closely the WKB formalism developed by Maslov [83], that might be easier to access for physicists.

We therefore want to describe the evolution of an initial density (at $t = t_0$) which is in the semi-classical form

$$m_0(\vec{x}) = \phi_0(\vec{x}) \exp[\lambda S_0(\vec{x})] , \quad (5.27)$$

with $\vec{x} \in \mathbb{R}^d$. Such form includes Gaussian densities such as equation (5.6), but are significantly more general.

By writing ($\sigma^{-2} \equiv \lambda$), FP equation reads in the more general case,

$$0 = \lambda^{-1} \partial_t m + \lambda^{-1} \nabla(\vec{a}(t, \vec{x})m) - \frac{1}{2} \lambda^{-2} \Delta m = \hat{L}m , \quad (5.28)$$

which, up to the i factors, very much looks like a λ -pseudo differential Maslov operator of symbol

$$L(\vec{x}, t; \vec{p}, E) = E + \vec{a}(\vec{x}, t) \cdot \vec{p} - \frac{\vec{p}^2}{2} . \quad (5.29)$$

Following Maslov's derivation [83], let us consider the ansatz

$$m(t, \vec{x}) = \phi(t, \vec{x}) \exp[\lambda S(t, \vec{x})] , \quad (5.30)$$

with $\phi(t_0, \vec{x}) = \phi_0(\vec{x})$ and $S(t_0, \vec{x}) = S_0(\vec{x})$.

Writing $\vec{X} \equiv (t, \vec{x})$, $\vec{P} \equiv (E, \vec{p})$, FP equation (5.28) becomes

$$\begin{aligned} \hat{L} \left[\phi(\vec{X}) e^{\lambda S(\vec{X})} \right] &= 0 \\ &= e^{\lambda S(\vec{X})} \left[R_0 \phi(\vec{X}) + \lambda^{-1} R_1 \phi(\vec{X}) + O(\lambda^{-2}) \right] , \end{aligned} \quad (5.31)$$

with

$$R_0 = L(\vec{X}; \partial_{\vec{X}} S) , \quad (5.32)$$

and

$$R_1 = \langle \partial_{\vec{p}} L(\vec{X}; \partial_{\vec{x}} S), \partial_{\vec{x}} \phi \rangle + \left\{ \frac{1}{2} \text{Tr} \left[\partial_{\vec{p}\vec{p}}^2 L(\vec{X}; \partial_{\vec{x}} S) \partial_{\vec{x}\vec{x}}^2 S \right] + \text{Tr} \left[\partial_{\vec{x}\vec{p}}^2 L(\vec{X}; \partial_{\vec{x}} S) \right] \right\} \phi . \quad (5.33)$$

Neglecting terms of order λ^{-2} and higher, solving FP equation (5.28) now amounts to solving $R_0 = 0$ and $R_1 = 0$.

5.2.1 $R_0 = 0$, Hamilton-Jacobi equation

The equation ($R_0 = 0$) can be written as an Hamilton-Jacobi equation on S

$$L(\vec{X}; \partial_{\vec{x}} S) = \partial_t S + \vec{a}(t, \vec{x}) \cdot \vec{\nabla} S - \frac{1}{2} (\nabla S)^2 = 0 , \quad (5.34)$$

with an initial condition at $t = t_0$

$$S(t_0, \vec{x}_0) = S_0(\vec{x}_0) . \quad (5.35)$$

Solution of this kind of equations is typically obtained through the method of characteristics as described in Appendix B. In this case it amounts to build a one parameter family of rays $(t, \vec{x}; E, \vec{p})_{\vec{x}_0}(s) \equiv \vec{r}(s, \vec{x}_0)$, indexed by \vec{x}_0 , which follow – for a fictitious time s – the Hamilton dynamics associated with L

$$\begin{cases} \dot{t} = \partial_E L = 1 & \dot{E} = \partial_t L = -\vec{p} \cdot \partial_t \vec{a} \\ \dot{\vec{x}} = \partial_{\vec{p}} L = \vec{a}(t, \vec{x}) - \vec{p} & \dot{\vec{p}} = -\partial_{\vec{x}} L = -\vec{p} \cdot \partial_{\vec{x}} \vec{a} \end{cases} , \quad (5.36)$$

with initial the conditions

$$\begin{cases} \vec{r}(0, \vec{x}_0) = (E_0, t_0, \vec{p}_0(\vec{x}_0), \vec{x}_0) \\ L(\vec{r}(0, \vec{x}_0)) = 0 \end{cases} , \quad (5.37)$$

corresponding to

$$\vec{p}_0(\vec{x}_0) = \partial_{\vec{x}_0} S_0(\vec{x}_0) . \quad (5.38)$$

Equations (5.37) fixes E_0 and it is clear from equations (5.36) that we can take $s \equiv t - t_0$.

As stressed in the previous section, the family of rays defined by equations (5.36)-(5.37) form a Lagrangian manifold, thus, according to the method of characteristics (cf appendix B), the solution of Hamilton-Jacobi equation (5.34) reads

$$S(t, \vec{x}) = \int_{\vec{X}_0}^{\vec{X}} E dt + \vec{p} \cdot d\vec{x} , \quad (5.39)$$

where the integral is taken on any path on the manifold starting above the point $\vec{X}_0 = (t_0, \vec{X}_0)$ such that $S_0(\vec{X}_0) = 0$ and ending on the point above $\vec{X} = (t, \vec{x})$.

5.2.2 $R_1 = 0$, transport equation

Looking at the first term of R_1 , one may notice that it can be rewritten in a more explicit fashion using the canonical Hamilton-Jacobi equations

$$\begin{aligned} \langle \partial_{\vec{p}} L(\vec{X}, \partial_{\vec{X}} S), \partial_{\vec{X}} \phi \rangle &= \partial_t \phi + (\vec{a}(t, \vec{x}) - \partial_{\vec{X}} S) \partial_{\vec{X}} \phi \\ &= \partial_t \phi + \dot{\vec{x}} \partial_{\vec{X}} \phi = \frac{D\phi}{Dt}, \end{aligned} \quad (5.40)$$

where $\frac{D}{Dt}$ represents the time derivative along the flow. This allows to write the equation ($R_1 = 0$) as a simple evolution equation

$$\frac{D\phi}{Dt} = - \left\{ \frac{1}{2} \text{Tr} \left[\partial_{\vec{p}\vec{p}}^2 L(\vec{X}, \partial_{\vec{X}} S) \partial_{\vec{X}\vec{X}}^2 S \right] + \text{Tr} \left[\partial_{\vec{X}\vec{p}}^2 L \right] \right\} \phi. \quad (5.41)$$

To solve this equation one may make use of Liouville's formula, which states that for a dynamical system

$$\frac{d\vec{x}}{dt} = f(\vec{x}), \quad (5.42)$$

and for any $(d-1)$ -parameter family of trajectories $\vec{x}(t, \vec{\alpha})$ indexed by $\vec{\alpha} \in \mathbb{R}^{(d-1)}$, the determinant $J(t, \vec{\alpha}) \equiv \det \left[\frac{\partial \vec{x}(t, \vec{\alpha})}{\partial (t, \vec{\alpha})} \right]$ fulfils

$$\frac{D \ln J}{Dt} = \text{Tr} \left[\frac{df}{d\vec{x}}(\vec{x}(t, \vec{\alpha})) \right]. \quad (5.43)$$

Elements of a demonstration are given in appendix K for the sake of completeness. Using the canonical equations yields

$$\dot{\vec{X}} = \partial_{\vec{p}} L, \quad (5.44)$$

and noting that one can write $\vec{X} \equiv (t, \vec{x}(t, \vec{x}_0))$ along with having J denote $\det[\partial_{t, \vec{x}_0} \vec{X}]$, Liouville's formula reads

$$\frac{D \ln(J)}{Dt} = \text{Tr} \left[\partial_{\vec{X}} (\partial_{\vec{p}} L) \right] = \text{Tr} \left[\partial_{\vec{p}\vec{X}}^2 L + \partial_{\vec{p}\vec{p}}^2 L \partial_{\vec{X}\vec{X}}^2 S \right]. \quad (5.45)$$

Hence equation (5.41) becomes

$$\frac{D\phi}{Dt} + \frac{1}{2} \frac{D}{Dt} (\ln J) \phi = -\frac{1}{2} \text{Tr} [\partial_{\vec{X}\vec{p}}^2 L] \phi, \quad (5.46)$$

and, multiplying both sides by \sqrt{J} ,

$$\frac{D}{Dt} \left[\sqrt{J} \phi \right] = -\frac{1}{2} \text{Tr} \left[\partial_{\vec{X}\vec{p}}^2 L \right] \sqrt{J} \phi. \quad (5.47)$$

Finally, we have

$$\begin{aligned} \phi(\vec{x}(t, \vec{x}_0)) &= \frac{\sqrt{J(\vec{x}(t_0, \vec{x}_0))}}{\sqrt{J(\vec{x}(t, \vec{x}_0))}} \phi(\vec{x}(t_0, \vec{x}_0)) \\ &\quad \times \exp\left(-\frac{1}{2} \int_{t_0}^t \text{Tr} \left[\partial_{\vec{x}\vec{p}}^2 L \right] d\tau\right), \end{aligned} \quad (5.48)$$

where $\sqrt{J(\vec{x}(t_0, \vec{x}_0))} = 1$ and, for L given by equation (5.29), $\text{Tr} \left[\partial_{\vec{x}\vec{p}}^2 L \right] = \vec{\nabla} \cdot \vec{a}$. In 1d J would simply become $\partial_{x_0} x$, yielding the pre-factor in equation (5.19).

It is also worth noting that equation (5.41) can be solved in multiple ways, another possibility would be

$$\frac{D}{Dt} [J\phi] = +\frac{1}{2} \text{Tr} \left[\left(\partial_{\vec{p}^2}^2 L \right) \cdot \left(\partial_{\vec{x}^2}^2 S \right) \right] J\phi, \quad (5.49)$$

implying

$$\begin{aligned} \phi(\vec{x}(t, \vec{x}_0)) &= \frac{J(\vec{x}(t_0, \vec{x}_0))}{J(\vec{x}(t, \vec{x}_0))} \phi(\vec{x}(t_0, \vec{x}_0)) \\ &\quad \times \exp\left(+\frac{1}{2} \int_{t_0}^t \text{Tr} \left[\left(\partial_{\vec{p}^2}^2 L \right) \cdot \left(\partial_{\vec{x}^2}^2 S \right) \right] d\tau\right). \end{aligned} \quad (5.50)$$

Here J serves only as a pre-factor, and either expressions can be used.

5.3 APPLICATION TO THE SEMINAR PROBLEM

For a 1d problem, and writing $\lambda^{-1} \equiv \sigma^2$, the semi-classical expression for m reads

$$m(t, x) = \frac{\mathcal{N}}{\sqrt{\partial_{x_0} x}} \exp \left[\frac{S(t, x)}{\sigma^2} - \frac{1}{2} \int_0^t (\partial_x a) d\tau \right]. \quad (5.51)$$

I will use this expression to study the different drift regimes, c.f. equation (5.5), presented by the seminar problem for Gaussian initial condition at $t=0$

$$m_0(x) = \mathcal{N} \exp \left[-\frac{\mu(x_0 - \underline{x}_0)^2}{2\sigma^2} \right] = \mathcal{N} \exp \left[\frac{S_0(x_0)}{\sigma^2} \right], \quad (5.52)$$

to which, through equation (5.13), is associated the one-parameter family of initial points in phase space

$$\vec{r}(x_0) = (t=0, x_0, E_0(x_0), p_0(x_0)) \quad (5.53)$$

corresponding to

$$p_0(x_0) = \partial_{x_0} S_0(x_0) = -\mu(x_0 - \underline{x}_0),$$

and

$$E_0(x_0) = \frac{p_0^2(x_0)}{2} - p_0(x_0)a(x_0, t=0).$$

5.3.1 Constant drift

I will start with the simple case of a constant drift a (this would correspond to regions (0) or (2) in Figure (21)). In order to obtain a density as expressed in equation (5.51), there are two terms one needs to compute: the pre-factor $\partial_{x_0}x(t, x_0)$ and the action $S(t, x)$. To do so, one should start from the canonical equations of motion

$$\begin{cases} \dot{p} = -\partial_x L = -p\partial_x a = 0 \\ \dot{x} = \partial_p L = a - p \quad (= \text{const. along a trajectory}) . \end{cases} \quad (5.54)$$

For the one-parameter family of trajectories given by equations (5.53), this leads to

$$\begin{cases} p(t, x_0) = \mu(x_0 - x_0) \\ x(t, x_0) = x_0 + [a - p(t, x_0)]t = x_0(1 + t\mu) + t(a - \mu x_0) . \end{cases} \quad (5.55)$$

The pre-factor is then readily obtained as

$$\partial_{x_0}x(t, x_0) = 1 + t\mu . \quad (5.56)$$

The action is computed noticing that, along the *center of mass trajectory* $x(t, \underline{x}_0)$, the momentum $p(t, \underline{x}_0)$ and energy $\mathcal{E}(t, \underline{x}_0)$ remain identically zero. Hence, $\mathcal{M} = \{(t, x(t, x_0), \mathcal{E}(t, x_0), p(t, x_0))\}$ being Lagrangian,

$$S(t, x) = \int_{x(t, \underline{x}_0)}^x p(t, x') dx' , \quad (5.57)$$

with $p(t, x)$, the momentum of the point above (x, t) on \mathcal{M} . Denoting $x_0(t, x)$ the initial position of a trajectory arriving at x at time t (i.e. such that $x = x(t, x_0)$), the second equation of system (5.55) gives

$$x_0(t, x) = \frac{x - at + \mu x_0 t}{1 + \mu t} , \quad (5.58)$$

and the first one

$$p(t, x) = -\frac{\mu}{1 + \mu t} (x - (x_0 + at)) . \quad (5.59)$$

After integration, this last expression yields,

$$S(t, x) = -\left(\frac{\mu t}{1 + \mu t}\right) \left(\frac{(x - x_0 - at)^2}{2t}\right) . \quad (5.60)$$

Finally, using the equation (5.51) one may reconstruct the semi-classical form

$$m(t, x) = \sqrt{\frac{\mu}{2\pi\sigma^2}} \frac{1}{\sqrt{1 + t\mu}} \exp \left[-\left(\frac{\mu t}{1 + \mu t}\right) \left(\frac{(x - x_0 - at)^2}{2t\sigma^2}\right) \right] , \quad (5.61)$$

which turns out to be the *exact expression* for the evolution of a initial Gaussian density in the case of a constant drift. This was actually to be expected since going back to the derivation of the semi-classical approximation, one may notice that the neglected terms only contain second (or higher) order spatial derivatives of a which are identically zero in the case of a constant drift.

If $\mu \rightarrow \infty$, $m(0, x) \rightarrow \delta(x - x_0)$, and

$$m(t, x) \rightarrow G(t, x, x_0) = \sqrt{\frac{1}{2\pi t\sigma^2}} \exp\left[-\frac{(x - x_0 - at)^2}{2t\sigma^2}\right], \quad (5.62)$$

which indeed is the exact Green function of FP equation for a constant drift.

Absorbing boundary condition at $x = 0$

To implement the absorbing boundary condition at $x = 0$, we follow the procedure discussed earlier in section 5.1.3 and construct the reflected action

$$\tilde{S}(t, x) = S(t, 0) + \int_0^x p_-(t, x') dx', \quad (5.63)$$

where $p_-(t, x)$ is the reflected momentum.

To compute this quantity, let us introduce

$$t_{\text{abs}} = \frac{x_0}{\mu(x_0 - x_0) - a}$$

the time at which the trajectory initiated at x_0 reaches 0 (and is thus “absorbed”). Since velocity is constant on a given trajectory, we can express the velocity before the bounce as $\dot{x}_+(x_0) = -x_0/t_{\text{abs}}$ and thus just after the bounce as $\dot{x}_-(x_0) = +x_0/t_{\text{abs}}$. Equations (5.54) then give

$$p_-(t > t_{\text{abs}}, x_0) = a - \frac{x_0}{t_{\text{abs}}} = 2a - \mu(x_0 - x_0), \quad (5.64)$$

and

$$\begin{aligned} x(t > t_{\text{abs}}, x_0) &= \frac{x_0}{t_{\text{abs}}}(t - t_{\text{abs}}) \\ &= -x_0(1 + \mu t) - at + \mu x_0 t \end{aligned} \quad (5.65)$$

Defining $\tilde{x}_0(t, x)$ the initial position of a trajectory arriving at $x(t, x_0) = x$ after reflection at $x = 0$, we thus infer from equation (5.65)

$$\tilde{x}_0(t, x) = \frac{\mu t x_0 - at - x}{1 + \mu t}, \quad (5.66)$$

which, inserted into equation (5.64), gives

$$p_-(t, x) = 2a - \left(\frac{\mu t}{1 + \mu t}\right) \left(\frac{x + x_0 + at}{t}\right). \quad (5.67)$$

Performing the integral in equation (5.63), and noting that the lower bound cancels the term $S(t, x=0)$, we thus write

$$\tilde{S}(t, x) = 2ax - \left(\frac{\mu t}{1 + \mu t} \right) \left(\frac{(x + x_0 + at)^2}{2t} \right), \quad (5.68)$$

yielding for the total (incident plus reflected) density

$$m_{\text{tot}}(t, x) = \sqrt{\frac{\mu}{2\pi\sigma^2}} \frac{1}{\sqrt{1 + t\mu}} \left\{ \exp \left[- \left(\frac{\mu t}{1 + \mu t} \right) \left(\frac{(x - x_0 - at)^2}{2t\sigma^2} \right) \right] - \exp \left(\frac{2ax}{\sigma^2} \right) \exp \left[- \left(\frac{\mu t}{1 + \mu t} \right) \left(\frac{(x + x_0 + at)^2}{2t\sigma^2} \right) \right] \right\}. \quad (5.69)$$

This fulfils the absorbing boundary conditions $m_{\text{tot}}(t, 0) = 0$ and, for the same aforementioned reason, is an exact solution of the FP equation. Note that, for finite μ , the Gaussian initial condition (5.52) fulfils the boundary condition $m_0(x = 0)$ up to exponentially small terms, and conversely equation (5.69), which satisfies the boundary condition exactly, only satisfies the initial condition $m_{\text{tot}}(t, 0) = m_0(x)$ up to exponentially small terms. As $\mu \rightarrow \infty$, however, the boundary condition is exactly met by m_0 and equation (5.69) provides the exact Green function of FP equation.

5.3.2 Linear drift

I will now consider a linear drift $a(x, t) = x/(t - T)$, with $T > t$ the time at which the seminar begins, associated with region (1) in Figure (21). The canonical equations become

$$\begin{cases} \dot{x} = \partial_p L = a - p = \frac{x}{t - T} - p \\ \dot{p} = -\partial_x L = -p \partial_x a = -\frac{p}{t - T}, \end{cases} \quad (5.70)$$

giving

$$\begin{cases} p(t, x_0) = p_0(x_0) \frac{T}{T - t} = \frac{\mu T(x_0 - x_0)}{T - t} \\ x(t, x_0) = \frac{x_0(T - t)}{T} - \mu t(x_0 - x_0). \end{cases} \quad (5.71)$$

We thus have

$$\partial_{x_0} x = \frac{(T - t + \mu t T)}{T}, \quad (5.72)$$

which, together with

$$\int_0^t (\partial_{x_0} a) d\tau = \log \left[\frac{(T - t)}{T} \right], \quad (5.73)$$

yields for the pre-factor

$$\frac{\mathcal{N}}{\sqrt{\partial_{x_0} x}} \exp \left[-\frac{1}{2} \int_0^t (\partial_x a) d\tau \right] = \sqrt{\frac{\mu}{2\pi\sigma^2}} \sqrt{\frac{T^2}{(\mu t T + T - t)(T - t)}}. \quad (5.74)$$

Turning now to the action, and looking at the second equation of (5.71), we have

$$x_0(t, x) = (x - \mu t \underline{x}_0) \frac{T}{T - t + \mu T t}, \quad (5.75)$$

which, inserted into the first equation of (5.71), gives for the momentum $p(t, x)$,

$$p(t, x) = \frac{\mu T (x_0(T - t) - Tx)}{(T - t)(T - t + \mu T t)}. \quad (5.76)$$

This leads to, after integration

$$S(t, x) = \int_{x(t, \underline{x}_0)}^x p(t, x') dx' = \frac{\mu (x_0(t - T) - Tx)^2}{2(T - t)(T - t + \mu T t)}. \quad (5.77)$$

Using the semi-classical form (5.51), and computing the reflected action $\tilde{S}(t, x)$ by following the same procedure discussed in section 5.3.1

$$\tilde{S}(t, x) = \frac{\mu (xT + (T - t)\underline{x}_0)^2}{2(t - T)(T - t + \mu T t)}, \quad (5.78)$$

one obtains the evolution of a Gaussian initial density with a linear drift velocity and absorbing boundary conditions at $x = 0$

$$m(t, x) = \sqrt{\frac{\mu}{2\pi\sigma^2}} \sqrt{\frac{T^2}{(\mu t T - T - t)(T - t)}} \left\{ \exp \left[\frac{\mu (xT - (T - t)\underline{x}_0)^2}{2\sigma^2(t - T)(T - t + \mu T t)} \right] - \exp \left[\frac{\mu (xT + (T - t)\underline{x}_0)^2}{2\sigma^2(t - T)(T - t + \mu T t)} \right] \right\}. \quad (5.79)$$

As $\mu \rightarrow \infty$ we recover the Green function of the corresponding FP equation

$$G(t, x, \underline{x}_0) = \sqrt{\frac{T}{2\pi\sigma^2 t(T - t)}} \left\{ \exp \left(-\frac{T(x - \frac{T-t}{T}\underline{x}_0)^2}{2\sigma^2 t(T - t)} \right) - \exp \left(-\frac{T(x + \frac{T-t}{T}\underline{x}_0)^2}{2\sigma^2 t(T - t)} \right) \right\}. \quad (5.80)$$

And, again because the second x derivative of the drift is zero, expressions (5.79) and (5.80) are exact.

5.3.3 Coupling the two solutions

I will now consider the full problem corresponding to the drift field equation (5.5), taking into account the possibility that agents beginning in region (0) or (2) (associated with constant drifts $a^{(0)}$ and $a^{(2)}$) may leak into region (1) (associated with a linear drift $a(x, t) = x/(t - T)$), and reciprocally. I focus here on times $t \leq T$ and on the configuration where the agents start their diffusion in region (1), which is the one of interest from the point of view of MFG theory. Corresponding expressions for a group of agents initially located in region (2) are given in appendix L.

Let me begin by defining $x^{*(n)}(x_0)$, $p^{*(n)}(x_0)$ and $t^{*(n)}(x_0)$, ($n = 0, 2$), the position, impulsion and time at which a trajectory initiated at $\vec{r}(x_0)$ (cf equation (5.53)) crosses the boundary between regions (1) and (n), n being either 0 or 2. Using equation (5.71) together with the fact that the boundary between two regions corresponds to the $x = a^{(n)}(t - T)$ straight line, one may write

$$\begin{aligned} x^{*(n)}(x_0) &= a^{(n)}(t^{*(n)} - T) \\ &= x_0 \frac{(T - t^{*(n)})}{T} - \mu(\underline{x}_0 - x_0)t^{*(n)}(x_0). \end{aligned} \quad (5.81)$$

It is then possible to compute $t^{*(n)}$, by inverting this last equation, and obtain $p^{*(n)}$, inserting this newly found $t^{*(n)}$ expression in equation (5.71)

$$\begin{cases} t^{*(n)}(x_0) = T \left[1 - \frac{\mu T(\underline{x}_0 - x_0)}{a^{(n)}T + x_0 + \mu T(\underline{x}_0 - x_0)} \right] \\ p^{*(n)}(x_0) = \frac{a^{(n)}T + \mu T(\underline{x}_0 - x_0) + x_0}{T} \end{cases}. \quad (5.82)$$

Before the crossing ($t < t^{*(n)}$) the agents do not feel the effects of the drift change, and their trajectories remain the same as in equation (5.71). In region (1), ($x^{*(0)} < x < x^{*(2)}$), the pre-factor is thus obtained, as in section 5.3.2, through equation (5.74) and the action through equation (5.77). After the crossing however, the density changes and one has to compute its new expression. The complete solution is then simply obtained by patching the linear and the leaking densities, imposing continuity of the solution.

Using the canonical equations in the region in which the agents are leaking, one has for $t > t^{*(n)}$,

$$\begin{cases} \mathcal{X}^{(n)}(t, x_0) = x^{*(n)} + (a^{(n)} - p^{*(n)})(t - t^{*(n)}) \\ \mathcal{P}^{(n)}(t, x_0) = p^{*(n)} \end{cases}. \quad (5.83)$$

Let $x_0(t, x)$ be the initial position of a trajectory arriving at position x at time t (thus $x^{(n)}(t, x_0) = x$), $t^{*(n)}(t, x)$ the time at which this tra-

Note that even if the derivative of the drift field $a(t, x)$ is discontinuous at the boundary, p , E and L are continuous, and thus the Lagrangian character of the manifold \mathcal{M} is trivially preserved.

jectory crosses the boundary between the two regions, and $p^{*(n)}(t, x)$ the momentum at the crossing

$$\begin{cases} x_0(t, x) = \frac{T(x - \mu t \underline{x}_0)}{T - t - \mu T t} \\ t^{*(n)}(t, x) = T \left\{ 1 - \frac{\mu T [\underline{x}_0 - x_0(t, x)]}{aT + x_0(t, x) + \mu T (\underline{x}_0 - x_0(t, x))} \right\} \\ p^{*(n)}(t, x) = \frac{aT + \mu T [\underline{x}_0 - x_0(t, x)] + x_0(t, x)}{T} \end{cases} \quad (5.84)$$

One may now compute the pre-factor

$$\frac{\mathcal{N}}{\sqrt{\partial_{x_0} \mathcal{X}_n}} \exp \left[-\frac{1}{2} \int_0^{t^{*(n)}(t, x)} (\partial_x a^{(1)}) d\tau \right] = \sqrt{\frac{\mu}{2\pi\sigma^2} \frac{T}{T - t + \mu T t} \frac{\mu T (\underline{x}_0 - x) + x + a^{(n)}(T - t + \mu T t)}{\mu T (\underline{x}_0 - x) - \mu t \underline{x}_0}}, \quad (5.85)$$

and the action

$$\begin{aligned} S_{\text{leak}}^{(n)}(t, x) &= \int_{\underline{x}}^{a^{(n)}(t-T)} p^{(1)}(t, x') dx' + \int_{a^{(n)}(t-T)}^x p^{*(n)}(t, x') dx' \\ &= \frac{1}{2(T - t + \mu T t)} \left[-(a^{(n)})^2 (t - T)(T - t + \mu T t) \right. \\ &\quad \left. + 2a^{(n)}(T - t + \mu T t)x + (1 - \mu T)x^2 + 2\mu T x \underline{x}_0 + \mu(t - T)\underline{x}_0^2 \right], \end{aligned} \quad (5.86)$$

with $p^{(1)}$ given by equation (5.76). It should be noted that if both x and \underline{x}_0 belong to the boundary between region (1) and region (n), the pre-factor diverges because of diffraction effects that would have to be treated specifically.

The reflected action is computed through the usual procedure, but, this time, taking into account that the reflected trajectory may also transit from a region to an other

$$\begin{aligned} \tilde{S}_{\text{leak}}(t, x) &= S_{\text{leak}}^{(n)}(t, 0) + \int_0^{\min[x; a^{(1)}(t-T)]} p_{-}^{*(0)}(t, x') dx' \\ &\quad + \int_{a^{(1)}(t-T)}^{\min[\max[x; a^{(1)}(t-T)]; a^{(2)}(t-T)]} p_{-}^{(1)}(t, x') dx' \\ &\quad + \int_{a^{(2)}(t-T)}^{\max[x; a^{(2)}(t-T)]} p_{-}^{*(2)}(t, x') dx', \end{aligned} \quad (5.87)$$

with $p_{-}^{*(n)}$ the reflected leaking momentum in region (n) and $p_{-}^{(1)}$ the reflected linear drift momentum. Complete, explicit, expressions are given in appendix L (c.f. equations (L.2), (L.3) and (L.4)). However, the contribution of reflected trajectories decay exponentially away from

the absorbing boundary $x = 0$. Assuming $t \leq T$, as we do here, this implies that unless $t \approx T$, we can assume the contribution of reflected trajectories are important only when they are still in region (0), and the reflected action can be approximated as

$$\begin{aligned} \tilde{S}_{\text{leak}}(t, x) = & 2a^{(0)}x \\ & - \frac{1}{2(T-t+\mu T)} \left[-(a^{(0)})^2(t-T)(T-t+\mu Tt) \right. \\ & + 2a^{(0)}(T-t+\mu Tt)x \\ & \left. + (1-\mu T)x^2 + 2\mu T x \underline{x}_0 + \mu(t-T)\underline{x}_0^2 \right]. \end{aligned} \quad (5.88)$$

One can then check that, for this specific drift field, the reflected prefactor is the same as the direct one and eventually, using equation (5.51), obtains

$$\begin{aligned} m_{\text{leak}}(t, x) = & \sqrt{\frac{\mu}{2\pi\sigma^2} \frac{T}{T-t+\mu Tt} \frac{\mu T(\underline{x}_0-x) + x + a^{(n)}(T-t+\mu Tt)}{\mu T(\underline{x}_0-x) - \mu t \underline{x}_0}} \left\{ \right. \\ & \left. \exp\left(\frac{S_{\text{leak}}(t, x)}{\sigma^2}\right) - \exp\left(\frac{\tilde{S}_{\text{leak}}(t, x)}{\sigma^2}\right) \right\}. \end{aligned} \quad (5.89)$$

Contrarily to constant and linear drifts which represent non-generic cases for which the WKB expression is exact, the above result is an approximation, valid only in the semi-classical regime of small σ . To be a bit more quantitative, it can be appropriate to introduce the dimensionless parameter K defined as the ratio between the drift time $\tau_{\text{drift}} = x(t, \underline{x}_0)/a$, time needed to get from $x = x(t, \underline{x}_0)$ to the location of the absorbing boundary condition $x = 0$ at speed a , and the diffusion time $\tau_{\text{diffusion}} = x^2(t, \underline{x}_0)/\sigma^2$, time it would take for a purely diffusive process to spread the density from its center in $x = x(t, \underline{x}_0)$ to $x = 0$. Thus

$$K = \frac{\tau_{\text{drift}}}{\tau_{\text{diffusion}}} = \left| \frac{\sigma^2}{ax(t, \underline{x}_0)} \right| \propto \sigma^2. \quad (5.90)$$

The weak noise [semi-classical] regime can be therefore characterized by $K \ll 1$ while the strong noise regime by $K \gg 1$. Note that K usually depends on time. Figure (24) shows a comparison between a numerical solution and the semi-classical approximation for different small values of K , fixing σ and varying t . As we can see the semi-classical approximation is almost indistinguishable from the numerical solution up to $K = 0.33$ and remains good for K slightly greater than one even if we can observe small discrepancies. Looking at larger values of σ (and hence K), c.f. Figure (25), we see that, even for the largest value of K considered here ($K = 6.66$), the agreement is still rather good although the difference with the exact result becomes more significant. The fact that the source of errors in the semi-classical treatment is gen-

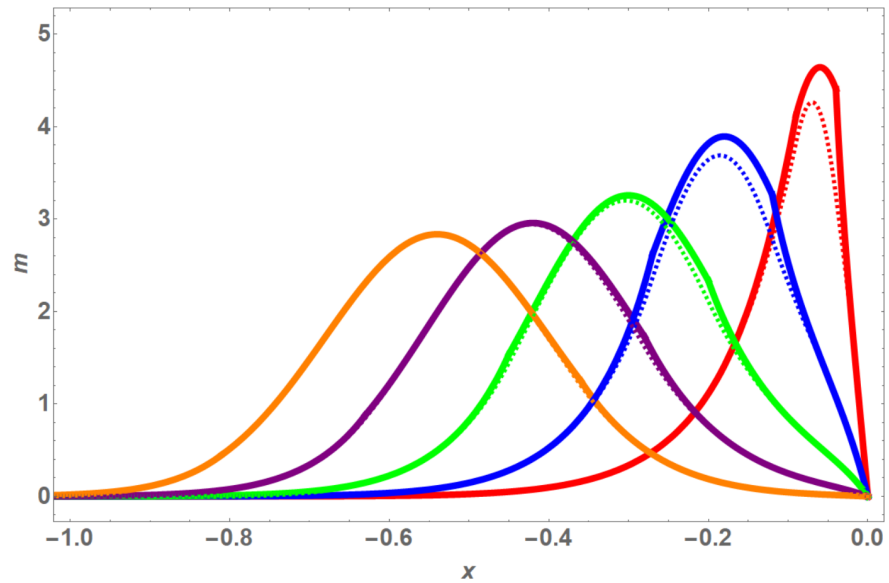


Figure 24: Spatial distribution of the agents at fixed time, dashed lines show the numerical solution while solid lines show the approximation. From left to right, $K = 0.19$ and $t = 1.1$, $K = 0.24$ and $t = 1.3$, $K = 0.33$ and $t = 1.5$, $K = 0.56$ and $t = 1.7$, $K = 1.67$ and $t = 1.9$. In this case $T = 2$, $a^{(0)} = 0.4$, $a^{(2)} = 0.9$, $\sigma = 0.2$, $x_0 = 1.2$ and $\mu = 10^6$.

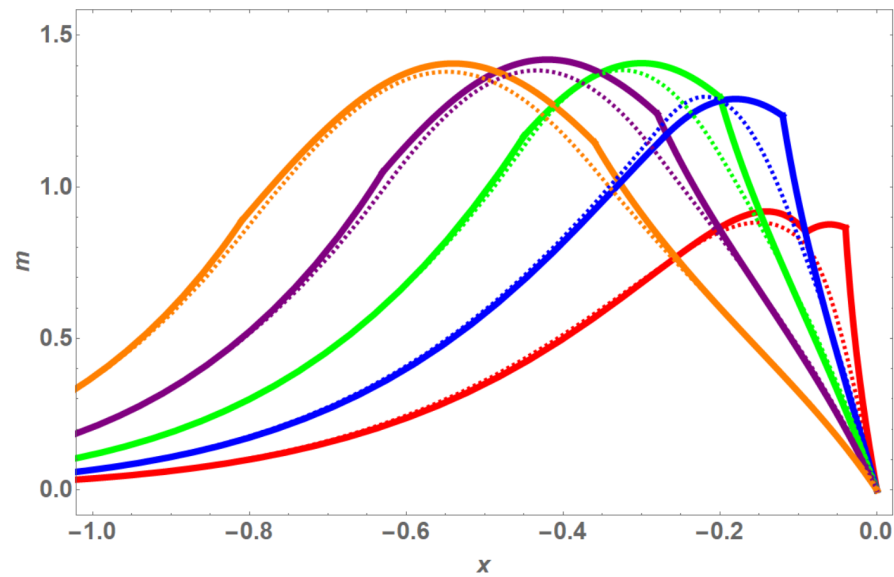


Figure 25: Spatial distribution of the agents at fixed time, dashed lines show the numerical solution while solid lines show the approximation. From left to right, $K = 0.74$ and $t = 1.1$, $K = 0.95$ and $t = 1.3$, $K = 1.33$ and $t = 1.5$, $K = 2.22$ and $t = 1.7$, $K = 6.66$ and $t = 1.9$. In this case $T = 2$, $a^{(0)} = 0.4$, $a^{(2)} = 0.9$, $\sigma = 0.4$, $x_0 = 1.2$ and $\mu = 10^6$.

erated only at the boundaries between the various regions explains the effectiveness of the approximation in this particular setup.

In this chapter I discussed a new take on the [WKB](#) approximation scheme to study [FP](#) equation. This approach, based on Maslov's geometric perspective, offers a transparent way of tackling [FP](#) equation and this was illustrated by the treatment of a problem motivated by a simple [MFG](#) toy-model.

As stressed in the introduction, this chapter aims more to discuss [FP](#) equation than [MFG](#), even if some application of this discussion can be exploited in the context of [MFG](#). I have addressed here only a very small part of the program which would consist in providing a *ray theory* of [MFG](#) in the small but non zero-noise limit. This program would require a few steps (defining a ray theory of [HJB](#) equation to start with and then dealing with the coupling between the two equations) which are significantly more involved. I leave these for future research, but this [WKB](#) approach provides a sound start for this program.

CONCLUSION

While **MFG** theory was initially introduced by mathematicians, and while its applications are the most prevalent in fields like Engineering Sciences and Economics, I believe physicists can provide such a discipline with an interesting and alternative point of view. Even in simplified forms, **MFG** problems are usually technically complicated and the exact mechanisms brought forward by their constitutive equations, along with their mixed initial/final boundary conditions, are still ill-understood. In this context, a physicist's approach, which aims to develop intuition and qualitative understanding through the examination of various limiting regimes and approximation schemes, can prove to be pertinent.

This manuscript can serve as a fairly accessible entry point for physicists in the realm of **MFG** theory, focusing on a particular class of models, dubbed quadratic, which display on the formal level some similarities to problems of physics. Chapter 2 introduced such models in a synoptic, albeit non-perfectly rigorous, way. Elements of Optimal Control, as well as Game Theory, were presented and parallels with Physics were drawn.

Chapter 3 investigated the particular case of integrable quadratic **MFG** for which exact analytical solutions can be computed. The small noise limit, for which there exists an instructive potential representation, was initially considered. The integrable character (in the physical sense) of those games was highlighted through the introduction of an infinite number of conserved quantities, equivalent to the traditional first integrals of motion, as coefficients of the multipole expansion of the potential from an auxiliary problem of electrostatics. Although what concrete effect each of those coefficients has on the actual solution of the game currently remains unclear, this multipole expansion presents several interesting features:

- In the long time limit, the auxiliary electrostatic potential can be approximated as one created by a simple monopole. This underlines the existence of a universal (as in independent of both the initial and terminal conditions) scaling behaviour, of a *pseudo-ergodic* state in a context where the ergodic state cannot be reached.
- The multipole expansion provides a generic way to approach this class of games and to interpret its solutions. Each coefficient has a proper physical meaning, independent of the boundary conditions.

- An easily controllable ansatz can be constructed as truncation to arbitrary finite order of the multipole expansion.

Noisy games were then considered and the possibility of using Inverse Scattering methods was explored. The applicability of these methods to MFG indicates the existence of a transformation to action-angle variables which can serve a role akin (and even complementary) to that of the multipole expansion in noiseless regimes. However, a few technical difficulties need to be addressed before all else:

- There should exist a simplifying hypothesis allowing the reduced monodromy matrix to be expressed in terms of two independent coefficients (just as Schrödinger monodromy) rather than four.
- The fact that Schrödinger variables do not vanish at infinity should be taken into account.
- A way to implement the MFG forward-backward structure should be devised, either through the addition of a self-consistent condition or by looking at the time monodromy.

Trying and solving any of those problems represents a reasonable axis for future research.

Chapter 4 proposed a simple, heuristic yet efficient, method to describe negatively coordinated MFG in one dimension. Three limiting regimes were emphasized: two dynamical ones describing the early stages of the game by way of two different ansätze, and a static one, also known as ergodic state, corresponding to the vast majority of the remaining game. Ways to couple those regimes, based on the concept of conservation of energy borrowed from Physics, were examined and characteristic length, as well as times, were introduced. That said, the finer details of the transition from one regime to another is still ill-described. Moreover this chapter focused on very particular, highly localized, initial conditions, it could be interesting to investigate more general ones. On a similar note, in a more general setting where center of mass of the distribution of players and maximum of the external gain do not coincide, collective motion of players towards this maximum is likely to occur. This, along with the possibility of an external gain displaying several local maxima, was not considered here. Finally, the existence of solutions to a counter-intuitive game, where interactions between players are repulsive and the effects of the external gain negligible but where players are actually gathering instead of dispersing, were briefly hinted at. These solutions could certainly be accounted for by the multipole expansion introduced chapter 3 and constitute a good argument as to why this particular representation should be further investigated.

Lastly, chapter 5 dealt with a WKB approach to Fokker-Planck equation in the weak noise limit, and, as such, does not strictly relate to

MFG theory. Nonetheless, this semi-classical approximation can find applications in the context of MFG and provides quantitatively satisfactory results, as was illustrated with the example of the seminar problem. Suggesting a similar treatment of Hamilton-Jacobi-Bellman equation, and then of the complete system of coupled MFG equations, is thus quite conceivable. This would represent an alternative approach to the weak noise limit of MFG, one which would probably be less abstract and more generic, albeit less insightful, than the potential representation of chapter 3.

Quadratic MFG form a brand new field for physicists to explore. They represent a simplification over more general models that can be addressed through methods originating from Physics, while still describing a reasonably large class of problems. This thesis takes a few steps in this fairly uncharted territory, examining by way of various approximation schemes what can be arguably considered the simplest non-trivial examples of negatively coordinated quadratic MFG, and highlights results that I believe to be encouraging. Although, at the moment, the models described in this manuscript still require further investigation, on a larger time-scale, one can wonder about enriched versions of those conundrums. The more natural extension of the previously discussed models would probably come as a generalisation to higher dimension. Another rather obvious extension would be to study non-local interactions. In a similar vein, examining effects of segregation (be it à la Schelling or in more simplistic ways) or frustration by looking at the interactions between different types of populations seems to be a reasonable direction to follow as well. Finally, it could be interesting to look for alternative MFG models that, maybe, fall outside of the quadratic class but are still simple enough to be studied thoroughly. Surely, one has to wonder if MFG, in the way they were described here, can accurately describe socio-economic phenomena, as the hypothesis of a perfectly rational and infinitely far-sighted player does not seem to be realistic. With this in mind, it may be feasible for one to devise a MFG toy-model featuring preference for the present and/or non-rational (possibly evolutionary) behaviours that can be approached through the lens of Physics.

Part III

APPENDIX

NUMERICAL SCHEME

The results of most simulations discussed in this manuscript were computed using the same C++ algorithm, this appendix provides details about the overall structure of the program as well as the discretization scheme. Numerical computations are done using the [NLS](#) representation of [MFG](#) equations

$$\begin{cases} \mu\sigma^2\partial_t\Phi = -\frac{\mu\sigma^4}{2}\partial_{xx}\Phi - (gm + U_0)\Phi \\ \mu\sigma^2\partial_t\Gamma = \frac{\mu\sigma^4}{2}\Delta\partial_{xx}\Gamma + (gm + U_0)\Gamma \\ u = -\mu\sigma^2\log\Phi \\ m = \Phi\Gamma \end{cases}, \quad (\text{A.1})$$

mainly because Φ and Γ follow the same equation (up to a sign) and it is obviously more convenient to have to program a solver for only one type of equation rather than two. Another important reason to use this representation comes from the fact that it makes it easy to adapt proven discretization schemes used in other contexts where [NLS](#) equation is present.

A.1 BASIC STRUCTURE

The main difficulties when trying to solve equations [\(A.1\)](#) come from the non-linear coupling between Φ and Γ along with the forward-backward structure of the system. The easiest way to bypass those difficulties is to assume a particular form of m , solve a linearized version of equations [\(A.1\)](#) and then iterate to obtain the "real" solutions in a self-consistent fashion. Essentially the algorithm can be broken down in such a way:

- Assume a plausible form of the density m^0 . The ergodic state, if one exists, can serve as a good initial guess.
- Compute a first solution Φ^1 of the equation

$$\mu\sigma^2\partial_t\Phi^1 = -\frac{\mu\sigma^4}{2}\partial_{xx}\Phi^1 - (gm^0 + U_0)\Phi^1, \quad (\text{A.2})$$

with initial condition $\exp\left[-\frac{u_T(x)}{\mu\sigma^2}\right]$. One should start by computing Φ because the initial condition for Γ is ill-defined.

- Compute Γ^1 , solution of

$$\mu\sigma^2\partial_t\Gamma^1 = \frac{\mu\sigma^4}{2}\partial_{xx}\Gamma^1 + (gm^0 + U_0)\Gamma^1, \quad (\text{A.3})$$

with initial condition $m^0(x, t = 0)/\Phi^1(x, t = 0)$.

- Update the initial guess $m^0 \rightarrow m^1 = \Phi^1\Gamma^1$ and repeat the process until m^i is sufficiently close to m^{i-1} .

This method is fairly efficient but self-consistency may prove difficult to achieve (probably because the solutions of the equations (A.1) constitute a saddle point of the action rather than a clear minimum) and convergence may never occur. A simple, yet not perfectly controlled, fix to this problem is to update the guess using a linear combination of the previous guess and what should be the new one

$$m^{i+1} = \alpha m^i + (1 - \alpha)\Phi^{i+1}\Gamma^{i+1}, \quad (\text{A.4})$$

α being an arbitrary number between 0 and 1.

A.2 CRANK-NICOLSON METHOD

Because equations (A.1) are based on NLS equation, we can make use of the well-known *Crank-Nicolson* discretization scheme [37].

A.2.1 Discretization scheme

Crank-Nicolson method is a finite difference method used mostly to deal with diffusion equations. For added stability, compared to Euler method for example, it is implicit in time.

TIME DISCRETIZATION

$$\partial_t \phi \rightarrow \frac{\phi_i^{j+1} - \phi_i^j}{\Delta t} \quad (\text{A.5})$$

(IMPLICIT) SPACE DISCRETIZATION

$$\partial_x \phi \rightarrow \frac{1}{2} \left(\frac{\phi_{i+1}^{j+1} - \phi_{i-1}^{j+1}}{2\Delta x} + \frac{\phi_{i+1}^j - \phi_{i-1}^j}{2\Delta x} \right) \quad (\text{A.6})$$

hence

$$\partial_{xx} \phi \rightarrow \frac{1}{2(\Delta x)^2} \left[\left(\phi_{i+1}^{j+1} - 2\phi_i^{j+1} + \phi_{i-1}^{j+1} \right) + \left(\phi_{i+1}^j - 2\phi_i^j + \phi_{i-1}^j \right) \right] \quad (\text{A.7})$$

DISCRETIZED EQUATION

$$\begin{aligned} & \phi_i^{j+1} \left(\frac{\mu\sigma^2}{\Delta t} + \frac{\mu\sigma^4}{2(\Delta x)^2} - \frac{U + gm_i^{j+1}}{2} \right) - \frac{\mu\sigma^4}{4(\Delta x)^2} (\phi_{i-1}^{j+1} + \phi_{i+1}^{j+1}) \\ &= \frac{\mu\sigma^4}{4(\Delta x)^2} (\phi_{i-1}^j + \phi_{i+1}^j) - \phi_i^{j+1} \left(-\frac{\mu\sigma^2}{\Delta t} + \frac{\mu\sigma^4}{2(\Delta x)^2} - \frac{U + gm_i^j}{2} \right) \end{aligned} \quad (\text{A.8})$$

Defining

$$\phi^j = \begin{pmatrix} \phi_1^j \\ \phi_2^j \\ \vdots \\ \phi_N^j \end{pmatrix}, \quad (\text{A.9})$$

one can write the discretized equation (A.8) in matrix form

$$A\phi^{j+1} = B\phi^j, \quad (\text{A.10})$$

where A and B are tridiagonal matrices with coefficients

$$\begin{cases} A_{\text{diag}} = \frac{\mu\sigma^2}{\Delta t} + \frac{\mu\sigma^4}{2(\Delta x)^2} - \frac{U_0 + gm_i^{j+1}}{2} \\ A_{\text{up}} = A_{\text{down}} = -\frac{\mu\sigma^4}{4(\Delta x)^2} \\ B_{\text{diag}} = -\frac{\mu\sigma^2}{\Delta t} + \frac{\mu\sigma^4}{2(\Delta x)^2} - \frac{U_0 + gm_i^j}{2} \\ B_{\text{up}} = B_{\text{down}} = \frac{\mu\sigma^4}{4(\Delta x)^2} \end{cases}. \quad (\text{A.11})$$

Because A and B are tridiagonal, numerical inversion is made using the $o(N)$ *Thomas algorithm* [42].

A.2.2 Neumann boundaries

In this case Dirichlet boundary conditions are trivially implemented in a $2L$ long box. To deal with Neumann boundaries, however, one needs to introduce ghost sites at each boundaries, in sites 0 and $N + 1$, and use either forward or backward finite difference to approximate the derivative

$$\begin{cases} 0 = \partial_x \phi(-L, t) \approx \frac{-3\phi(-L, t) + 4\phi(-L + \Delta x, t) - \phi(-L + 2\Delta x, t)}{2\Delta x} \\ 0 = \partial_x \phi(L, t) \approx \frac{3\phi(L, t) - 4\phi(L - \Delta x, t) + \phi(L - 2\Delta x, t)}{2\Delta x} \end{cases}, \quad (\text{A.12})$$

using $o(\Delta x^2)$ approximations [57]. This leads to the discretized equations

$$\begin{cases} \phi_0^j = \frac{4\phi_1^j - \phi_2^j}{3} \\ \phi_{N+1}^j = \frac{4\phi_N^j - \phi_{N-1}^j}{3} \end{cases}, \quad (\text{A.13})$$

which modify the first and last row of A and B

$$\begin{cases} A_{\text{diag},1}^{\text{N}} = A_{\text{diag},1} + \frac{4}{3}A_{\text{up},1} & B_{\text{diag},1}^{\text{N}} = B_{\text{diag},1} + \frac{4}{3}B_{\text{down},1} \\ A_{\text{diag},N}^{\text{N}} = A_{\text{diag},N} + \frac{4}{3}A_{\text{down},N} & B_{\text{diag},N}^{\text{N}} = B_{\text{diag},N} + \frac{4}{3}B_{\text{up},N} \\ A_{\text{up},1}^{\text{N}} = -\frac{A_{\text{down},1}}{3} + A_{\text{up},1} & B_{\text{up},1}^{\text{N}} = B_{\text{up},1} - \frac{B_{\text{down},1}}{3} \\ A_{\text{up},N}^{\text{N}} = -\frac{A_{\text{up},1}}{3} + A_{\text{down},N} & B_{\text{up},N}^{\text{N}} = B_{\text{down},N} - \frac{B_{\text{up},1}}{3} \end{cases} \quad (\text{A.14})$$

A.2.3 Von Neumann stability analysis

Crank-Nicolson method is supposed to be unconditionally stable and one can easily check that it is, at least is under *Von Neumann stability analysis*. To that end, one can study the growths of plane waves: suppose $\phi = \exp(ikx + \omega t)$ and plug it in the discretized version of Eqs (A.1)

$$\begin{aligned} \mu\sigma^2 \frac{e^{\omega\Delta t} - 1}{\Delta t} &= \frac{\mu\sigma^4}{2(\Delta x)^2} (\cos(k\Delta x) - 1) (e^{\omega\Delta t} + 1) \\ &\quad + \frac{U_0 + gm}{2} (e^{\omega\Delta t} + 1) \end{aligned} \quad (\text{A.15})$$

One can now compute the growth factor

$$e^{\omega\Delta t} = \frac{A + B + C}{A - B - C}, \quad (\text{A.16})$$

with

$$\begin{cases} A = \mu\sigma^2/\Delta t > 0 \\ B = \mu\sigma^4 (\cos(k\Delta x) - 1) / 2(\Delta x)^2 < 0 \\ C = (U + gm)/2 < 0 \end{cases} \quad (\text{A.17})$$

and check that it remains smaller than 1 for all Δt and Δx .

Even if Crank-Nicolson itself is unconditionally stable, it is of important note that the complete scheme is not. Noise, σ in other words, plays a critical regularizing role, particularly if interactions are repulsive.

METHOD OF CHARACTERISTICS

The method of characteristics is typically used to solve first-order partial differential equations. It aims to reduce a PDE to a family of ODEs that can be easily integrated. Let us consider a PDE

$$F(x_1, \dots, x_n, u, p_1, \dots, p_n) = 0 \quad (\text{B.1})$$

where $p_i \equiv \partial_{x_i} u$. Introducing a parameter s , and denoting by $(\dot{})$ its associated derivative, let $\gamma = (x_1, \dots, x_n, u, p_1, \dots, p_n)(s)$ be a curve of \mathbb{R}^{2n+1} . Assuming that u is a solution of PDE (B.1), one can infer three remarkable relations. First, by applying the chain rule to a solution u one can deduce

$$\dot{u} = \sum_i p_i \dot{x}_i, \quad (\text{B.2})$$

then, taking the exterior derivative of du yields

$$d(du) = 0 = \sum_i \dot{x}_i dp_i - \dot{p}_i dx_i, \quad (\text{B.3})$$

and finally, differentiating equation (B.1) with respect to s , one finds

$$\sum_i (\partial_{x_i} F + p_i \partial_u F) \dot{x}_i + \dot{p}_i \partial_{p_i} F = 0. \quad (\text{B.4})$$

Combining the last three equations, one can obtain the Lagrange-Charpit equations

$$\frac{\dot{x}_i}{\partial_{p_i} F} = - \frac{\dot{p}_i}{\partial_{x_i} F + p_i \partial_u F} = \frac{\dot{u}}{\sum_i p_i \partial_{p_i} F}, \quad (\text{B.5})$$

that can be used to find a *characteristic curve* γ along which PDE (B.1) simplifies to an ODE.

In the particular case of the Hamilton-Jacobi equation

$$\partial_t S + a \partial_x S - \frac{1}{2} (\partial_x S)^2 = 0, \quad (\text{B.6})$$

it is straightforward to check that the action defined by equation (5.15) is a solution, as Lagrange-Charpit equations are essentially equivalent to the canonical equations of Hamiltonian mechanics (5.10). Using the least action principle, one can check that for any $X = (x, t)$, $\partial_x S = p$ and $\partial_t S = E$, where p and E are the momentum and energy of the trajectory reaching x at time t . Since all the trajectories involved have to fulfil the compatibility condition (5.14), reading $L(x, t; \partial_x S, \partial_t S) = 0$ in this case, which is precisely the Hamilton-Jacobi equation.

A rather complete discussion of this method can be found for instance in chapter II of monograph [39].

RIEMANN INVARIANTS

As mentioned in section (3.1.3), Riemann's method can be considered as an extension of the method of characteristics. It amounts to finding curves (*characteristics*) on which some quantities (*Riemann invariants*) are conserved. Let $\Omega(t, x)$ be a curve (of tangent \vec{s} and normal \vec{n}) on which m, v , solutions of system (3.6), and their derivatives are known. Let $\theta(t, x)$ be the angle between \vec{s} and the x -axis, one can write

$$\begin{cases} \frac{dv}{ds} = \partial_x v \cos \theta + \partial_t v \sin \theta \\ \frac{dm}{ds} = \partial_x m \cos \theta + \partial_t m \sin \theta \end{cases} . \quad (\text{C.1})$$

The Cauchy problem for the system (3.6) can only be solved if the initial (or boundary) data is not specified on a characteristic curve because one cannot use a Taylor expansion in its vicinity (information only propagates along the characteristic). As a consequence the determinant Δ of the combined system (3.6)+(C.1) is non zero unless Ω is a characteristic. Computing Δ

$$\begin{aligned} \Delta &= \begin{vmatrix} 1 & v & 0 & m \\ 0 & g/\mu & 1 & v \\ \sin \theta & \cos \theta & 0 & 0 \\ 0 & 0 & \sin \theta & \cos \theta \end{vmatrix} , \\ &= -(\cos \theta - v \sin \theta)^2 + \frac{g}{\mu} m \sin^2 \theta \end{aligned} \quad (\text{C.2})$$

reveals that Ω is a characteristic if

$$\cot \theta_{\pm} = v \pm i \sqrt{\frac{m|g|}{\mu}} . \quad (\text{C.3})$$

This is the major difference with traditional NLS equation, the characteristics, here, are complex and have no physical meaning and thus solutions cannot feature discontinuous derivatives anywhere. Another way to look at this is to acknowledge that the system (3.6) is elliptic rather than hyperbolic: its solutions are not wave-like, a perturbation propagates instantly to all points of the domain. Nevertheless, the fact that characteristics are complex bears no consequence for the hodograph transform itself as we only need the Riemann invariants to do so.

Now that we have identified the characteristics of the problem, let us show that there exists a pair (λ_+, λ_-) of Riemann invariants associated to the pair (θ_+, θ_-) , and extract their dynamics. To do so we

start by multiplying the first equation of (3.6) by $-\frac{g}{\mu} \sin \theta$, the second by $(\cos \theta - v \sin \theta)$, and subtract one from the other

$$-\frac{g}{\mu} \sin \theta [\partial_t m + \partial_x(mv)] - (\cos \theta - v \sin \theta) \left(\partial_t v + v \partial_x v + \frac{g}{\mu} \partial_x m \right) = 0. \quad (\text{C.4})$$

Using equations (C.1) and the fact that $\Delta = 0$ along a characteristic curve, one can rewrite the previous equation in a more compact manner

$$\frac{dv}{ds} \pm i \sqrt{\frac{|g|}{\mu m}} \frac{dm}{ds} = 0, \quad (\text{C.5})$$

the left-hand side of which has the form of a total derivative. Introducing λ_{\pm} such that

$$\begin{cases} \partial_m \lambda_{\pm} = \pm i \sqrt{\frac{|g|}{\mu m}} \\ \partial_v \lambda_{\pm} = 1 \end{cases}, \quad (\text{C.6})$$

it then becomes clear that

$$\frac{d\lambda_{\pm}}{ds} = 0, \quad (\text{C.7})$$

the definition of a Riemann invariant. From there, computing (λ_+, λ_-) , as well as their dynamics, is fairly straightforward. One can integrate equations (C.6) and reformulate equation (C.7) in terms of (x, t) using equations (C.1) and (C.3) so that one is able to construct

$$\begin{cases} \lambda_{\pm} = v \pm 2i \sqrt{\frac{|g|m}{\mu}} \\ \partial_t \lambda_{\pm} + \left(\frac{3}{4} \lambda_{\pm} + \frac{1}{4} \lambda_{\mp} \right) \partial_x \lambda_{\pm} = 0 \end{cases}, \quad (\text{C.8})$$

the equations introduced in section (3.1.3).

GREEN'S THEOREM AND THE LAPLACE EQUATION

Traditionally the boundary value problem for elliptic PDEs, and in particular for Laplace equation, can be solved by means of Green's theorem. In other words, if one is able to compute the impulse response, also known as Green's function, G of Laplace equation (3.18), one should be able to define the potential χ as the convolution of G with the boundary data.

D.1 GREEN FUNCTION OF LAPLACE EQUATION IN CYLINDRIC COORDINATES

Green's function for Laplace equation is defined as its impulse response

$$\Delta G = -\frac{4\pi}{\eta} \delta(\eta - \eta') \delta(\xi - \xi'), \quad (\text{D.1})$$

where Δ is the cylindrical Laplacian and the Dirac deltas have been expressed in cylindrical coordinates. Equations of this type are quite well-known and can be solved by separation of variables. To that end, it is convenient to introduce Dirac deltas in their Fourier representation

$$\delta(\xi - \xi') = \frac{1}{\pi} \int_0^\infty \cos(k(\xi - \xi')) dk, \quad (\text{D.2})$$

and assume G can take the form

$$G = \frac{1}{\pi} \int_0^\infty \cos(k(\xi - \xi')) g_k(\eta, \eta') dk, \quad (\text{D.3})$$

so as to write equation (D.1) as

$$\partial_{\eta,\eta} g_k + \frac{1}{\eta} \partial_\eta g_k - k^2 g_k = -\frac{4\pi}{\eta} \delta(\eta - \eta'). \quad (\text{D.4})$$

As long as $\eta \neq \eta'$ and the right-most term is equal to 0, this equation is known as Bessel's differential equation and it admits first order modified Bessel functions of the first and second kind, $I_0(k\eta)$ and $K_0(k\eta)$, as solution. For G to make sense, it has to be continuous, bounded for $\eta \rightarrow 0$ as well as $\eta \rightarrow \infty$ and symmetric by inversion of η and η' . Given the properties of I_0 and K_0 , the only acceptable solution for equation (D.1) is

$$g_k = A I_0(k\eta_{<}) K_0(k\eta_{>}), \quad (\text{D.5})$$

where $\eta_{<} = \eta$ and $\eta_{>} = \eta'$ when $\eta < \eta'$ but $\eta_{<} = \eta'$ and $\eta_{>} = \eta$ when $\eta > \eta'$. The prefactor A is then determined by the discontinuity in the slope induced by the δ function

$$\left. \frac{dg_k}{d\eta} \right|_+ - \left. \frac{dg_k}{d\eta} \right|_- = -\frac{4\pi}{\eta'} = AkW[I_0(k\eta), K_0(k\eta)], \quad (D.6)$$

$W[I_0(x), K_0(x)] = -\frac{1}{x}$ being the Wronskian of the modified Bessel functions of first and second kind, yielding $A = 4\pi$.

D.2 SOLVING THE BOUNDARY VALUE PROBLEM

In order to specify the boundary problem one needs to solve, one has to relate equation (3.18) to the original problem, namely, MFG equations (2.24) along with their mixed-type boundary conditions on u and m . Let $S_\Omega(\xi_\Omega, \eta_\Omega, \theta)$ be a curve in the hodograph space where

$$\begin{cases} \xi_\Omega = \xi(t(s), x(s)) \\ \eta_\Omega = \eta(t(s), x(s)) \end{cases}, \quad (D.7)$$

represent the boundary conditions of the initial problem. Using the compatibility equations (3.19) one may then compute χ on S_Ω

$$\begin{cases} \partial_\xi \chi_\Omega = 2(x(s) - \xi_\Omega t(s)) \\ \partial_\eta \chi_\Omega = \eta_\Omega t(s) \\ \partial_s \chi_\Omega = \partial_\xi \chi_\Omega \partial_s \xi_\Omega + \partial_\eta \chi_\Omega \partial_s \eta_\Omega \end{cases}, \quad (D.8)$$

and the boundary problem is specified. One can now apply Green's theorem, in the hodograph coordinates (η, θ, ξ) , to χ and G

$$\begin{aligned} & \int_{V_\Omega} [\chi(\xi', \eta') \Delta G(\xi, \eta; \xi', \eta') - G(\xi, \eta; \xi', \eta') \Delta \chi(\xi', \eta')] \eta' d\eta' d\theta d\xi' \\ &= \int_{S_\Omega} [\chi(\xi', \eta') \vec{\nabla} G(\xi, \eta; \xi', \eta') - G(\xi, \eta; \xi', \eta') \vec{\nabla} \chi(\xi', \eta')] \cdot \vec{n} dS \end{aligned} \quad (D.9)$$

where V_Ω is the volume enclosed by S_Ω in which χ is meant to be computed, $\vec{\nabla}$ is the cylindrical gradient and \vec{n} is the normal to S_Ω . By definition, G being an impulse response and χ being solution to Laplace equation (3.18), the volume integral in equation (D.9) can be easily rewritten

$$\chi(\xi, \eta) = -\frac{1}{4\pi} \int_{S_\Omega} \left[\chi(\xi', \eta') \vec{\nabla} G(\xi, \eta; \xi', \eta') - G(\xi, \eta; \xi', \eta') \vec{\nabla} \chi(\xi', \eta') \right] \cdot \vec{n} dS \quad (D.10)$$

Note that this is an integral statement, not a solution to a boundary-value problem as a problem where both χ and $\vec{\nabla} \chi$ are known is over-specified. In the context of MFG, the initial-value problem would specify both $\eta(t=0, x)$ and $\xi(t=0, x)$, and hence $\vec{\nabla} \chi$ through the compatibility equations (3.19), on a surface S_Ω . Then, observing that the

impulse response G is actually defined up to an harmonic function F , one can choose $G_N = G + F$ as Green's function of the problem so that the $\vec{n} \cdot \vec{\nabla} G_N(\xi, \eta; \xi', \eta')$ term in integral (D.10) vanishes on S_Ω . As such

$$\chi(\xi, \eta) = \frac{1}{4\pi} \int_{S_\Omega} G_N(\xi, \eta; \xi', \eta') \vec{\nabla} \chi(\xi', \eta') \cdot \vec{n} dS, \quad (\text{D.11})$$

is solution to Laplace equation (3.18) with Neumann boundary conditions. A remarkable advantage of this method is that G_N does not depend on the details of the boundary conditions, but only on S_Ω , simplifying the original problem greatly. However, determining G_N can become rather involved depending on the shape of S_Ω .

The main problem with such an approach comes from the fact that S_Ω does not exist in the context of MFG because there is no point at which we know both m and u, η and ξ . Seemingly, one could look for particular cases where the problem simplifies, the most obvious one being the limit we considered in the simulation illustrated Figure (3), where $\{\xi(T, x) \rightarrow 0 \forall x\}$. In this case the system (D.8) reduces to

$$\begin{cases} \partial_\xi \chi_\Omega = 2x \\ \partial_\eta \chi_\Omega = \eta_\Omega T \\ \chi_\Omega = \frac{\eta_\Omega^2 T}{2} \end{cases}, \quad (\text{D.12})$$

and equation (D.9) to

$$\chi(\xi, \eta) = -\frac{1}{4\pi} \int_0^{\bar{\eta}} \eta' \left[\frac{\eta'^2 T}{2} \partial_{\xi'} G(\xi, \eta; \xi', \eta') - 2x G(\xi, \eta; \xi', \eta') \right] d\eta', \quad (\text{D.13})$$

$\bar{\eta} = \eta(T, 0)$ being the maximum of η at time T . The second term in the integrand is problematic as it contains x which is an unknown function of η at $t = T$. But, because this relation holds for all function G that verifies equation (D.1) on the domain where χ is defined, if one can find a valid function G so that $G = 0$ if $\xi' = 0$ one can also compute the potential regardless of if $\eta(T, x)$ is known or not. Let us call G_0 the free Green function computed in last section

$$G_0 = 4 \int_0^\infty \cos(k(\xi - \xi')) I_0(k\eta_{<}) K_0(k\eta_{>}) dk, \quad (\text{D.14})$$

and define

$$F = 4 \int_0^\infty \cos(k(\xi)) I_0(k\eta_{<}) K_0(k\eta_{>}) dk, \quad (\text{D.15})$$

then

$$G = G_0 - F = 4 \int_0^\infty [\cos(k(\xi - \xi')) - \cos(k\xi)] I_0(k\eta_{<}) K_0(k\eta_{>}) dk,$$

(D.16)

is a valid candidate. Hence, one should be able to obtain a fairly simple expression for the potential

$$\chi(\xi, \eta) = -\frac{1}{\pi} \int_0^{\eta} \int_0^{\infty} k \sin(k\xi) \frac{\eta'^3 T}{2} I_0(k\eta') K_0(k\eta'') d\eta' dk. \quad (\text{D.17})$$

The reason this is not the case in the aforementioned simulation is only because σ , there, is small but non zero.

Unfortunately this does not work either, because for the terminal cost to be flat, $\xi(t = T, x) = 0$ for all x , the charge distribution at the origin ρ_0 (and by extension all of the exterior multipole moments) also needs to be zero. This means that the only way to observe a flat terminal cost in the weak noise limit is for both m and u to be stationary which corresponds to a highly unsatisfactory solution. In that sense, the limit of flat terminal cost is ill-defined for $\sigma = 0$. Or rather, the limit $\sigma \rightarrow 0$ does not commute with the one $c_T(x) \rightarrow 0$. To my knowledge no matter the (mixed-type) boundary conditions and the simplification they bring, one will end up facing a similar problem.

NON-ABELIAN STOKES THEOREM

This appendix aims to introduce the non-Abelian Stokes theorem in the context of the [IST](#) presented in section [3.2](#). While I want to keep this discussion concise, more details on this subject can be found in [\[24\]](#).

E.1 STOKES THEOREM

We start by briefly recalling the traditional, Abelian, Stokes theorem. Let N be a d -dimensional manifold, ∂N its $(d-1)$ -dimensional boundary and ω a $(d-1)$ -form with differential $d\omega$. Then this theorem states that

$$\int_N d\omega = \int_{\partial N} \omega, \quad (\text{E.1})$$

converting an integral over a closed surface into a volume integral.

E.2 GENERALIZATION TO NON ABELIAN FORMS

To generalize the previous result, one can introduce the covariant derivative

$$D_i = \partial_i - A_i, \quad (\text{E.2})$$

where A_i is the i component of a connection. Then, the non Abelian version of the relation [\(E.1\)](#) naturally reads

$$\mathcal{P} \exp \oint A = \mathcal{P} \exp \int DA, \quad (\text{E.3})$$

where \mathcal{P} denotes the path ordering. Now, let us recall the compatibility condition [\(3.54\)](#) of the auxiliary problem [\(3.53\)](#)

$$\partial_t U + \partial_x V + [U, V] = 0. \quad (\text{E.4})$$

As I mentioned in section [3.2](#), U and V can be interpreted as a connection (or gauge potential), used to define the parallel transport Ω through equation [\(3.58\)](#). We can make this more explicit by noticing that the compatibility condition [\(3.54\)](#) can be rewritten in a very compact way

$$[D_0, D_1] = 0, \quad (\text{E.5})$$

with

$$\begin{cases} \partial_0 - A_0 = \partial_x - U \\ \partial_1 - A_1 = \partial_t - V \end{cases}, \quad (\text{E.6})$$

which is equivalent to saying that the differential form $A = A_i dx^i$ has a vanishing covariant derivative

$$DA = D_j A_i dx^i \wedge dx^j = 0 . \quad (\text{E.7})$$

By way of the non-Abelian Stokes theorem, this means that

$$\mathcal{P} \exp \oint A = \mathbb{1} , \quad (\text{E.8})$$

hence the name *zero-curvature condition*.

POISSON COMMUTATIVITY OF THE FIRST INTEGRALS OF MOTION

For the MFG equations (3.1) to be completely integrable in the Liouville sense, the (infinite number of) conserved quantities generated section 3.2.4 need to be in involution. In this appendix I will introduce a Poisson structure in the context of integrable MFGs and use it to show the Poisson commutativity of the aforementioned conserved quantities.

F.1 GENERALISATION OF POISSON BRACKETS TO INFINITE DIMENSIONAL SYSTEMS

For N-dimensional Hamiltonian systems, given two functions $f(p_i, q_i, t)$ and $g(p_i, q_i, t)$ of Darboux coordinates (p_i, q_i) on the phase space, *Poisson brackets* take the form

$$\{f, g\} = \sum_{i=1}^N \left(\frac{\partial f}{\partial q_i} \frac{\partial g}{\partial p_i} - \frac{\partial f}{\partial p_i} \frac{\partial g}{\partial q_i} \right). \quad (\text{F.1})$$

However, MFG equations (3.1) constitute an infinite-dimensional system and definition (F.1) needs to be extended. In this case the phase space \mathcal{M} is an infinite-dimensional real space with positive coordinates defined by pairs of functions $\Phi(x, t)$ and $\Gamma(x, t)$. On this phase space, the algebra of observables is made up of smooth, real, analytic functionals, on which one can define a *Poisson structure* by the following bracket

$$\{F, G\} = \int_{\mathbb{R}} \left(\frac{\delta F}{\delta \Phi} \frac{\delta G}{\delta \Gamma} - \frac{\delta F}{\delta \Gamma} \frac{\delta G}{\delta \Phi} \right) dx, \quad (\text{F.2})$$

which possesses the standard properties of Poisson brackets: it is skew-symmetric and satisfies Jacobi identity. The coordinates Φ and Γ may themselves be considered functionals on \mathcal{M} (albeit with generalized functions for variational derivative) such that

$$\begin{aligned} \{\Phi(x, t), \Gamma(y, t)\} &= \delta(x - y) \\ \{\Phi(x, t), \Phi(y, t)\} &= \{\Gamma(x, t), \Gamma(y, t)\} = 0 \end{aligned} \quad (\text{F.3})$$

These formulae directly yield that, for any observable F

$$\frac{\delta F}{\delta \Phi} = \{F, \Gamma\} \quad \text{and} \quad \frac{\delta F}{\delta \Gamma} = -\{F, \Phi\}, \quad (\text{F.4})$$

By analogy with finite-dimensional coordinates, x may be thought of a coordinate label.

and in particular, if this observable is the energy defined by equation (2.35), $F = E$, one obtains *Hamilton's equations of motion*

$$\begin{cases} \frac{\delta E}{\delta \Phi} = \{E, \Gamma\} = \mu \sigma^2 \partial_t \Gamma \\ \frac{\delta E}{\delta \Gamma} = -\{E, \Phi\} = \mu \sigma^2 \partial_t \Phi \end{cases}, \quad (\text{F.5})$$

which are perfectly equivalent to MFG equations (3.1). The Poisson structure defined by the non-degenerate bracket (F.2) highlights the symplectic nature of the phase space \mathcal{M} and each of the Poisson commuting integrals of motion correspond to a leaf of the regular foliation of this phase space. This provides yet another, Hamiltonian, representation of MFG problems.

F.2 CLASSICAL R-MATRIX

The simplest way to check that all the invariant observables generated section 3.2.4 are in involution (and prove that the system is completely integrable in the Liouville sense) is probably to verify that the Poisson bracket of the trace of the monodromy matrix with itself vanishes

$$\{\text{Tr}[T], \text{Tr}[T]\} = 0, \quad (\text{F.6})$$

as $\text{Tr}[T]$ can serve as generating functions for the constant of motion. In this section I will introduce a powerful tool that will help me with these computations: the *classical r-matrix*.

To that end, let us define a *tensorial Poisson bracket* for any 2×2 matrix functionals A and B

*This can naturally
be generalized to
 $n \times n$ matrices, but
I restrict the
discussion to
matrices of the size
of T .*

$$\{A \otimes B\} = \int_{\mathbb{R}} \left(\frac{\delta A}{\delta \Phi} \otimes \frac{\delta B}{\delta \Gamma} - \frac{\delta A}{\delta \Gamma} \otimes \frac{\delta B}{\delta \Phi} \right) dx, \quad (\text{F.7})$$

such that

$$\{A \otimes B\}_{j,k,m,n} = \{A_{j,m}, B_{k,n}\}. \quad (\text{F.8})$$

Hence, using relations (F.3), one can compute the bracket of U , x -component of the Lax connection, with itself

$$\{U(x, \lambda) \otimes U(y, \mu)\} = v(\sigma_- \otimes \sigma_+ - \sigma_+ \otimes \sigma_-) \delta(x - y), \quad (\text{F.9})$$

which can also be written as

$$\{U(x, \lambda) \otimes U(y, \mu)\} = [r(\lambda - \mu), U(x, \lambda) \otimes \mathbb{I} + U(x, \mu) \otimes \mathbb{I}] \delta(x - y), \quad (\text{F.10})$$

where the classical r-matrix takes the form

$$r(\lambda) = -\frac{v}{\lambda} \begin{pmatrix} 1 & 0 & 0 & 0 \\ 0 & 0 & 1 & 0 \\ 0 & 1 & 0 & 0 \\ 0 & 0 & 0 & 1 \end{pmatrix}. \quad (\text{F.11})$$

The point of this formulation is to express tensorial Poisson brackets, which may be difficult to compute for the monodromy matrix T , as simple commutators. The existence of the r -matrix and formulation (F.10) underlies integrability and has a natural Lie-algebraic interpretation. As such, this relation takes the name of *fundamental Poisson bracket*.

F.3 SKLYANIN FUNDAMENTAL RELATION

To compute the Poisson bracket of T with itself one can evaluate an integral version of the fundamental Poisson bracket (F.10)

$$\{T_{ab}(x, y, \lambda), T_{cd}(x, y, \mu)\} = \int_x^y \frac{\delta T_{ab}(x, y, \lambda)}{\delta U_{jk}(z, \lambda)} \{U_{jk}(z, \lambda), U_{lm}(z', \mu)\} \frac{\delta T_{cd}(x, y, \mu)}{\delta U_{lm}(z', \mu)} dz dz' . \quad (\text{F.12})$$

By varying the differential equation (3.70), that serves as definition of the monodromy matrix T

$$\partial_x \delta T(x, y, \lambda) = \delta U(x, \lambda) T(x, y, \lambda) + U(x, \lambda) \delta T(x, y, \lambda) , \quad (\text{F.13})$$

the solution of which is

$$\delta T(x, y, \lambda) = \int_y^x T(x, z) \delta U(z) T(z, y) dz , \quad (\text{F.14})$$

it follows that

$$\frac{\delta T_{ab}(x, y, \lambda)}{\delta U_{jk}(z, \lambda)} = T_{aj}(x, z, \lambda) T_{kb}(z, y, \lambda) . \quad (\text{F.15})$$

Inserting this last expression in equation (F.12) one eventually gets

$$\begin{aligned} \{T(x, y, \lambda) \otimes T(x, y, \mu)\} &= \int_y^x (T(x, z, \lambda) \otimes T(x, z, \mu)) \\ &\quad [r(\lambda - \mu), U(z, \lambda) \otimes \mathbb{I} + \mathbb{I} \otimes U(z, \mu)]' \\ &\quad (T(z, y, \lambda) \otimes T(z, y, \mu)) dz \end{aligned} \quad (\text{F.16})$$

that simplifies, noticing the integrand is a total derivative with respect to z ,

$$\{T(x, y, \lambda) \otimes T(x, y, \mu)\} = -[r(\lambda - \mu), T(x, y, \lambda) \otimes T(x, y, \mu)] . \quad (\text{F.17})$$

This formulation is sometimes called *RTT Poisson structure* or *Sklyanin fundamental relation*.

F.4 INVOLUTION OF THE FIRST INTEGRALS OF MOTION

From Sklyanin fundamental relation (now that integrals depending on unknown fields Φ and Γ that constitute Poisson brackets are dealt with implicitly) it is easy to show the constants of motion are in involution. In particular, recalling that, for any pair of matrices (A, B)

$$\text{Tr}(A \otimes B) = \text{Tr}[A]\text{Tr}[B] , \quad (\text{F.18})$$

yields from equation (F.17), since the trace of a commutator is zero,

$$\{\text{Tr}[T(x, y, \lambda)], \text{Tr}[T(x, y, \mu)]\} = 0 , \quad (\text{F.19})$$

proving the involution of the first integrals of motion.

DERIVATION OF THE SEMI-CLASSICAL
APPROXIMATION FOR QUADRATIC EXTERNAL
POTENTIAL

This appendix deals with the semi-classical approximation of equation (4.15). Such approximation consists at looking for solution of the form

$$\Psi_{\text{SC}}(x) = \psi(x) \exp\left(\frac{S(x)}{\sqrt{\mu\sigma^4}}\right), \quad (\text{G.1})$$

that verify the aforementioned equation up to the second order in σ^2 .

Order σ^0

At zeroth order, equation (4.15) reduces to

$$(U_0(x) + \lambda) \psi(x) + \frac{(\partial_x S(x))^2}{2} \psi(x) = 0, \quad (\text{G.2})$$

which can be analytically integrated given the external potential is not too complicated. Taking once again the example of a quadratic potential, we get

$$\begin{aligned} S(x) &= \int_{\sqrt{\frac{2\lambda}{\mu\omega_0^2}}}^x \sqrt{2\left(\frac{\mu\omega_0^2 s^2}{2} - \lambda\right)} ds \\ &= \frac{\lambda}{\sqrt{\mu\omega_0^2}} \left[x \sqrt{\frac{\mu\omega_0^2}{2\lambda}} \sqrt{x^2 \frac{\mu\omega_0^2}{2\lambda} - 1} - \operatorname{argcosh}\left(x \sqrt{\frac{\mu\omega_0^2}{2\lambda}}\right) \right]. \end{aligned} \quad (\text{G.3})$$

Order σ^2

At first order in σ^2 , equation (4.15) becomes

$$\partial_{xx} S(x) \psi(x) + 2\partial_x S(x) \partial_x \psi(x) = 0 \quad \Rightarrow \quad \psi(x) = \frac{C^{1/4}}{\sqrt{\partial_x S(x)}}, \quad (\text{G.4})$$

easily computed using equation (G.2)

$$\psi(x) = \left[\frac{-C}{2(U_0(x) + \lambda)} \right]^{1/4}, \quad (\text{G.5})$$

up to a multiplicative constant C obtained numerically.

Uniform approximation

In order to avoid the use of complex numbers, one has to consider different versions of the semi-classical action S , depending on the sign of $(U_0 + \lambda)$. For $x < \sqrt{\frac{2\lambda}{\mu\omega^2}}$

$$\begin{aligned} S_{\text{left}}(x) &= \int_x^{\sqrt{\frac{2\lambda}{\mu\omega_0^2}}} \sqrt{2 \left(\lambda - \frac{\mu\omega_0^2 s^2}{2} \right)} ds \\ &= \frac{\lambda}{\sqrt{\mu\omega_0^2}} \left[\frac{\pi}{2} - x \sqrt{\frac{\mu\omega_0^2}{2\lambda}} \sqrt{1 - x^2 \frac{\mu\omega_0^2}{2\lambda}} - \arcsin \left(x \sqrt{\frac{\mu\omega_0^2}{2\lambda}} \right) \right], \end{aligned} \quad (\text{G.6})$$

while, as earlier, if $x > \sqrt{\frac{2\lambda}{\mu\omega^2}}$

$$S_{\text{right}}(x) = \frac{\lambda}{\sqrt{\mu\omega_0^2}} \left[x \sqrt{\frac{\mu\omega_0^2}{2\lambda}} \sqrt{x^2 \frac{\mu\omega_0^2}{2\lambda} - 1} - \operatorname{argcosh} \left(x \sqrt{\frac{\mu\omega_0^2}{2\lambda}} \right) \right]. \quad (\text{G.7})$$

PROOF THAT THE OPERATOR \hat{D} HAS ONLY REAL
NON-NEGATIVE EIGENVALUES

This appendix investigates the operator \hat{D} introduced in equation (4.24), and in particular provides a proof of why it has only real non-negative eigenvalues.

Consider any two function with compact support (φ, φ') . Applying the operator \hat{D} and integrating by part twice gives that

$$\begin{aligned}\langle \varphi | \hat{D} | \varphi' \rangle &= \int dx \varphi(x) \hat{D} [\varphi'(x)] \\ &= \int dx \hat{D} [\varphi(x)] [\varphi'(x)] \cdot \\ &= \langle \varphi' | \hat{D} | \varphi \rangle\end{aligned}\tag{H.1}$$

The operator \hat{D} is therefore real and symmetric and, as such, has only real eigenvalues.

Now, introducing ϵ_i eigenvalue of \hat{D} , and $\varphi_i(x)$ the corresponding eigenvector, one has

$$\begin{aligned}\langle \varphi_i | \hat{D} | \varphi_i \rangle &= \epsilon_i \int dx \varphi_i^2(x) \\ &= \int dx [\partial_x \varphi(x)]^2 \bar{m}(x) \cdot\end{aligned}\tag{H.2}$$

Since $\varphi(x)^2$, $[\partial_x \varphi(x)]^2$, and $\bar{m}(x)$ are all positive quantities, this implies that ϵ_i too has to be positive.

DECREASING SOLUTIONS OF THE EFFECTIVE GAME

As mentioned in section 4.2.2, this appendix provides expressions for the decreasing families of solutions of the effective game

$$z(t) = \begin{cases} z_* \xi^+(\alpha z_*^{-3/2}(t_0 - t)) & \text{if } \epsilon = 1 \\ \xi^0(\alpha(t_0 - t)) & \text{if } \epsilon = 0 \\ z_* \xi^-(\alpha z_*^{-3/2}(t_0 - t)) & \text{if } \epsilon = -1 \end{cases} . \quad (\text{I.1})$$

Contrary to increasing solutions, decreasing solutions can only be defined on $[0, t_0]$, and with $t_0 < \frac{\pi z_*^{3/2}}{2\alpha}$ if $\epsilon = -1$. Using those properties we can also construct a mixed type solution by patching together an increasing "-" type solution with a decreasing one of same z_*

$$z(t) = \begin{cases} z_* \xi^-\left(\frac{\pi}{2} + \alpha z_*^{-3/2}(t - T_m)\right) & \text{for } 0 \leq t \leq T_m \\ z_* \xi^-\left(\frac{\pi}{2} - \alpha z_*^{-3/2}(t - T_m)\right) & \text{for } T_m \leq t \leq T \end{cases} , \quad (\text{I.2})$$

with T_m the the time at which the solutions starts decreasing, with

$$T - \frac{\pi z_*^{3/2}}{2\alpha} \leq 0 \leq T_m \leq \frac{\pi z_*^{3/2}}{2\alpha} . \quad (\text{I.3})$$

Increasing "+", decreasing or mixed type solutions can all be observed numerically, however they refer to configurations where variations of the terminal cost are important in front of $\tilde{u} = \mu\sigma^2$ and fall outside the scope of chapter 4. Still, I mention them, once again, for the sake of completeness.

NON-HERMITIAN CORRECTION TO THE
SEMI-CLASSICAL TREATMENT OF
FOKKER-PLANCK EQUATION

As mentioned in section 5.1.2, the additional term $\frac{1}{2} \int_{t_0}^t \partial_x a d\tau$ in the semi-classical expression (5.19) can be seen as coming from the perturbation of the non-Hermitian operator

$$\hat{L}_1 = \hat{L} - \hat{L}_0, \quad (\text{J.1})$$

on the Hermitian approximation of \hat{L}

$$\hat{L}_0 = \left\{ \lambda^{-1} \partial_t \cdot + \frac{\lambda^{-1}}{2} [\partial_x(a \cdot) + a \partial_x(\cdot)] - \frac{1}{2} (\lambda^{-1} \partial_x)^2 \cdot \right\}. \quad (\text{J.2})$$

This can be made clearer by applying \hat{L}_1 on $m(t, x)$

$$\begin{aligned} \hat{L}_1 m &= \frac{\lambda^{-1}}{2} [\partial_x(am) - a \partial_x(m)] \\ &= \frac{\lambda^{-1}}{2} (\partial_x a) m, \end{aligned} \quad (\text{J.3})$$

and then defining its classical symbol

$$L_1 = \frac{\lambda^{-1}}{2} \partial_x a. \quad (\text{J.4})$$

Using traditional first order perturbation theory for the action we thus obtain $S \rightarrow S_0 + \delta S$ with

$$\delta S \equiv - \int_{t_0}^t L_1 d\tau = - \frac{\lambda^{-1}}{2} \int_{t_0}^t (\partial_x a) d\tau, \quad (\text{J.5})$$

where the integral is taken on the unperturbed trajectory.

LIOUVILLE'S FORMULA

For completeness, in this appendix, we provide a brief derivation of the Liouville formula used in Section 5.2, as presented in [101]. We consider a dynamic system described by

$$\frac{d\vec{x}}{dt} = f(\vec{x}) \quad (\vec{x} \in \mathbb{R}^d), \quad (\text{K.1})$$

and consider a $(d-1)$ -family of trajectories $\vec{x}(t, \vec{\alpha})$ indexed by $\vec{\alpha} \in \mathbb{R}^{(d-1)}$. Defining $J(t, \vec{\alpha}) \equiv \det \left[\frac{\partial \vec{x}(t, \vec{\alpha})}{\partial (t, \vec{\alpha})} \right]$, the Liouville's formula states that

$$\frac{d \ln J}{dt} = \text{Tr} \left[\frac{\partial f}{\partial \vec{x}}(\vec{x}(t, \vec{\alpha})) \right]. \quad (\text{K.2})$$

Derivation

Let A a $d \times d$ matrix. Naturally $\det A = \exp[\text{Tr} \ln A]$, and thus

$$\frac{d(\ln \det A)}{dt} = \frac{d(\text{Tr} \ln A)}{dt}. \quad (\text{K.3})$$

Now, for any function g of A , writing $g(A) = \sum_n g_n A^n$ and using the cyclicity of the trace

$$\frac{d(\text{Tr} g(A))}{dt} = \text{Tr} \left[g'(A) \frac{dA}{dt} \right]. \quad (\text{K.4})$$

Thus, if $A \equiv \frac{\partial \vec{x}}{\partial (t, \vec{\alpha})}$ and $J(t, \vec{\alpha}) \equiv \det A$, one obtains

$$\frac{d \ln J}{dt} = \text{Tr} A^{-1} \frac{dA}{dt}. \quad (\text{K.5})$$

Noting that, here, the total derivative $\frac{d}{dt}$ is the same as the partial derivative ∂_t taken at constant $\vec{\alpha}$, one furthermore has

$$\frac{dA}{dt} = \frac{\partial^2 \vec{x}(t, \vec{\alpha})}{\partial t \partial (t, \vec{\alpha})} = \frac{\partial f(\vec{x}(t, \vec{\alpha}))}{\partial (t, \vec{\alpha})}, \quad (\text{K.6})$$

and in the end

$$\frac{d \ln J}{dt} = \text{Tr} \left[\frac{\partial (t, \vec{\alpha})}{\partial \vec{x}} \frac{\partial f(\vec{x}(t, \vec{\alpha}))}{\partial (t, \vec{\alpha})} \right] = \text{Tr} \left[\frac{\partial f}{\partial \vec{x}}(\vec{x}(t, \vec{\alpha})) \right]. \quad (\text{K.7})$$

COUPLING TWO SEMI-CLASSICAL SOLUTIONS OF FOKKER-PLANCK EQUATION

This appendix aims at addressing what was left out of 5.3.3 for the sake of succinctness. I will first provide explicit expressions for the reflected action equation (5.87), then I will discuss the configuration where the agents begin in a constant drift region.

Explicit expression of the reflected action

Recalling equation (5.87)

$$\begin{aligned} \tilde{S}_{\text{leak}}(t, x) = & S_{\text{leak}}^{(n)}(t, 0) + \int_0^{\min[x; a^{(1)}(t-T)]} p_-^{*(0)}(t, x') dx' \\ & + \int_{a^{(1)}(t-T)}^{\min[\max[x; a^{(1)}(t-T)]; a^{(2)}(t-T)]} p_-^{(1)}(t, x') dx' \quad (\text{L.1}) \\ & + \int_{a^{(2)}(t-T)}^{\max[x; a^{(2)}(t-T)]} p_-^{*(2)}(t, x') dx' , \end{aligned}$$

there are three domains in which $\tilde{S}_{\text{leak}}(t, x)$ takes slightly different expressions.

- $x < a^{(1)}(t - T)$

$$\begin{aligned} \tilde{S}_{\text{leak}}(t, x) = & 2a^{(0)}x - \frac{1}{2(T-t+\mu tT)} \left[-(a^{(0)})^2(t-T)(T-t+\mu tT) \right. \\ & + 2a^{(0)}(T-t+\mu tT)x \\ & + (1-\mu T)x^2 + 2\mu Tx\bar{x}_0 \\ & \left. + \mu(t-T)\bar{x}_0^2 \right] \quad (\text{L.2}) \end{aligned}$$

- $a^{(1)}(t - T) < x < a^{(2)}(t - T)$

$$\begin{aligned} \tilde{S}_{\text{leak}}(t, x) = & \frac{1}{2(T-t+\mu tT)(t-T)} \left[(t-T)^2 x_0^2 \right. \\ & \left. + \mu(T^2 x^2 - 2T(T-t)(2a^{(0)}(T-t) + x)x_0) \right] \quad (\text{L.3}) \end{aligned}$$

- $x > a^{(2)}(t - T)$

$$\begin{aligned} \tilde{S}_{\text{leak}}(t, x) = \frac{1}{2(T - t + \mu t T)} & \left[(a^{(2)})^2 (t - T)(T - t + \mu t T) \right. \\ & - 2a^{(2)}(T - t + \mu t T)x \\ & + (\mu T - 1)x^2 4a^{(2)}\mu T(T - t)x_0 \\ & \left. + 2\mu T x x_0 + \mu(T - t)(4a^{(1)}T - x_0)x_0 \right] \end{aligned} \quad (\text{L.4})$$

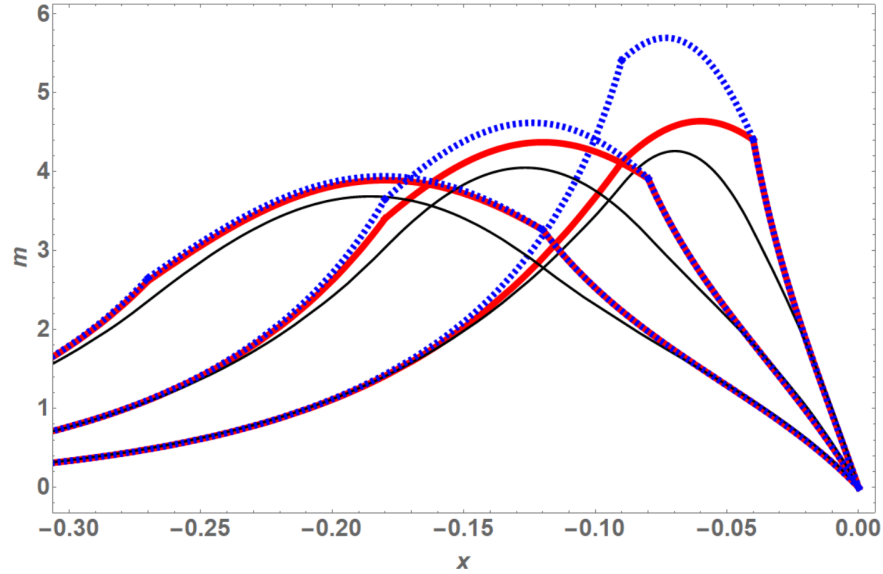


Figure 26: Spatial distribution of the agents, the thin line represents the numerical solution, the thick straight line the approximation using equation (5.87) and the thick dashed line the approximation using only equation (L.2). In this case $T = 2$, $a^{(0)} = 0.4$, $a^{(2)} = 0.9$, $\sigma = 0.2$, $\bar{x}_0 = 1.2$ and $\mu = 10^6$. From left to right, $t = 1.7$, $t = 1.8$, $t = 1.9$.

However, as mentioned in section 5.3.3, equation (5.87) can be approximated using only equation (L.2). This is illustrated in Figure 26 where the results of the two approximations, although obviously different for $t \approx T$ become more and more similar the smaller t gets.

Leak from a constant to a linear drift region

I begin, as in Section 5.3.3, by computing the position, time and momentum of the agents as they cross the boundary between a region

of constant drift $a^{(n)}$ and region (1). Keeping the same notations and using the same method as earlier one has

$$\begin{cases} x^{*(n)}(x_0) = a^{(n)}(t^{*(n)} - T) = x_0(1 + t^{*(n)}\mu) + t^{*(n)}(a^{(n)} - \mu x_0) \\ t^{*(n)}(x_0) = \frac{a^{(n)}T + x_0}{\mu(\bar{x}_0 - x_0)} \\ p^{*(n)}(x_0) = \mu(\bar{x}_0 - x_0) \end{cases} . \quad (\text{L.5})$$

Using the canonical equations in region (1), one can compute for $t > t^{*(n)}(x_0)$

$$\begin{cases} \mathcal{P}^{(n)}(t, x_0) = \frac{aT + x_0 - \mu T(\bar{x}_0 - x_0)}{t - T} \\ \mathcal{X}^{(n)}(t, x_0) = at + x_0 - \mu t(\bar{x}_0 - x_0) \\ x_0(t, x) = \frac{x - at + \mu t\bar{x}_0}{1 + \mu t} \end{cases} , \quad (\text{L.6})$$

from which one gets the prefactor

$$\frac{\mathcal{N}}{\sqrt{\partial_{x_0} x_n(t, x_0)}} \exp \left[-\frac{1}{2} \int_{t^{*(n)}(t, x)}^t (\partial_x a^{(1)}) d\tau \right] = \sqrt{\frac{\mu}{2\pi\sigma^2(1 + t\mu)} \frac{\mu(t - T)(at - x + \bar{x}_0)}{a(T - t) + x + \mu Tx - \mu(T - t)\bar{x}_0}} , \quad (\text{L.7})$$

and the action

$$S_{\text{leak}}^{(n)}(t, x) = \int_{x(t, \bar{x}_0)}^{a^{(n)}(t-T)} p^{(n)}(t, x') dx' + \int_{a^{(n)}(t-T)}^x p^{*(1)}(t, x') dx' , \quad (\text{L.8})$$

with $p^{(n)}$ the constant drift momentum of region (n) given by equation (5.59) and $p^{*(1)}$ the leaking momentum in region (1) obtained by inserting the third equation of system (L.6) into the second, yielding

$$\begin{aligned} S_{\text{leak}}^{(n)}(t, x) = \frac{1}{2(1 + \mu t)(t - T)} & \left[-a^{(n)2}(t - T)(T - t + \mu tT) \right. \\ & + x^2(1 + \mu T) \\ & + 2\mu(t - T)x\bar{x}_0 \\ & + \mu(T - t)x_0^2 \\ & \left. - 2a^{(n)}(t - T)(x + \mu t\bar{x}_0) \right] \quad . \quad (\text{L.9}) \end{aligned}$$

In the case where agents begin in region (2), they may diffuse up to region (0), using, once again the same scheme, one may compute the new prefactor

$$\frac{\mathcal{N}}{\sqrt{\partial_{x_0} x_0(t, x_0)}} \exp \left[-\frac{1}{2} \int_{t^{*(1)}(t, x)}^{t^{*(2)}(t, x)} (\partial_x a^{(1)}) d\tau \right] = \sqrt{\frac{\mu}{2\pi\sigma^2(1 + t\mu)} \frac{\mu(a^{(2)}t - x + \bar{x}_0)}{a^{(0)} - a^{(2)} + a^{(0)}\mu t + \mu(\bar{x}_0 - x)}} , \quad (\text{L.10})$$

and the new action

$$S_{\text{leak}}^{(0)}(t, x) = \int_{x(t, \bar{x}_0)}^{a^{(2)}(t-T)} p^{(n)}(t, x') dx' + \int_{a^{(2)}(t-T)}^{a^{(0)}(t-T)} p^{*(1)}(t, x') dx' + \int_{a^{(0)}(t-T)}^x p^{*(0)}(t, x') dx' , \quad (\text{L.11})$$

takes the explicit form

$$S_{\text{leak}}^{(0)}(t, x) = -\frac{1}{2(1+\mu t)} \left[a^{(2)2}(3+\mu t)(t-T) - a^{(0)2}(T-t+\mu t T) - 2a^{(2)}x + 2a^{(0)} \left(-a^{(2)}(2+\mu t)(t-T) + x + \mu t(x - \bar{x}_0) \right) - \mu(x - \bar{x}_0)^2 \right] . \quad (\text{L.12})$$

Finally the reflected action is computed as

$$\begin{aligned} \tilde{S}_{\text{leak}}(t, x) = & S_{\text{leak}}^{(0)}(t, 0) + \int_0^{\min[x; a^{(1)}(t-T)]} p_-^{*(0)}(t, x') dx' \\ & + \int_{a^{(1)}(t-T)}^{\min[\max[x; a^{(1)}(t-T)]; a^{(2)}(t-T)]} p_-^{*(1)}(t, x') dx' \\ & + \int_{a^{(2)}(t-T)}^{\max[x; a^{(2)}(t-T)]} p_-^{(2)}(t, x') dx' , \end{aligned} \quad (\text{L.13})$$

that can be approximated, as in section 5.3.3, as

$$\begin{aligned} \tilde{S}_{\text{leak}}(t, x) = & 2a^{(0)}x + \frac{1}{2(1+\mu t)} \left[a^{(2)2}(3+\mu t)(t-T) - a^{(0)2}(T-t+\mu t T) - 2a^{(2)}x + 2a^{(0)} \left(-a^{(2)}(2+\mu t)(t-T) + x + \mu t(x - \bar{x}_0) \right) - \mu(x - \bar{x}_0)^2 \right] . \end{aligned} \quad (\text{L.14})$$

LIST OF FIGURES

Figure 1	There are infinite possibilities for the system to reach state \vec{q}_2 starting from \vec{q}_1 , however the chosen path (red) is the one that minimizes the action.	9
Figure 2	Evolution of the density of players with time. Initially the density is localized around $x = 0$ and then spreads up to the point when the system reaches the ergodic state where it remains for most of the game. Towards the end, players gather once again not to pay too high of a terminal cost. For this simulation we chose a potential featuring repulsive interactions between players and a (confining) environmental gain $V[m] = -2m - 0.1x^2$, with $T = 10$, $\mu = 1$ and $\sigma = 0.4$. The terminal cost $c_T = 10x^2$ is also confining to ensure players effectively gather at the end. All numerical solutions of system (2.24) are obtained using a C++ algorithm described in appendix A.	18
Figure 3	Time evolution of the density of agents. In this case $T = 200$, $g = -2$, $\sigma = 0.5$ and $\mu = 1$. The initial distribution is a Gaussian of variance 0.1, and the terminal cost is flat $c_T(x) = 0$ (for better legibility).	29
Figure 4	On the left is plotted the evolution of $m(t, 0) = 3/4z(t)$ with time (full line) compared to the $t^{2/3}$ scaling behaviour (dashed). On the right are plotted an inverted parabola, and the density $m(x, t)$ rescaled by $z(t)$ for three different times.	30
Figure 5	Representation of the contraction of constant-time surfaces S_t in the (η, ζ) plane for the simulation presented in Figure 3. From smallest to largest, $t = 195, 100, 50$ and 20	33

Figure 6	Potential representation in the hodograph space of the simulation illustrated Figure (3). The small slit in the center of the figure represents the terminal condition, that is where charges are located with distribution ρ_0 . As we go further from the origin, the potential seems to flatten indicating the presence of charges at infinity, distributed according to ρ_∞	34
Figure 7	Comparison between the $N = 2$ approximation (blue) and the boundary conditions (red). For this Figure I chose $T = 10$, $g = -2$, $\mu = 1$, $m_0(x) = \frac{3(0.25^2 - x^2)}{4(0.25)^3}$ and $v_T(x) = 0.07x$, while the optimization of c yields $Q_0 = -2$, $Q_1 = 0$, $Q_2 = -0.12$, $I_0 = 0$, $I_1 = 0$, $I_2 = 0.034$	44
Figure 8	Comparison between the $N = 2$ approximation (blue) and the results of the brute force resolution described in Appendix A (red). For this Figure I chose $T = 10$, $g = -2$, $\mu = 1$, a Gaussian of variance 0.1 as initial distribution $m_0(x)$ and $v_T(x) = 0.07x$, while the optimization of c yields $Q_0 = -2$, $Q_1 = 0$, $Q_2 = -0.12$, $I_0 = 0$, $I_1 = 0$, $I_2 = 0.0225$. Simulations have been made with non-zero noise, $\sigma = 0.4$	45
Figure 9	Comparison between the $N = 2$ approximation (blue) and the boundary conditions (red). For this Figure I chose $T = 10$, $g = -2$, $\mu = 1$, a Gaussian of variance 0.1 as initial distribution $m_0(x)$ and $v_T(x) = 8.10^{-4}x^3$, while the optimization of c yields $Q_0 = -2$, $Q_1 = 0$, $Q_2 = 0.025$, $I_0 = 0$, $I_1 = 0$, $I_2 = 0.0225$	45
Figure 10	Comparison between the $N = 2$ approximation (blue) and the results of the brute force resolution described in Appendix A (red). For this Figure I chose $T = 10$, $g = -2$, $\mu = 1$, a Gaussian of variance 0.1 as initial distribution $m_0(x)$ and $v_T(x) = 8.10^{-4}x^3$, while the optimization of c yields $Q_0 = -2$, $Q_1 = 0$, $Q_2 = 0.025$, $I_0 = 0$, $I_1 = 0$, $I_2 = 0.0225$. Simulations have been made with non-zero noise, $\sigma = 0.4$	46
Figure 11	A rectangular loop γ_R in the (x, t) plane. The vanishing of the curvature imposes that the parallel transport along it is the identity.	49

Figure 12	Computational solution of the Gross-Pitaevskii equation (full) and Thomas-Fermi approximation (dashed). In this case $g = -2$, $\sigma = 0.4$, $\mu = 1$ and $U_0(x) = -x^2$	62
Figure 13	Computational solution of the Gross-Pitaevskii equation (full), Thomas-Fermi approximation (dashed) and semi-classical approximation (dot). The inset shows the same curves in Log-Linear plot focusing on the tail of the distribution. Parameters for this figure are $g = -2$, $\sigma = 0.4$, $\mu = 1$, $U_0(x) = -x^2$ and $C = 8.10^{-4}$	65
Figure 14	Computational solution of the Gross-Pitaevskii equation (full), Thomas-Fermi approximation (dashed), semi-classical approximation (dot) and uniform approximation (dash-dot). Parameters for this figure are to $g = -2$, $\sigma = 0.4$, $\mu = 1$, $U_0(x) = -x^2$, $C_{\text{left}} = 0.14$ and $C_{\text{right}} = 0.07$	65
Figure 15	First order Legendre polynomial of the second kind. Its effect on the ergodic state would be to add feet to the distribution.	68
Figure 16	Computational solution of the Gross-Pitaevskii equation with Gaussian initial condition (blue dot) and variational ansatz (red dashed). The inset shows the time evolution of the numerical variance (blue full) and Σ_t (red dashed) as defined in equation (4.38). In this case $g = -2$, $\sigma = 3.5$, $\mu = 1$, $\Sigma_0 = 0.2$ and $T = 20$	72
Figure 17	Computational solution of the Gross-Pitaevskii equation (blue dot) and parabolic ansatz (red dashed). The inset shows the time evolution of z numerically (blue full) and analytically (red dashed). In this case, parameters are chosen to be $g = -2$, $\sigma = 0.45$ and $\mu = 1$, meaning $\nu \approx 0.02$. The actual (numerical) game takes place from $t = 0$, when it starts as an inverted parabola of extension 0.4, to $t = T = 20$ when the terminal cost is flat. The effective game essentially starts at time $t \approx -0.07$ as a Dirac delta function and its effective duration is $\tilde{T} \approx 20.07$. The only difference between the numerical results and the parabolic ansatz comes from the fact that σ is non-zero in the simulation. This figure also illustrates how the Thomas-Fermi approximation becomes more and more effective as the typical extension of the density becomes larger in front of ν	77

Figure 18	Time evolution of the variance (left) and the width of the parabola (right). The numerical solution for the density of players has been numerically fitted with a Gaussian and an inverted parabola, full curves are obtained through the extraction of the fitting parameters. Dashed curves are obtained using either the Gaussian or parabolic ansatz with energy $E = -9.95 \times 10^{-3}$ computed through the self-consistent condition. Parameters for this figure are $g = -2$, $\sigma = 1.2$, $\mu = 1$, $\nu = 1$, $\Sigma_0 = 0.2$ and $T = 300$	80
Figure 19	Density of players at different times, numerical results are plotted (solid line) along with the Gaussian (dotted line) and the parabolic ansatz (dashed line). At the beginning of the game, Figs (19a) and (19b), the Gaussian ansatz is the most accurate. Then in the middle of the game, Figs (19c) and (19d), the parabolic constitutes a better approximation. At the end of the game, Figs (19e) and (19f), the parabolic ansatz becomes less and less accurate as we near the terminal condition. Here $g = -2$, $\sigma = 1.2$, $\mu = 1$, $\nu = 1$, $\Sigma_0 = 0.2$ and $T = 300$, while $E = -9.95 \times 10^{-3}$ has been computed through the self-consistent condition.	81
Figure 20	The full blue line represents the numerical density of players, the dashed green line is obtained through a parabolic ansatz of intrinsic time $\bar{\tau} = \tilde{T}_{IV}(3/2)^{3/2} = 2.5$ and the dashed red line corresponds to the ergodic density. In the inset the full line shows the time evolution of the maximum of the player density $m(x = 0, t)$, while the dashed horizontal line is set at $\bar{m}(0)$, maximum of the density during the ergodic state, and the dotted vertical at $t = \bar{\tau} = 2.5$. Here $g = -2$, $\sigma = 0.4$, $\mu = 1$, $\omega_0^2 = 0.2$, $E = -0.36$ and $T = 15$	83
Figure 21	Regions of the (t, \vec{x}) space, where $T = 2$ is the time when the seminar effectively begins, and their associated optimal drift $a(t, \vec{x})$. In regions (0) and (2) the drift stays constant and is denoted respectively $a^{(0)}$ and $a^{(2)}$ (here 5 and 2). In region (1), the drift is linear in x	87

Figure 22 A typical manifold generated by the classical trajectories in region (1) of the drift field. In this case $a = \frac{-x}{T-t}$, $\mu = 1.5$, $\sigma = 0.4$, $T = 2$ and $\text{pop}x_0 = -5$. The dashed curves represent specific trajectories beginning at $x_0 = -5.5$, -5 and -4.5 from left to right. 90

Figure 23 Same manifold as in Figure (22) where are highlighted two paths with same beginning and end. Because of the Lagrangian nature of the manifold we can write $\int_{C_1} (Et + p\dot{x})dt = \int_{C_2} (Et + p\dot{x})dt$ 91

Figure 24 Spatial distribution of the agents at fixed time, dashed lines show the numerical solution while solid lines show the approximation. From left to right, $K = 0.19$ and $t = 1.1$, $K = 0.24$ and $t = 1.3$, $K = 0.33$ and $t = 1.5$, $K = 0.56$ and $t = 1.7$, $K = 1.67$ and $t = 1.9$. In this case $T = 2$, $a^{(0)} = 0.4$, $a^{(2)} = 0.9$, $\sigma = 0.2$, $\text{pop}x_0 = 1.2$ and $\mu = 10^6$ 104

Figure 25 Spatial distribution of the agents at fixed time, dashed lines show the numerical solution while solid lines show the approximation. From left to right, $K = 0.74$ and $t = 1.1$, $K = 0.95$ and $t = 1.3$, $K = 1.33$ and $t = 1.5$, $K = 2.22$ and $t = 1.7$, $K = 6.66$ and $t = 1.9$. In this case $T = 2$, $a^{(0)} = 0.4$, $a^{(2)} = 0.9$, $\sigma = 0.4$, $\text{pop}x_0 = 1.2$ and $\mu = 10^6$ 104

Figure 26 Spatial distribution of the agents, the thin line represents the numerical solution, the thick straight line the approximation using equation (5.87) and the thick dashed line the approximation using only equation (L.2). In this case $T = 2$, $a^{(0)} = 0.4$, $a^{(2)} = 0.9$, $\sigma = 0.2$, $\bar{x}_0 = 1.2$ and $\mu = 10^6$. From left to right, $t = 1.7$, $t = 1.8$, $t = 1.9$ 142

BIBLIOGRAPHY

- [1] Y. Achdou, F. Camilli, and I. Capuzzo-Dolcetta. “Mean field games: numerical methods for the planning problem.” In: *SIAM J. Control Optim.* 50.1 (2012), pp. 77–109. URL: <http://epubs.siam.org/doi/abs/10.1137/100790069>.
- [2] Y. Achdou, F. J. Buera, J.-M. Lasry, Lions P.-L., and B. Moll. “Partial differential equation models in macroeconomics.” In: *Phil. Trans. R. Soc. A* 372 (2014), p. 20130397. URL: <http://dx.doi.org/10.1098/rsta.2013.0397>.
- [3] Y. Achdou, P.-N. Giraud, J.-M. Lasry, and P.-L. Lions. “A long-term mathematical model for mining industries.” In: *Appl. Math. Optim.* 74 (2016), 579–618.
- [4] Yves Achdou, Martino Bardi, and Marco Cirant. “Mean field games models of segregation.” In: *Mathematical Models and Methods in Applied Sciences* 27.01 (2017), pp. 75–113.
- [5] Noha Almulla, Rita Ferreira, and Diogo Gomes. “Two numerical approaches to stationary mean-field games.” In: *Dynamic Games and Applications* 7.4 (2017), pp. 657–682.
- [6] Warren Ambrose and Isadore M Singer. “A theorem on holonomy.” In: *Trans. Amer. Math. Soc* 75.3 (1953), pp. 428–443.
- [7] Vladimir Igorevich Arnol’d. *Mathematical methods of classical mechanics*. Vol. 60. Springer Science & Business Media, 2013.
- [8] Robert J Aumann. *Markets with a Continuum of Traders I*. Princeton University, 1962.
- [9] Robert J Aumann and Lloyd S Shapley. *Values of non-atomic games*. Princeton University Press, 2015.
- [10] Jean Avan and Vincent Caudrelier. “On the origin of dual Lax pairs and their r-matrix structure.” In: *Journal of Geometry and Physics* 120 (2017), pp. 106–128.
- [11] O. Babelon, D. Bernard, M. Talon, Cambridge University Press, P.V. Landshoff, D.R. Nelson, D.W. Sciama, and S. Weinberg. *Introduction to Classical Integrable Systems*. Cambridge Monographs on Mathematical Physics. Cambridge University Press, 2003. ISBN: 9780521822671. URL: <https://books.google.fr/books?id=Hboa9NvpvdAC>.
- [12] M. Ballerini et al. “Interaction ruling animal collective behavior depends on topological rather than metric distance: Evidence from a field study.” In: *PNAS* 105 (2008), pp. 1232–1237. DOI: <https://doi.org/10.1073/pnas.0711437105>.

- [13] M. Bardi. “Explicit solutions of some linear-quadratic mean field games.” In: *Networks and Heterogeneous Media* 7.2 (2012), pp. 243–261. DOI: [10.3934/nhm.2012.7.243](https://doi.org/10.3934/nhm.2012.7.243).
- [14] R. Bellman, R.E. Bellman, and Rand Corporation. *Dynamic Programming*. Rand Corporation research study. Princeton University Press, 1957. URL: <https://books.google.fr/books?id=rZW4ugAACAAJ>.
- [15] A. Bensoussan, J. Frehse, and S. C. P. Yam. “The master equation in mean field theory.” In: *J. Math. Pures Appl.* 103.6 (2015), 1441–1474.
- [16] James Binney and Scott Tremaine. *Galactic dynamics*. Vol. 20. Princeton university press, 2011.
- [17] Giulio Biroli, Guy Bunin, and Chiara Cammarota. “Marginally stable equilibria in critical ecosystems.” In: *New J. Phys.* 20 (2018), p. 083051.
- [18] F. Bonnans and P. Rouchon. *Commande et optimisation de systèmes dynamiques*. Mathématiques appliquées. Éditions de l’École Polytechnique, 2005. ISBN: 9782730212519. URL: <https://books.google.fr/books?id=F1bIQSGf57sC>.
- [19] Thibault Bonnemain, Thierry Gobron, and Denis Ullmo. “Universal behavior in non stationary Mean Field Games.” In: *arXiv e-prints* (2019).
- [20] Thibault Bonnemain and Denis Ullmo. “Mean field games in the weak noise limit: A WKB approach to the Fokker–Planck equation.” In: *Physica A: Statistical Mechanics and its Applications* 523 (2019), pp. 310–325.
- [21] Thibault Bonnemain, Denis Ullmo, and Thierry Gobron. “Schrödinger approach to Mean Field Games with negative coordination.” In: *HAL archives-ouvertes* (2019).
- [22] J.-P. Bouchaud and M. Mezard. “Wealth condensation in a simple model of economy.” In: *PHYSICA A* 282 (2000), pp. 536–545. DOI: [10.1016/S0378-4371\(00\)00205-3](https://doi.org/10.1016/S0378-4371(00)00205-3).
- [23] V. A. Brazhnyi, A. M. Kamchatnov, and V. V. Konotop. “Hydrodynamic flow of expanding Bose-Einstein condensates.” In: *Phys. Rev. A* 68 (3 2003), p. 035603.
- [24] Boguslaw Broda. “Non-Abelian Stokes theorem.” In: *Advances in Chemical Physics* 119.2 (2001), pp. 429–468.
- [25] Arthur E Bryson. “Optimal control-1950 to 1985.” In: *IEEE Control Systems Magazine* 16.3 (1996), pp. 26–33.
- [26] P. Cardaliaguet. “Notes on mean field games (from P.-L. Lions’ lectures at Collège de France).” URL: <https://www.ceremade.dauphine.fr/~cardaliaguet/MFG20130420.pdf>.

- [27] P. Cardaliaguet and Lehalle C.-A. “Mean Field Game of Controls and An Application To Trade Crowding.” In: *Math Finan Econ* (2017).
- [28] P. Cardaliaguet, J.-M. Lasry, P.-L. Lions, and A. Porretta. “Long Time Average of Mean Field Games with a Nonlocal Coupling.” In: *SIAM J. Control Optim.* 51.5 (2013), pp. 3558–3591. DOI: [10.1137/120904184](https://doi.org/10.1137/120904184). eprint: <http://dx.doi.org/10.1137/120904184>. URL: <http://dx.doi.org/10.1137/120904184>.
- [29] Pierre Cardaliaguet, François Delarue, Jean-Michel Lasry, and Pierre-Louis Lions. *The Master Equation and the Convergence Problem in Mean Field Games:(AMS-201)*. Vol. 381. Princeton University Press, 2019.
- [30] R. Carmona and F. Delarue. “Probabilistic Analysis of Mean-Field Games.” In: *SIAM J. Control Optim.* 51.4 (2013), pp. 2705–2734. DOI: [10.1137/120883499](https://doi.org/10.1137/120883499). eprint: <http://dx.doi.org/10.1137/120883499>. URL: <http://dx.doi.org/10.1137/120883499>.
- [31] R. Carmona and F. Delarue. *Probabilistic Theory of Mean Field Games with Applications : vol. I*. Probability Theory and Stochastic Modelling, 83. Springer, 2018.
- [32] R. Carmona and F. Delarue. *Probabilistic Theory of Mean Field Games with Applications : vol. II*. Probability Theory and Stochastic Modelling, 84. Springer, 2018.
- [33] René Carmona, François Delarue, and Aimé Lachapelle. “Control of McKean–Vlasov dynamics versus mean field games.” In: *Mathematics and Financial Economics* 7.2 (2013), pp. 131–166. URL: <http://link.springer.com/article/10.1007/s11579-012-0089-y> (visited on 08/18/2014).
- [34] Rene Carmona, Jean-Pierre Fouque, and Li-Hsien Sun. “Mean field games and systemic risk.” In: *arXiv preprint arXiv:1308.2172* (2013). URL: <http://arxiv.org/abs/1308.2172> (visited on 09/03/2014).
- [35] B. Caroli, C. Caroli, and B. Roulet. “Diffusion in a Bistable Potential: A Systematic WKB Treatment.” In: *Journal of Statistical Physics* 21 (1979), pp. 415–437.
- [36] D. Challet and Y.C. Zhang. “Emergence of cooperation and organization in an evolutionary game.” In: *PHYSICA A* 246 (1997), pp. 407–418. DOI: [10.1016/S0378-4371\(97\)00419-6](https://doi.org/10.1016/S0378-4371(97)00419-6).
- [37] Yaan Yee Choy, Wooi Nee Tan, Kim Gaik Tay, and Chee Tiong Ong. “Crank-Nicolson implicit method for the nonlinear Schrödinger equation with variable coefficient.” In: *AIP Conference Proceedings* 1605.1 (2014), pp. 76–82. DOI: [10.1063/1.4887568](https://doi.org/10.1063/1.4887568). eprint: <https://aip.scitation.org/doi/pdf/10.1063/1.4887568>.

- URL: <https://aip.scitation.org/doi/abs/10.1063/1.4887568>.
- [38] Jack K. Cohen and Robert M. Lewis. "A Ray Method for the Asymptotic Solution of the Diffusion Equation." In: *J. Inst. Maths Applics* 3 (1967), pp. 266–290.
- [39] Richard Courant and David Hilbert. *Methods of Mathematical Physics: Partial Differential Equations*. John Wiley & Sons, 2008.
- [40] F. Dalfovo, L. Pitaevskii, and S. Stringari. "Order parameter at the boundary of a trapped Bose gas." In: *Phys. Rev. A* 54 (5 1996), pp. 4213–4217.
- [41] Franco Dalfovo, Stefano Giorgini, Lev P. Pitaevskii, and Sandro Stringari. "Theory of Bose-Einstein condensation in trapped gases." In: *Reviews of Modern Physics* 71.3 (Apr. 1999), pp. 463–512. DOI: [10.1103/revmodphys.71.463](https://doi.org/10.1103/revmodphys.71.463). URL: <http://dx.doi.org/10.1103/revmodphys.71.463>.
- [42] B.N. Datta. *Numerical Linear Algebra and Applications, Second Edition*. Other Titles in Applied Mathematics. Society for Industrial and Applied Mathematics (SIAM, 3600 Market Street, Floor 6, Philadelphia, PA 19104), 2010. ISBN: 9780898717655. URL: <https://books.google.fr/books?id=-tW8-FUoxWwC>.
- [43] Stanislav A. Derevyanko, Sergei K. Turitsyn, and Dennis A. Yakushev. "Fokker-Planck equation approach to the description of soliton statistics in optical fiber transmission systems." In: *J. Opt. Soc. Am. B* 22.4 (), pp. 743–752.
- [44] B. Diu. *Éléments de physique statistique*. Collection Enseignement des sciences. Hermann, 1989. ISBN: 9782705660659. URL: <https://books.google.fr/books?id=I67gAAAAMAAJ>.
- [45] G.A. El and M.A. Hoefer. "Dispersive shock waves and modulation theory." In: *Physica D: Nonlinear Phenomena* 333 (2016). Dispersive Hydrodynamics, pp. 11–65. ISSN: 0167-2789. DOI: <https://doi.org/10.1016/j.physd.2016.04.006>. URL: <http://www.sciencedirect.com/science/article/pii/S0167278916301580>.
- [46] Ludwig Faddeev and Leon Takhtajan. *Hamiltonian methods in the theory of solitons*. Springer Science & Business Media, 2007.
- [47] Irving Fisher. *Mathematical investigations in the theory of value and prices (1892)*. Augustus M. Kelley, 1965.
- [48] C.W. Gardiner. *Handbook of stochastic methods for physics, chemistry, and the natural sciences*. Springer series in synergetics. Springer-Verlag, 1985. ISBN: 9783540113577. URL: <https://books.google.fr/books?id=cRfvAAAAMAAJ>.

- [49] L. Gauvin, J. Vannimenus, and J.-P. Nadal. "Phase diagram of a Schelling segregation model." In: *Eur. Phys. J. B* 70 (2009), pp. 293–304.
- [50] D. A. Gomes and J. Saúde. "Mean Field Games Models – A Brief Survey." English. In: *J. Dyn. Games Appl.* 4.2 (2014), pp. 110–154. ISSN: 2153-0785. DOI: [10.1007/s13235-013-0099-2](https://doi.org/10.1007/s13235-013-0099-2). URL: <http://dx.doi.org/10.1007/s13235-013-0099-2>.
- [51] O. Guéant. "A reference case for mean field games models." In: *J. Math. Pures Appl.* 92.3 (2009), pp. 276–294. DOI: [doi:10.1016/j.matpur.2009.04.008](https://doi.org/10.1016/j.matpur.2009.04.008).
- [52] O. Guéant. "Mean field games equations with quadratic Hamiltonian: a specific approach." In: *Math. Models Methods Appl. Sci.* 22 (2012), p. 1250022.
- [53] O. Guéant. "Mean field games equations with quadratic Hamiltonian: a specific approach." In: *Math. Models Methods Appl. Sci.* 22 (2012), p. 1250022.
- [54] O. Guéant. "Existence and Uniqueness Result for Mean Field Games with Congestion Effect on Graphs." In: *Applied Mathematics & Optimization* 72 (2015), 291–303.
- [55] O. Guéant, J.-M. Lasry, and P.-L. Lions. "Mean Field Games and Applications." In: *Paris-Princeton Lectures on Mathematical Finance 2010*. Heidelberg: Springer, 2011, pp. 205–266. DOI: [10.1007/978-3-642-14660-2_3](https://doi.org/10.1007/978-3-642-14660-2_3). URL: http://dx.doi.org/10.1007/978-3-642-14660-2_3.
- [56] AV Gurevich, AL Krylov, and NG Mazur. "Quasi-simple waves in Korteweg-de Fries hydrodynamics." In: *Zh. Eksp. Teor. Fiz* 95 (1989), p. 1674.
- [57] D. Harder. "The Crank-Nicolson Method and Insulated Boundaries." 2012. URL: <https://fr.scribd.com/doc/292534942/3-CrankNicolson>.
- [58] E. Hopf. "The partial differential equation $u_t + uu_x = u_{xx}$." In: *Comm. Pure Appl. Math.* 3 (1950), pp. 201–230.
- [59] M. Huang, R. P. Malhamé, and P. E. Caines. "Large population stochastic dynamic games: closed-loop McKean–Vlasov systems and the Nash certainty equivalence principle." In: *Commun. Inf. Syst.* 6.3 (2006), pp. 221–252. URL: <http://projecteuclid.org/euclid.cis/1183728987> (visited on 08/28/2014).
- [60] Swiecicki I, Gobron T., and Ullmo D. "'Phase diagram' of a mean field game." In: *Physica A* 442 (2016), pp. 467–485. DOI: [http://dx.doi.org/10.1016/j.physa.2015.09.018](https://doi.org/10.1016/j.physa.2015.09.018). URL: <http://www.sciencedirect.com/science/article/pii/S0378437115007451>.

- [61] M Isoard, AM Kamchatnov, and N Pavloff. "Long-time evolution of pulses in the Korteweg–de Vries equation in the absence of solitons reexamined: Whitham method." In: *Physical Review E* 99.1 (2019), p. 012210.
- [62] M Isoard, AM Kamchatnov, and N Pavloff. "Wave breaking and formation of dispersive shock waves in a defocusing nonlinear optical material." In: *Physical Review A* 99.5 (2019), p. 053819.
- [63] John David Jackson. *Classical electrodynamics*. 3rd ed. New York, NY: Wiley, 1999. ISBN: 9780471309321. URL: <http://cdsweb.cern.ch/record/490457>.
- [64] A.M. Kamchatnov. *Nonlinear Periodic Waves and Their Modulations: An Introductory Course*. World Scientific, 2000. ISBN: 9789810244071. URL: <https://books.google.fr/books?id=yM99QgAACAAJ>.
- [65] V. Kaplunovsky. "Multipole Expansion of the Electrostatic Potential." URL: <http://bolvan.ph.utexas.edu/~vadim/Classes/2017f/mme.pdf>.
- [66] D. J. Kaup. "Perturbation theory for solitons in optical fibers." In: *Phys. Rev. A* 42 (9 1990), pp. 5689–5694. DOI: [10.1103/PhysRevA.42.5689](https://doi.org/10.1103/PhysRevA.42.5689). URL: <https://link.aps.org/doi/10.1103/PhysRevA.42.5689>.
- [67] M. Ali Khan. "Non-cooperative games with many players." In: *Handbook of Game Theory with Economic Applications* 3 (2002), pp. 1761–1808.
- [68] C. Kharif, E. Pelinovsky, and A. Slunyaev. *Rogue Waves in the Ocean*. Advances in Geophysical and Environmental Mechanics and Mathematics. Springer, 2008. ISBN: 9783540884194.
- [69] Arman C. Kizilkale and Roland P. Malhamé. "Load Shaping via Grid Wide Coordination of Heating-Cooling Electric Loads: A Mean Field Games Based Approach." submitted paper to IEEE Transactions on Automatic Control.
- [70] Arman C Kizilkale, Rabih Salhab, and Roland P Malhamé. "An integral control formulation of mean field game based large scale coordination of loads in smart grids." In: *Automatica* 100 (2019), pp. 312–322.
- [71] A. Lachapelle and M.-T. Wolfram. "On a mean field game approach modeling congestion and aversion in pedestrian crowds." In: *Transportation Research Part B* 45.10 (2011), pp. 1572–1589. DOI: [10.1016/j.trb.2011.07.011](https://doi.org/10.1016/j.trb.2011.07.011).
- [72] Aimé Lachapelle, Julien Salomon, and Gabriel Turinici. "Les Cahiers de la Chaire/N 16." In: (). URL: http://www.ifd.dauphine.fr/fileadmin/mediatheque/recherche_et_valo/FDD/CAHIER_CHAIRE_16.pdf (visited on 08/18/2014).

- [73] L. Laguzet and G. Turinici. "Individual Vaccination as Nash Equilibrium in a SIR Model with Application to the 2009-2010 Influenza A (H1N1) Epidemic in France." In: *Bull. Math. Biol.* 77.10 (2015), pp. 1955–1984. DOI: [10.1007/s11538-015-0111-7](https://doi.org/10.1007/s11538-015-0111-7).
- [74] L.D. Landau and E.M. Lifshitz. *Fluid Mechanics*. vol. 6. Elsevier Science, 2013. ISBN: 9781483140506. URL: <https://books.google.fr/books?id=CeBbAwAAQBAJ>.
- [75] L.D. Landau, E.M. Lifshitz, J.B. Sykes, and J.S. Bell. *Mechanics*. Butterworth-Heinemann. Elsevier Science, 1976. ISBN: 9780750628969. URL: <https://books.google.fr/books?id=e-xASAehg1sC>.
- [76] Rudolph E Langer. "On the connection formulas and the solutions of the wave equation." In: *Physical Review* 51.8 (1937), p. 669.
- [77] J.-M. Lasry and P.-L. Lions. "Jeux à champ moyen. I – Le cas stationnaire." In: *C. R. Acad. Sci. Paris, Ser. I* 343.9 (2006), pp. 619–625. DOI: <http://dx.doi.org/10.1016/j.crma.2006.09.019>. URL: <http://www.sciencedirect.com/science/article/pii/S1631073X06003682>.
- [78] J.-M. Lasry and P.-L. Lions. "Jeux à champ moyen. II – Horizon fini et contrôle optimal." In: *C. R. Acad. Sci. Paris, Ser. I* 343.10 (2006), pp. 679–684. ISSN: 1631-073X. DOI: <http://dx.doi.org/10.1016/j.crma.2006.09.018>. URL: <http://www.sciencedirect.com/science/article/pii/S1631073X06003670>.
- [79] Jean-Michel Lasry and Pierre-Louis Lions. "Mean field games." In: *Japanese Journal of Mathematics* 2.1 (Mar. 2007), pp. 229–260. ISSN: 0289-2316, 1861-3624. DOI: [10.1007/s11537-007-0657-8](https://doi.org/10.1007/s11537-007-0657-8). URL: <http://link.springer.com/10.1007/s11537-007-0657-8> (visited on 09/03/2014).
- [80] Adrien Marie Legendre. "Recherches sur l'attraction des spheroides homogenes." In: *Memoires de mathematique et de physique : pres. à l'Academie Royale des Sciences, par divers savans, et lûs dans ses assemblees* 1785 (2007), pp. 411–434.
- [81] Joseph Liouville. "Note sur l'intégration des équations différentielles de la Dynamique, présentée au Bureau des Longitudes le 29 juin 1853." In: *Journal de Mathématiques pures et appliquées* (1855), pp. 137–138.
- [82] N. Gregory Mankiw. *Principles of Microeconomics*. vol. 1. Dryden Press, 1998. ISBN: 9780030245022. URL: <https://books.google.fr/books?id=xoztFMavGCcC>.
- [83] V. P. Maslov and M. V. Fedoriuk. *Semi-Classical Approximation in Quantum Mechanics*. Mathematical Physics and Applied Mathematics, vol. 7. Translated from the Russian by J. Niederle and J. Tolar. Dordrecht-Boston, Mass.: Reidel Publishing Co., 1981.

- [84] F. Mériauxi, V. Varma, and S. Lasaulce. “Mean field energy games in wireless networks.” In: *2012 Conference Record of the Forty Sixth Asilomar Conference on Signals, Systems and Computers (ASILOMAR)*. 2012, pp. 671–675. DOI: [10.1109/ACSSC.2012.6489095](https://doi.org/10.1109/ACSSC.2012.6489095).
- [85] John Stuart Mill. “Utilitarianism.” In: *Seven masterpieces of philosophy*. Routledge, 2016, pp. 337–383.
- [86] Philip Mirowski. *More heat than light: economics as social physics, physics as nature’s economics*. Cambridge University Press, 1991.
- [87] Thierry Mora and William Bialek. “Are biological systems poised at criticality?” In: *Journal of Statistical Physics* 144.2 (2011), pp. 268–302.
- [88] Alexandre Nicolas, Marcelo Kuperman, Santiago Ibañez, Sebastián Bouzat, and Cécile Appert-Rolland. “Mechanical response of dense pedestrian crowds to the crossing of intruders.” In: *Scientific reports* 9.1 (2019), p. 105.
- [89] S Novikov, SV Manakov, LP Pitaevskii, and Vladimir E Zakharov. *Theory of solitons: the inverse scattering method*. Springer Science & Business Media, 1984.
- [90] R. Penrose. *The Road to Reality: A Complete Guide to the Laws of the Universe*. Vintage Series. Vintage Books, 2007. ISBN: 9780679776314. URL: <https://books.google.fr/books?id=coahAAAACAAJ>.
- [91] V. M. Pérez-García, H. Michinel, J. I. Cirac, M. Lewenstein, and P. Zoller. “Dynamics of Bose-Einstein condensates: Variational solutions of the Gross–Pitaevskii equations.” In: *Phys. Rev. A* 56 (2 1997), pp. 1424–1432. DOI: [10.1103/PhysRevA.56.1424](https://doi.org/10.1103/PhysRevA.56.1424). URL: <https://link.aps.org/doi/10.1103/PhysRevA.56.1424>.
- [92] C. J. Pethick and H. Smith. *Bose-Einstein Condensation in Dilute Gases*. 2nd ed. Cambridge University Press, 2008. DOI: [10.1017/CB09780511802850](https://doi.org/10.1017/CB09780511802850).
- [93] L. Pitaevskii and S. Stringari. *Bose-Einstein Condensation*. Oxford: Clarendon Press, 2003.
- [94] W. Poundstone. *Prisoner’s Dilemma*. Oxford paperbacks. Oxford University Press, 1993. ISBN: 9780192861627. URL: https://books.google.fr/books?id=v_-4vswEACAAJ.
- [95] H. Risken. *The Fokker-Planck Equation: Methods of Solution and Applications*. Springer Series in Synergetics. Heidelberg: Springer, 1996. ISBN: 9783642968075.
- [96] H. Risken. *The Fokker-Planck Equation*. 2nd Edition. Springer, 1996.
- [97] T. Schelling. “Dynamic models of segregation.” In: *Journal of Mathematical Sociology* 1 (1971), pp. 143–186.

- [98] Lawrence S Schulman. *Techniques and applications of path integration*. Courier Corporation, 2012.
- [99] A Shabat and V Zakharov. “Exact theory of two-dimensional self-focusing and one-dimensional self-modulation of waves in nonlinear media.” In: *Soviet physics JETP* 34.1 (1972), p. 62.
- [100] Bernie Shizgal and Takeo Nishigori. “A uniform WKB approach to electron thermalization in gases.” In: *Chemical Physics Letters* 171.5 (1990), pp. 493–498. ISSN: 0009-2614. DOI: [https://doi.org/10.1016/0009-2614\(90\)85252-8](https://doi.org/10.1016/0009-2614(90)85252-8). URL: <http://www.sciencedirect.com/science/article/pii/0009261490852528>.
- [101] V. I. Smirnov. *A Course of Higher Mathematics. Volume IV*. Elsevier, 1964.
- [102] John Maynard Smith. *Evolution and the Theory of Games*. Cambridge University Press, 1982. DOI: [10.1017/CB09780511806292](https://doi.org/10.1017/CB09780511806292).
- [103] A. Sommerfeld. *Partial differential equations in physics*. Pure and applied mathematics. Academic Press, 1949. URL: <https://books.google.fr/books?id=COFEAAAIAAJ>.
- [104] Robert Stalnaker. “On the evaluation of solution concepts.” In: *Theory and decision* 37.1 (1994), pp. 49–73.
- [105] I. Swiecicki. *Étude de quelques modèles issus de la théorie des jeux en champs moyens*. Université Cergy-Pontoise: PhD thesis, 2016.
- [106] I. Swiecicki, T. Gobron, and D. Ullmo. “Schrödinger Approach to Mean Field Games.” In: *Phys. Rev. Lett.* 116 (12 2016), p. 128701. DOI: [10.1103/PhysRevLett.116.128701](https://doi.org/10.1103/PhysRevLett.116.128701). URL: <http://link.aps.org/doi/10.1103/PhysRevLett.116.128701>.
- [107] V. I. Talanov. “Self Focusing of Wave Beams in Nonlinear Media.” In: *ZhETF Pisma Redaktsiiu* (1965).
- [108] Denis Ullmo, Igor Swiecicki, and Thierry Gobron. “Quadratic Mean Field Games.” In: *ArXiv:1708.07730* (2018). URL: <https://arxiv.org/abs/1708.07730>.
- [109] Denis Ullmo, Igor Swiecicki, and Thierry Gobron. “Quadratic mean field games.” In: *Physics Reports* 799 (2019). Quadratic mean field games, pp. 1–35. ISSN: 0370-1573. DOI: <https://doi.org/10.1016/j.physrep.2019.01.001>. URL: <http://www.sciencedirect.com/science/article/pii/S0370157319300018>.
- [110] Joachim Moser Von Filseck, Luca Barberi, Nathaniel Talledge, Isabel Johnson, Adam Frost, Martin Lenz, and Aurelien Roux. “Anisotropic ESCRT-III architecture governs helical membrane tube formation.” In: *BioRxiv* (2019), p. 716308.
- [111] John Von Neumann, Oskar Morgenstern, and Harold William Kuhn. *Theory of games and economic behavior (commemorative edition)*. Princeton university press, 2007.

- [112] Pierre Weiss. "L'hypothèse du champ moléculaire et la propriété ferromagnétique." In: *J. Phys. Theor. Appl.* 6.1 (1907), pp. 661–690.
- [113] Anthony Zee. *Quantum field theory in a nutshell*. Vol. 7. Princeton university press, 2010.

COLOPHON

This document was typeset using the typographical look-and-feel `classicthesis` developed by André Miede. The style was inspired by Robert Bringhurst's seminal book on typography "*The Elements of Typographic Style*". `classicthesis` is available for both \LaTeX and \LyX :

<https://bitbucket.org/amiede/classicthesis/>